CHALMERS
UNIVERSITY OF TECHNOLOGY

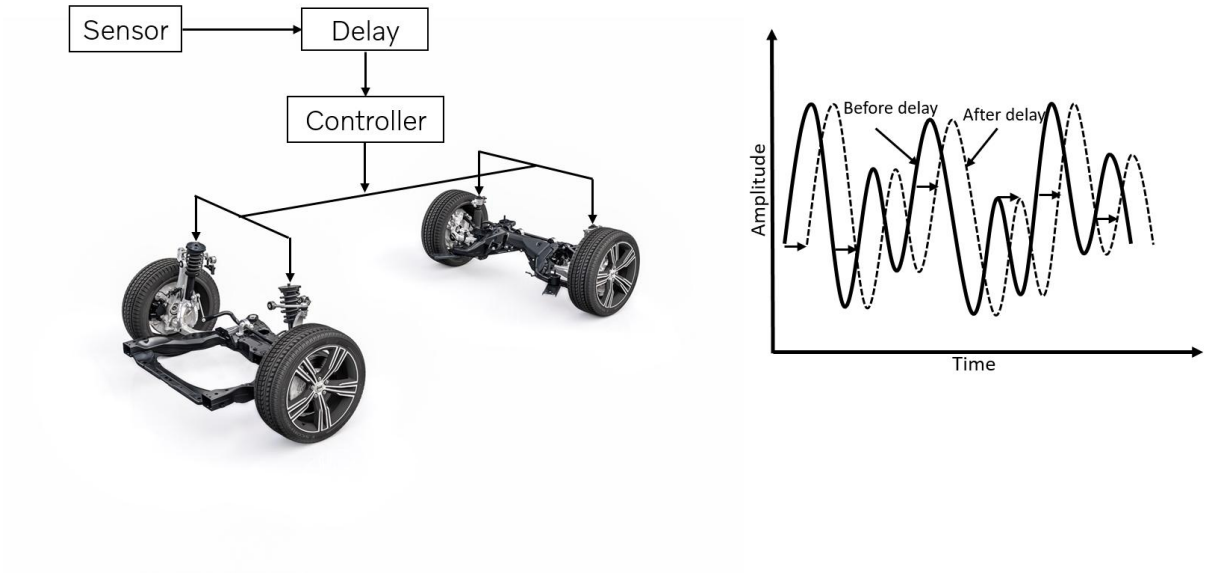

Influence of signal delays and accuracy, on the performance of suspension control system and controller design

Master's thesis in Systems, Control and Mechatronics and Automotive Engineering

DHURAI ISAAC PRABHAHAR

MOHAMMAD SHAIKH EBRAHIM KAMARDEEN

Department of Mechanics and Maritime Sciences
CHALMERS UNIVERSITY OF TECHNOLOGY
Gothenburg, Sweden 2020

Master's thesis in systems, control and mechatronics
and automotive engineering

Influence of signal delays and accuracy, on the performance of suspension control system and controller design

DHURAI ISAAC PRABHAKAR
MOHAMMAD SHAIKH EBRAHIM KAMARDEEN

CHALMERS
UNIVERSITY OF TECHNOLOGY

Department of Mechanics and Maritime Sciences
Division of Vehicle Dynamics and Autonomous Systems
Chalmers University of Technology
Gothenburg, Sweden 2020

Influence of signal delays and accuracy, on the performance of suspension control system and controller design

DHURAI ISAAC PRABHAHAR
MOHAMMAD SHAIKH EBRAHIM KAMARDEEN

Industrial Supervisor: Pontus Carlsson, Anton Albinsson, Volvo Car Corporation
Academic Supervisor: Mats Jonasson ,Vehicle Dynamics and Autonomous Systems
Examiner: Bengt Jacobson, Vehicle Dynamics and Autonomous Systems

Master's Thesis 2020:56
Department Mechanics and Maritime Sciences
Division of Vehicle Dynamics and Autonomous Systems
Chalmers University of Technology
SE-412 96 Gothenburg
Sweden
Telephone +46 31 772 1000

Cover: Structure of system with delays in suspension system and it's output response.

Typeset in LaTeX
Printed by Chalmers Reproservice
Gothenburg, Sweden 2020

Influence of signal delays and accuracy, on the performance of suspension control system and controller
Master's thesis in Systems, Control and Mechatronics and Automotive Engineering
DHURAI ISAAC PRABHAHAR
MOHAMMAD SHAIKH EBRAHIM KAMARDEEN
Department of Mechanics and Maritime Sciences
Division of Vehicle Engineering and Autonomous Systems
Chalmers University of Technology

Abstract

Abstract : Ride comfort, handling, and road holding are important vehicle dynamics characteristics, and at Volvo cars, these are actively controlled by Electronic dampers through software and control algorithm. The complexity of the software adds different sources of delays and errors within these controllers. And this presence of delays and errors leads to performance degradation, and in some cases, it could also result in system instability. Thus it's important to consider the delays and errors when designing the controllers. So in the thesis work, we first focus on studying the influence of the delays and errors on the performance and stability of three different suspension control systems: Semi-active, Active and system with preview. Here we have modelled different mathematical delays and quantization error models, and they are used based on the test case and performance metrics. In the second part of the work, an LQG controller for the Active suspension system and Smith predictor compensator for both active and semi-active suspension system was implemented and evaluated, to compensate for the delays. This entire work is carried out in the simulation environment, using IPG Carmaker and Matlab/Simulink. Finally, experimental tests were conducted on the current controller at Hällered Proving Ground to validate the trends, and perform a subjective and objective assessment for different sensor delays.

Keywords: Signal delay, Quantization error, Active Suspension, Control system, Performance analysis, Signal processing, Markov chain.

Acknowledgements

First, we would like to express our immense gratitude to our industrial supervisors **Anton Albinsson** and **Pontus Carlsson** for their incredible support and advice throughout the thesis. Each and every feedback from both of them were incredibly valuable in successfully finishing this project and we are super grateful for that. Then, we would like to thank **Angelis Stavros** for supporting with technical related doubts during our supervisor's parental leave. We would also like to thank **Axel Jonson** for his excellent guidance and help with the experimental results. Furthermore, we would like to thank **Fredrik Skoglund** for his excellent support. A special thanks to **Johan Ericson** for this amazing opportunity to work at Volvo cars with brilliant and passionate minds on an incredibly interesting and challenging problem, and also for his kind support throughout the project.

Finally, we would also like to thank our Academic Supervisor **Mats Jonasson** for his continuous support and constructive feedback, in both technical and non-technical aspect of this project throughout our thesis.

Dhurai Prabhahar & Mohammad Kamardeen, Gothenburg, June 2020

Nomenclature

Abbreviations

COG	Center Of Gravity
DOF	Degree Of Freedom
FL	Front Left
FR	Front Right
LQG	Linear Quadratic Gaussian
LQR	Linear Quadratic Regulator
LTI	Linear Time Invariant
QE	Quantization Error
RL	Rear Left
RMS	Root Mean Square
RR	Rear Right

Contents

List of Figures

List of Tables

1
Introduction

The primary purpose of the suspension system is to improve the grip and handling of the vehicle, and comfort for the passenger. Grip and handling affect the safety of the system and are mainly influenced by the tires, which in turn are influenced by the shock absorbers, springs and the suspension kinematics. Comfort is primarily achieved by the system capability to isolate the passenger compartment from road irregularities through shock absorbers and springs. Most often in suspension design, there is a compromise between the grip, handling and comfort. This tradeoff has resulted in Active and semi-active suspension technology. As the name suggests, in these systems, the suspension shock absorbers are actively controlled by the control algorithms with inputs from different sensors.

In premium suspension systems, the passive springs and dampers are replaced by advanced active or semi-active damper and springs with complex controls systems. The main functionality of these active and semi-active suspension systems is to actively control the ride of the vehicle to provide better comfort for the passengers in all possible scenarios. Today, the functionality and algorithms of these active suspensions are complex with lots of data being fed into them. The primary input data to these controllers are from the accelerometer, level sensor and camera to estimate the future road profile. As the complexities grow, the source of errors and signal delays within these systems becomes greater as well. This problem becomes significant in cases of high speeds as it could lead to loss of grip, thus the safety of the passenger. This becomes even more critical for active suspension, as long delays could lead to controller instability. Hence the need for a better robust and reliable controller that takes signal delay and quantization error becomes important.

1.1 Background

Comfort is one of the key criteria in determining the performance of the vehicle. This becomes challenging as cars are becoming more and more autonomous. According to [1], every human has different levels of threshold to motion sickness. This motion sickness could be a function of many different parameters like age, gender, previous health issue etc. Usually, these parameters are considered by the driver, and he/she make changes to their driving style by driving more or less aggressive. But the current ADAS and AD are not advanced enough to consider these uncertainties and take human comfort into account. Hence the need for active and semi-active

suspension systems becomes more important. These systems are part of the overall vehicle (or chassis) control system, designed to make the vehicle safe and give excellent ride experience for the passengers.

In recent studies, the active suspension model and usage of various types of controllers have been observed [2]. For which the LQR control is found to be better. Similarly sliding mode control (SMC), vehicle stability control (VSC), quantitative feedback theory (QFT), linear quadratic gaussian (LQG) and loop transfer recovery (LTR) are also other controllers that have been tested but these studies have shown that LQR is found to be better. But it is also noted that LQR is not robust to the signal delay on these semi-active and active suspension system. Due to this signal delay between the sensor to controller or controller to actuator, the existing active suspension is inefficient which results in performance issue and controller instability.So it is important to compensate for the effect of delay for improving the system stability. One of the oldest and most used mathematical models for capturing the structure of the delay component in a control system is the smith predictor. The idea of smith predictor is to compensate the delay component in the closed-loop system. The reason is because only the delay in the closed-loop system causes system instability [3].

1.2 Purpose

The purpose of the first part of the thesis work is to provide the necessary data to specify constraints on the sensor specifications and accuracy. Then the second part is to investigate and evaluate delay compensated controllers, to check to what extent these delays can be compensated and how much performance improvement can be guaranteed.

1.3 Objectives

The main objective of this thesis is to first evaluate the performance and stability of the state-of-the-art controller both with and without road preview and for semi-active and active dampers in simulations using IPG Carmaker and Matlab. And then to develop control methods that are robust to the signal delays for semi-active and active systems.

1.4 Deliverables

1. *How the signal delays affect the active and semi-active suspension in terms of comfort, and in which test cases these performance degradation becomes prominent?.*

2. *Which sensor has the most impact on the performance of the system when considering the signal delay and how much delays can be tolerated.*

3. *What are the effects of unsynchronized signal delay on the performance of the active and semi-active suspension.*

4. *How much accuracy of resolution of the signal delay do we need before the performance degradation becomes prominent.*

5. *Which modelling technique is most suitable for modelling the time-varying signal delays.*

6. *Which control method is suitable for a system with delays.*

7. *To what extend will the simulation environment be able to capture the expected vehicle performance in the presence of signal delay?*

1.5 Limitations

- Only the input from the level, accelerometer and road preview sensors are studied. The computation delay is neglected in this thesis work.

- Only comfort is studied in this thesis work. Road hold and handling are neglected.

- Effects of the Vehicle dynamic parameters like mass, inertia etc on delays are not studied in detail.

- The testing conditions are limited to standard environment with dry road condition.

- The work will be done on the existing vehicle and controller models. Hence no improvements will be done on these.

- From the complete system architecture, some delays and errors that are negligible and insignificant will not be considered.

1.6 Thesis Outline

Chapter 2 : presents the **theories** about vertical dynamics, time-delay system, controllers, compensators and some other performance metrics of interest.

Chapter 3 : contains an overview of **vehicle models** that were used in the thesis work. The vehicle model section starts with the description of the quarter car model;then the full car model is presented with state space representation. Finally, the IPG Carmaker model is defined with process flow diagram.

Chapter 4 : Contains the description of the current **state-of-the-art controller** implementations that were used in this thesis work.

Chapter 5 : Presents a brief description and classification of the mathematical models of the **time delays** and mathematical model of **quantization error** that were implemented and evaluated in the thesis work.

Chapter 6 : The methodology, the structure of the **work flow** is discussed briefly with flow charts and description.

Chapter 7 : The results from the analytical method were presented and then the results from the **performance analysis**, both from simulation and experimental data, and controllers are shown and discussed in detail.

Chapter 8 : The final **conclusion** is discussed based on the obtained results, and then the future scope of this has been included.

2

Theory

In this chapter, a general introduction of the systems, some important concepts and terminology are discussed in brief.

First, the theory behind the vertical dynamics of a vehicle is discussed. Here we have explained the fundamental objective of the vertical dynamics and its importance. Then the main overall system architecture is shown to visualize the different sources of delay and errors in a controlled system. Next, a brief explanation of the controllers that were implemented and damper models that were used are given. Finally, a general theory about the time delay system is discussed.

2.1 Vertical dynamics

Vehicle dynamics is fundamentally the study of the physics of the car, in terms of their behaviour and response. The area of vehicle dynamics is broad and covers a variety of performance and stability aspects of a vehicle. Hence for convenience, they are usually split into three different subfields: longitudinal, lateral and vertical dynamics. And vertical dynamics is fundamentally the study of the vehicle motion in the vertical plane. Although longitudinal, lateral and vertical dynamics interchangeably affect each other, for convenience, they are studied and analysed individually. Most aspects of suspension, like springs, dampers and a part of kinematics comes under the vertical dynamics, among them the springs and dampers are the area of study in this current thesis work.

Importance of studying vertical dynamics

Most of the real world roads are stochastic and random. Even the straight roads in highway have some amount of variations in their height. The random variation road height/profile causes **discomfort** to the passenger, **loss of grip**, and at a severe scenario like bump or pothole, it could also lead to a breakdown and material fatigue. Hence the need for studying and analysis vertical dynamics of a vehicle is fundamental. Although several factors need to be taken into when studying and designing vertical dynamics, due to time limitation, the thesis work is limited specifically to comfort analysis focusing on pitch, heave and roll of the vehicle.

Main Objective

There are two primary objectives in the design and analysis of vertical dynamics of a vehicle. The first objective is to improve comfort. This is achieved by **minimizing the fluctuation of the vehicle body acceleration** in the presence of any road disturbance. This, in turn, reduces the discomfort to the passenger. The second objective is to improve road hold and grip. This is achieved by designing the suspension system such that the wheels perfectly track the road height and **minimize the tire load fluctuation**. This reduces road contact loss, thus improving road hold.

Challenges and current trend

Although it is very challenging to achieve this ideal state, there has been a significant improvement in the development of the suspension system, both from the mechanical and Software side. Both sides of these areas have their advantages and flaws. For example, the mechanical system is usually very robust but lacks flexibility and optimality. In general, it is hard to tune the mechanical part as it involves modifying parts like springs, dampers bushings etc. But on the other hand, Electronic and software systems are less robust but allows for more flexibility, leading to better performance. This results in the development of semi-active and active dampers, which are continuously controlled by advanced algorithms to minimize the fluctuations of the state parameters.

To analyse the vehicle for comfort and dynamics in general, a mathematical model is employed, which captures the response of the mass, spring and dampers system in the presence of disturbance. These models are usually called the mass-spring-damper system and are as shown in fig below.

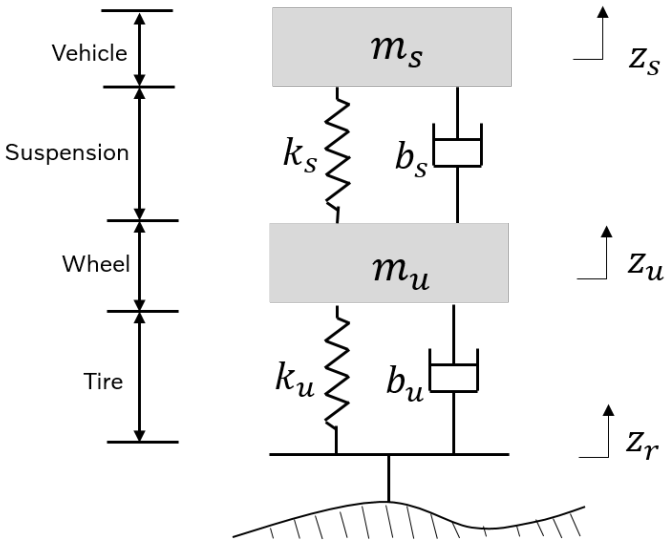

Figure 2.1: Mathematical model of a quarter car

As can be seen from the above figure, there are two different masses: sprung and unsprung mass. These two masses are separated by springs and dampers. Here, the

springs and damper between the sprung and unsprung masses represent the actual springs and dampers in the vehicle that controls the body motion. Whereas the one between the unsprung mass and the road represents the dynamics of the tires. The presence of these two masses results in two resonant frequency in the frequency domain. Therefore the comfort of the vehicle is in turn also divided into two: **primary and secondary ride comfort**. Here, primary comfort refers to body vibration, and it has the frequency at which the vehicle body is in resonance with the disturbance. This is called the body natural frequency. This is usually around the range of 1 - 2 Hz for a passenger car. Secondary comfort essentially deals with wheel hop frequency, and it is when the unsprung mass of the vehicle is in resonance with the disturbance. This value usually lies around 7 - 10 Hz.

Since this thesis work is primarily focused on mechatronic systems of the suspension, a brief introduction of the control system, damper models and architecture is given in this current chapter. Then more detailed vehicle models, delay and quantization models that are used for the analysis of these systems are discussed in detail in the upcoming chapters.

2.2 System architecture/ Mechatronics system

The architecture of the current wheel suspension control system is quite complex. The current overall architecture is as shown in the figure,

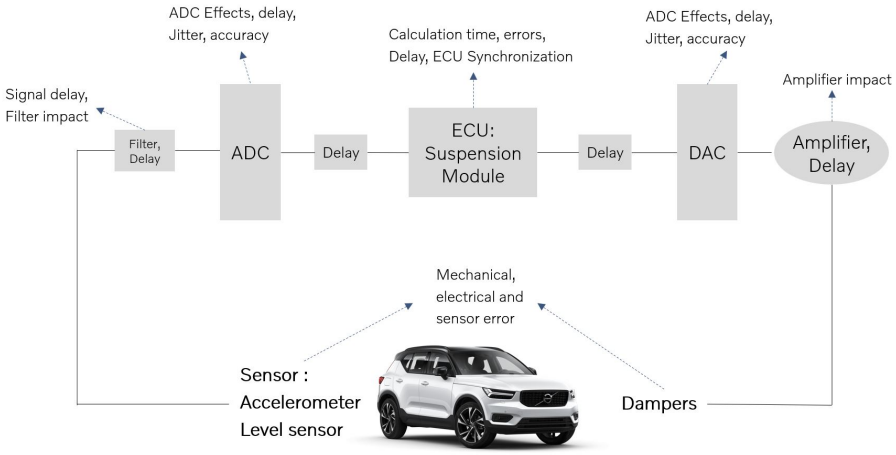

Figure 2.2: Architecture of the wheel suspension system

The above figure represents the vehicle plant model. The states of the system: body acceleration in heave, pitch and roll direction, and damper displacement are measured by accelerometer and level sensor. Before the signal reaches the central controller, they are first filtered. Then this filtering process induces delay. After the signals are filtered, it is then converted to digital by the ADC component. This conversion causes delays, but most importantly, it induces also signal errors and jitter due to the conversion. There is also an additional delay due to transportation. Then, finally, these sensed signals are used by the controller to compute the control

signals. Here, within the controller/ECU there is also the problem of latency in computation, Synchronization, error etc.

Once the control signals are calculated, these signals are then converted to the analogous, continuous signal through a DAC and are then amplified by an amplifier before reaching the damper model. This amplification and signal conversion, in turn, induces signal inaccuracies, error and delays. Finally, the damper generates the appropriate forces based on the control signals to control the body motion of the plant/ vehicle model.

2.3 Time delay

Delays are common in every engineering and non-engineering real-world application. All the system has some delay. The delay in perceiving/sensing, calculation and then applying the processed information. Even in the case of human being, it is considered as a time to be perceived, and then process the information, before applying the decision onto the environment. A most common example of the issue with time delay is shower example as shown,

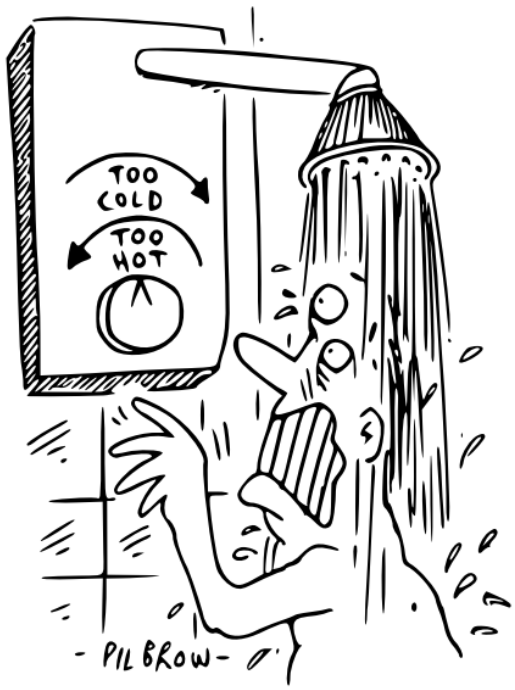

Figure 2.3: Shower example [4]

Suppose the person taking the shower wants the water to be medium hot, he/she must then turn the knob towards the "hot" direction side. As soon as the person turns the knob, there exists a delay between the time the person turns the knob to the time hot water is perceived/sensed by that person. This delay is due to the time it takes the heater to convert the water to hot water and the transportation from the

sink to the person. Due to this delay, the person tries to rotate the knob even further towards the hot direction as he/she is using the "old/outdated" information. Then as soon as the hot water reaches the person, he/she quickly realizes that the water is too hot. So he/she turns the knob towards the opposite direction to cool down the water. This goes back and forth until the water temperature finally reaches the requested equilibrium temperature.

So, in general, it can also be said that the effect of delays in the closed-loop control system resembles the same effect as of lowering the sampling frequency. This is because the controller is forced to use the "old" delayed information to compute the control signal for the current state of the system.

Solution to time delay

One way to prevent this situation is to simply **lower the control bandwidth/gain**. In case of our example, the person who is turning the knob should respond slower to the change in water temperature. This reduces the fluctuation/oscillation in the system and reaches the equilibrium, but slowly, thus performance loss. The other way would be to build a **compensator** around it, given the transportation delay value is known/predicted. As it sounds, its a bit tedious. The easier approach would be to just buy some really expensive shower system that instantly (or atleast close to) provides the request water temperature.

Overall, for the time-delay system, it can be concluded that any control system connected in networks with sensors and actuators induces delays and are inevitable due to limited bandwidth and overhead in the network. And the time delays in the control system loops induce/give rise to phase lag, and it also degenerates the system stability and performance of the system. These are the main issue with time-delay system. Thus it's important to consider delays when designing the control system.

Types of Delays

Deadtime delay is often confused with transport lag and vice versa. So it is important to distinguish between the two. The figure below shows the difference between **deadtime delay** and **lag**.

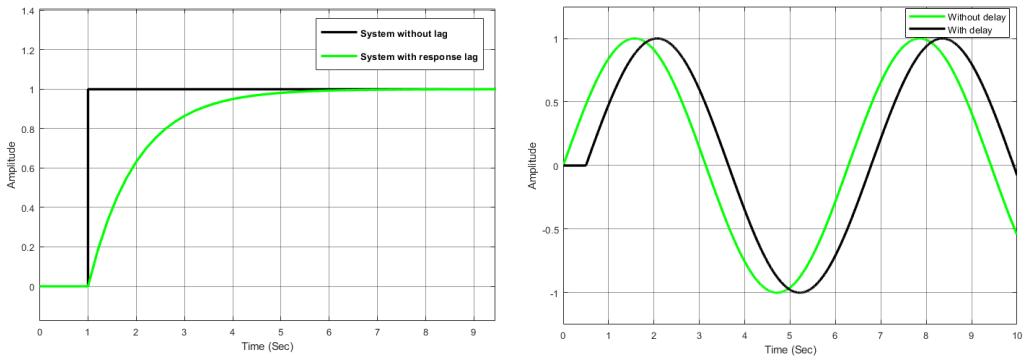

Figure 2.4: Difference of response lag(left) and dead time delay(right)

As it can be seen from the figure, the dead time delay is the delay in the initialization of the signal in itself whereas the response lag is the time delay that takes for the system to reach the target value.

2.3.1 Sensor delay

In this thesis work, the main focus of study is the transportation dead time delay from the sensor to the controllers for both level and accelerometer delay. So in this case, an analytical description of the system with delay is briefly discussed.

A typical closed-loop control system with a single sensor delay is as shown,

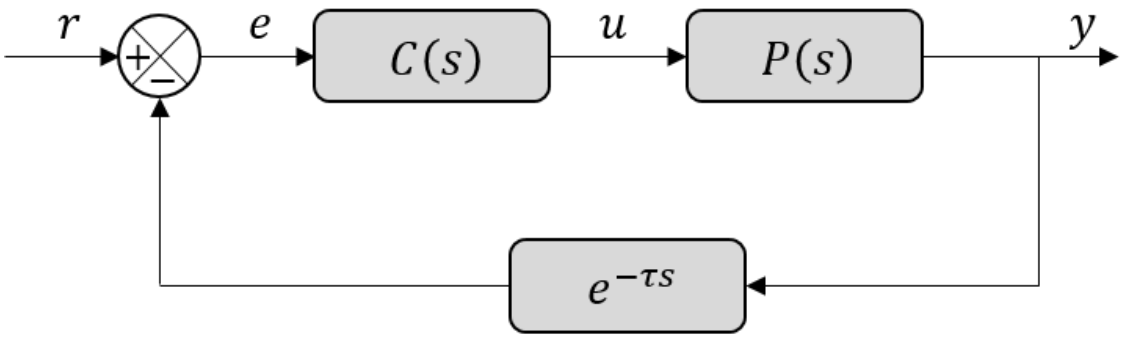

Figure 2.5: Closed loop system with sensor delay

From above figure, there is a controller $C(s)$ and plant $P(s)$. The 's' here represents that the system is in the Laplace domain. The output of the signal 'Y' is delayed by 'τ'. So the output delayed signal then becomes $Y(t-\tau)$. This, in turn, is represented in the Laplace domain, $e^{-s\tau}Y(s)$. And this delayed signal is fed back to the controllers through negative feedback. The transfers function of a system, in general, is defined as the output response of the system to the input control signal,

and it is given by $G(s) = Y(s)/R(s)$. The final form of the above system is given by,

$$G(s) = \frac{C(s)P(s)}{1 + C(s)P(s)e^{-s\tau}} \tag{2.1}$$

A simulation of this simple system with transfer function($\frac{2}{s+2}$) with step input results in the results as shown,

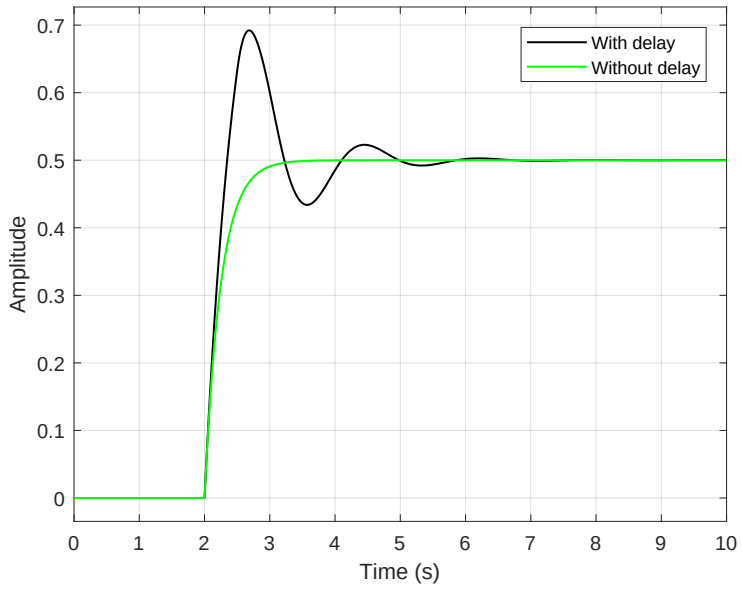

Figure 2.6: Effect of delays on the performance

Note: This is the case for any typical actuator that is fully active and depends only on the control signal.

2.3.2 Effect of delays on stability

To study the effects of delays on the stability of a system, first consider a simple SISO system with sensor delay. And we can use the system equation that was described before. In this, We can take the plant model $P(s)$ as a simple integrator $1/s$ and controller $C(s)$ as constant gain K. The transfer function of a simple system without delay is given by, $G = L(s)/(1 + L(s))$. Here L is $P(s) * C(s)$. After substituting the values, the system equation is given by,

$$G(s) = \frac{K}{(K + s)} \tag{2.2}$$

The dynamics of the equation is given by,

$$\dot{x}(t) = -Kx(t) + Kr(t) = K[r(t) - x(t)] \tag{2.3}$$

Here, $r(t) - x(t)$ is the error signal that is constantly being regulated by the control gain K. For a constant input, $\hat{r} = r(t)$, the solution is a constant exponential delay towards the equilibrium setpoint.

For simplicity, the setpoint is taken as $\hat{r} = 0$ and the solution to this equation is written as,

$$x(t) = x_0 e^{-Kt} \tag{2.4}$$

The final system transfer function of the equation including the delay is given as,

$$G(s) = \frac{K}{Ke^{-s\tau} + s} \tag{2.5}$$

Here $e^{-s\tau}$ represents the delay in the system. The differential equation of the system with delay is given by,

$$\dot{x} = k[r(t) - x(t - \tau)] \tag{2.6}$$

Again the reference is kept zero in this case, $\hat{r} = 0$. Then the equation becomes,

$$\dot{x} = -Kx(t - \tau) \tag{2.7}$$

This is the final delay differential equation. If the delay, tau, is large enough could result in instability in the system. Since the controller tries to control the system based on the old information, this, in turn, causes a very high system rate of change towards the equilibrium position.

In a closed-loop feedback system, the controller/regulator constantly regulates the system by multiplying the error between the setpoint and measured signal by the gain "k". And since the system state is delayed, there will be a deviation from the actual error value. This deviation from the true error signal causes the controller to destabilize the system.

2.4 Damper Model

The electronically controlled wheel suspension system, in general, is classified into active and semi-active system. Although there are semi-active and active springs, the work is limited to only the dampers.

These electronic dampers are controlled by the control signals which are generated by the controllers in the Suspension module. There are several different controllers to control the vertical dynamics of the suspension like optimal control strategies(LQR, MPC), skyhook, fuzzy, adaptive controllers etc. But first, the main differences and theories behind the semi and active suspension system are discussed.

2.4.1 Active suspension

In an active damper system, the damper model is **highly flexible**, meaning they can provide any force values in any operating condition, with some limitation. This allows a higher degree of controllability and thus makes it easier to achieve the targets on comfort and road hold with less tradeoff. Here, the passivity constraint is fully overcome by the active suspension system. But this vast controllability range takes a significant toll on power requirements and increases the complexity of the system. This, in turn, increases both cost and the need for redundancies in the system. The operating region of the fully active suspension is as shown in the figure.

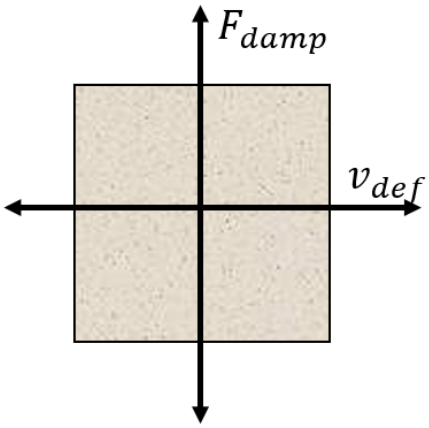

Figure 2.7: Operating region for active suspension

2.4.2 Semi-Active suspension

This system features an electronic shock absorber which varies the damping constant based on the request current signal from the controllers. The main difference between this and the active system is that the amount of force that can be delivered/produced by the damper is limited. Thus the name "semi-active suspension".

This delivered force follows the passivity constraint (based on velocity signal) of the damper, meaning only opposite forces to body motion may be introduced into the system. So it conveys that the semi-active suspension cannot add energy into the system and can only dissipate energy from the system. This makes the system stable compared to a fully active suspension system. Due to these features, the requested power is relatively low, around tens of Watts [5]. The operating region of the semi-active suspension is as shown in the figure.

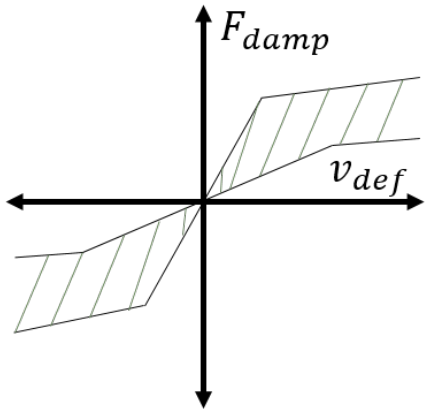

Figure 2.8: Operating region for Semi active suspension

2.5 Controllers/Compensators

In this section, a brief introduction about different controllers is discussed in brief. The detailed introduction of the controllers and compensators along with their architecture is discussed in the next chapter.

2.5.1 Linear Quadratic Control

Linear Quadratic Regulator guarantees closed-loop system stability and high performance of the system by enhancing the location of the closed-loop eigenvalues of the system. Linear Quadratic Regulator is a state feedback controller, in which it's controller gain accomplishes an objective function by optimizing the cost function. Consider a MIMO linear system [6],

$$\begin{aligned} \dot{x}(t) &= Ax(t) + Bu(t) \qquad x \in \mathbb{R}^n, u \in \mathbb{R}^p \\ y(t) &= Cx(t) + Du(t) \end{aligned} \tag{2.8}$$

Where A, B, C, D are Constant matrices. The assumption made is that only suspension deflection and body acceleration are the states considered for the measurement output and system states are available for controlling.
The optimal control law is given by [17]:

$$\begin{aligned} u(t) &= -\bar{K}x(t) \\ \bar{K} &= R^{-1}B^T\bar{P} \end{aligned} \tag{2.9}$$

Where K is the state feedback gain matrix and it is subjected to minimize J as cost function. A cost function describes a performance and behaviour of the system with equation and results out how well the control algorithm performs optimization problem. Minimization of cost function carried out by LQR is [6].

$$\begin{aligned} \min_{u(t)} J &= \min_{u(t)} \frac{1}{2} \int_0^\infty (x^T(t)Qx(t) + u^T(t)Ru(t))dt \\ &= \min_{u(t)} \frac{1}{2} ||Q^{\frac{1}{2}}x(t)||_2^2 + ||R^{\frac{1}{2}}u(t)||_2^2 \end{aligned} \tag{2.10}$$

Where $Q \geq 0$ is a symmetric and positive semi-definite matrix and $R > 0$ is symmetric positive-definite matrix. Matrix $\bar{P}$ in (2.10) is the solution to Algebraic Riccati equation, namely

$$A^T\bar{P} + \bar{P}A + \bar{P}BR^{-1}B^T\bar{P} = 0 \tag{2.11}$$

The simplicity to trade-off state errors against control effort through weighting of Q and R is one of the advantages of LQR. This results in a possibility to prioritize the states which are critical to minimize their deviations. And also some limitation in the actuator can be taken into account.
when selecting a weight factor matrices, the largest desired state response $x_{i,max}$ and the largest desired control input $u_{i,max}$ used to normalize the weight matrices. Parameters α_1,...,α_n and β_1,...,β_m are used to add relative weighting on the various states and inputs.

$$Q = \begin{bmatrix} \frac{\alpha_1^2}{x_{1,max}^2} & 0 & \dots & 0 \\ 0 & \frac{\alpha_2^2}{x_{2,max}^2} & \dots & 0 \\ \dots & \dots & \ddots & \dots \\ 0 & 0 & \dots & \frac{\alpha_n^2}{x_{1,max}^n} \end{bmatrix} \tag{2.12}$$

$$R = \begin{bmatrix} \frac{\beta_1^2}{u_{1,max}^2} & 0 & \dots & 0 \\ 0 & \frac{\beta_2^2}{u_{2,max}^2} & \dots & 0 \\ \dots & \dots & \ddots & \dots \\ 0 & 0 & \dots & \frac{\beta_n^2}{u_{1,max}^n} \end{bmatrix} \tag{2.13}$$

2.5.2 State derivative penalization in a cost function

The minimization of roll motion and vertical acceleration results in improved ride comfort therefore it should be kept low. Heave rate, roll rate and pitch rate are available as states so they can be penalized through the weighting matrices. However, accelerations $\ddot{z}$, $\ddot{\theta}$ and $\ddot{\phi}$ are not included in the states and but LQR can be extended to penalize state derivatives .
In order to control the state derivatives $\dot{x}(t)$, a new cost function can be specified as [7]:

$$J = \frac{1}{2} \int_0^\infty (\dot{x}^T(t)Q_1\dot{x(t)} + x^T(t)Q_2x(t) + u^T(t)Ru(t))dt \tag{2.14}$$

where Q_1, Q_2,R are weight matrices. With the state space described as,

$$\begin{aligned} \dot{x}(t) &= Ax(t) + Bu(t) \\ y(t) &= Cx(t) + Du(t) \end{aligned} \tag{2.15}$$

Substituting the state space into the cost function gives [7].

$$\begin{aligned} J &= \frac{1}{2}\int_0^\infty ((Ax(t)+Bu(t))^T(t)Q_1(Ax(t)+Bu(t)) + x^T(t)Q_2x(t) + u^T(t)Ru(t))dt \\ &= \frac{1}{2}\int_0^\infty ((x^T(t)A^T + u^T(t)B^T)(Q_1Ax(t)+Q_1Bu(t)) + x^T(t)Q_2x(t) + u^T(t)Ru(t))dt \\ &= \frac{1}{2}\int_0^\infty ((x^T\tilde{Q}x^T + x^T(t)\tilde{N}u(t)) + u^T(t)\tilde{N}x(t) + u^T(t)\tilde{R}u(t))dt \end{aligned} \tag{2.16}$$

where $\tilde{Q} = (A^TQ_1A + Q_2), \tilde{R} = (B^TQ_1B + R)$ and $\tilde{N} = A^TQ_1B$.

2.5.3 Discretization

The augmented state space is of the form,

$$\begin{aligned} \dot{\tilde{x}}(t) &= \tilde{A}x(t) + \tilde{B}u(t) \\ y(t) &= \tilde{C}x(t) + \tilde{D}u(t) \end{aligned} \tag{2.17}$$

is the non-linear model. The augmented model can be dicretized using zero-order hold method(ZOH). Equation (2.17) can be converted into following discrete-time form with sampling period T_s.

$$\begin{aligned} \tilde{x}(k+1) &= \Phi\tilde{x(k)} + \tilde{\Gamma}u(k) \\ y(t) &= \tilde{C}\tilde{x}(k) + \tilde{D}u(k) \end{aligned} \tag{2.18}$$

with $\tilde{x}(k) = \begin{bmatrix} x^T(k) & x_d^T(k) & x_e^T(k) \end{bmatrix}$. where,

$$\begin{aligned} \Phi &= e^{\tilde{A}T_s} = I + \tilde{A}\Psi \\ \Gamma &= \int_0^{T_s} e^{\tilde{A}s}ds\tilde{B} = \Psi\tilde{B} \end{aligned} \tag{2.19}$$

$$\Psi = \int_0^{T_s} e^{\tilde{A}s}ds = IT_s + \frac{\tilde{A}T_s^2}{2!} + \frac{\tilde{A}^2T_s^3}{3!} + ... + \frac{\tilde{A}^iT_s^{i+1}}{(i+1)!} + ... \tag{2.20}$$

Substituting the above parameters results in a discretized augmented system which is also a non-linear model and can be represented in the following general form:

$$\begin{aligned} \tilde{x}(k+1) &= f(\tilde{x(k)}, u(k)) + w \\ y(k) &= h(\tilde{x}(k), u(k)) + v \end{aligned} \tag{2.21}$$

where $f(\cdot)$ and $h(\cdot)$ are the functions of non-linear systems. w and v represents the process noise and measurement noise of the system respectively with the known covariance matrix $W = E(ww^T)$ and $V = E(vv^T)$ and also both are assumed to be white Gaussian process and uncorrelated.

2.5.4 LQG Design

Optimal stochastic control

Consider the controlled process with process noise which is assumed to be,

$$\dot{x}(t) = Ax(t) + Bu(t) + v(t) \tag{2.22}$$

The objective of LQG control problem is to find the optimal control law which minimizes the following cost function:

$$J = \sum_{k=0}^{\infty} [\bar{x}^T(k) Q \bar{x}(k) + u^T(K) R u(k)] \tag{2.23}$$

where Q is a non-negative definite state weight matrix and R is the positive definite control matrix.
The optimal state feedback control law is given by:

$$u(k) = -K_d \bar{x}(k),\ K_d = [\bar{\Gamma}^T P_r \bar{\Gamma} + R]^{-1} \bar{\Gamma}^T P_r \Phi \tag{2.24}$$

The structure of the kalman filter can be represented as follows,

$$\hat{\bar{x}}(k+1) = \bar{\Phi}\hat{\bar{x}}(k) + \bar{\Gamma}u(k) + L(y(k) - \bar{C}\hat{\bar{x}}(k)) \tag{2.25}$$

where $L = \bar{\Phi} P_f \bar{C}^T + [\bar{C} P_f \bar{C}^T + V]^{-1}$ is the kalman filter gain that minimizes estimation error variance $E\{[\bar{x} - \hat{\bar{x}}]^T [\bar{x} - \hat{\bar{x}}]\}$.$P_r$ and P_f is the unique non-negative definite solution of Discrete Algebraic Ricatti Equation(DARE).

$$\begin{aligned} P_r &= \bar{\Phi}^T P_r \bar{\Phi} - (\bar{\Gamma}^T P_r \bar{\Phi})^{-1} [\bar{\Gamma}^T P_r \bar{\Gamma} + R]^{-1} (\bar{\Gamma}^T P_r \bar{\Phi}) + Q \\ P_f &= \bar{\Phi} P_f \bar{\Phi}^T - (\bar{\Phi} P_f \bar{C})^T [\bar{C}^T P_f \bar{C}^T + V]^{-1} (\bar{C}^T P_f \bar{\Phi})^T + W \end{aligned} \tag{2.26}$$

Then the optimal control law is given by,

$$u(k) = -k_d \hat{\bar{x}}(k) \tag{2.27}$$

where k_d is the Kalman gain.

2.5.5 Smith Predictor Compensation Scheme

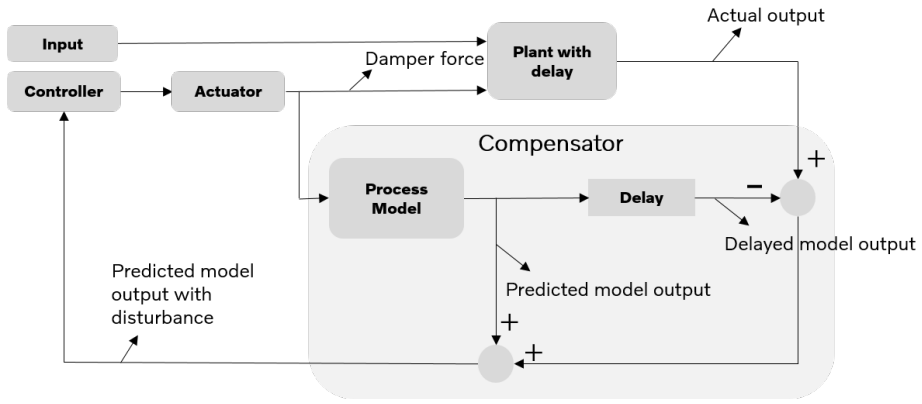

Figure 2.9: The structure of smith predictor

The Smith predictor is a control strategy which is a form of predictive control to mitigate the challenges of dead time in a control system. It is found to be the easiest and most implemented dead time compensation scheme employed to stabilize the control system. The principle of smith predictor is that the desired output from a controlled system with delay k is the same as that output from the desired delay-free system, only delayed by the delay of k. Let the delay be k, the delay-free series controller be $G_c(z)$, the desired delay controller be $\hat{G}_c(z)$ and the plant be $G_p(z)$. The transfer function of delay-free system can be written as [3],

$$CL(z) = \frac{G_c(z)G_p(z)}{1 + G_c(z)G_p(z)} \tag{2.28}$$

2.5.5.1 Smith predictor control

If a controller $\hat{G}_c$ is designed for the plant with network delays $G_p(z^{-k})$ the closed loop transfer function $CL(z)$ become $CL(z^{-k})$. The transfer function of delayed system with its desired controller can be written as,

$$\hat{CL}(z^{-k}) = \frac{\hat{G}_c G_p(z) z^{-k}}{1 + \hat{G}_c G_p(z) z^{-k}} \tag{2.29}$$

This control function has a time delay included in its denominator which means that its transition behaviour will depend on the time delay. According to smith's principle, $CL(z) = \hat{CL}(z^{-k})$, the equation (2.29) can be written as,

$$\frac{\hat{G}_c G_p(z) z^{-k}}{1 + \hat{G}_c G_p(z) z^{-k}} = z^{-k} \frac{G_c G_p}{1 + G_c G_p} \tag{2.30}$$

$$\hat{G}_c = \frac{G_c}{1 + G_c G_p (1 - z^{-k})} \tag{2.31}$$

equation (2.31) shows that required $CL(z)$ will be obtained if the designed closed-loop controller incorporates the transfer function of the controller designed for the system without time delay, the process model and with time delay. From the above figure 2.9, the outer feedback loop feeds the outdated information back to the input due to network time delays. As a result, there exist a degradation of system performance. So, for k seconds no new information is available, the system is controlled by an inner loop which contains a predictor of what is the output of the plant $G_p(z)$ currently is. the outcome is that outer and middle loop cancels while the system makes use of the inner loop to give a satisfactory performance. The performance loss is due to the model mismatches between the process model and the original model. This mismatches or difference between those model results as a disturbance to the original model in the feedback loop.

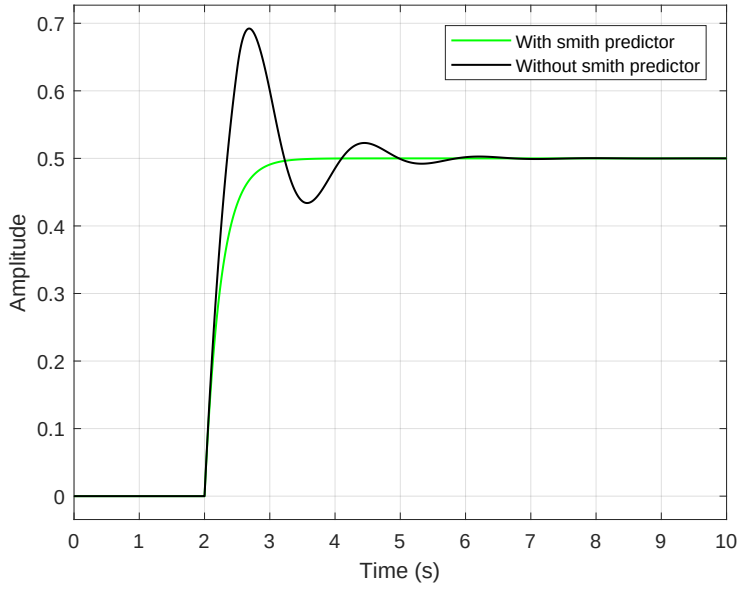

Figure 2.10: Response of smith predictor compared to delay with first order system

In figure 2.10, the first-order system with transfer function $(\frac{2}{s+2})$ was simulated for two cases, first-order system with delay 50 ms and first-order system with smith predictor with 50 ms in both plant and process model. As can be seen from the above figure, smith predictor compensates the effect of delays perfectly with knowledge of current delay value 50 ms. One of the reason for this response is that both plant and process model has the same transfer function and delayed by the same value, therefore there is no mismatch between plant and process model.

2.6 Statistical Terminology

To analyze the performance and trends of the suspension system, some statistical results were extrapolated from the simulation results. The results of the analysis are shown and discussed in brief in Chapter 7. In this chapter, some terminology and definition used in the analysis and their implication are discussed.

Histogram Peak or Height of the Zero Bin

The histogram peak or the zero bin height represents the peak value of the data in the histogram plot at its mean value. The zero bin height in the histogram plot is as shown,

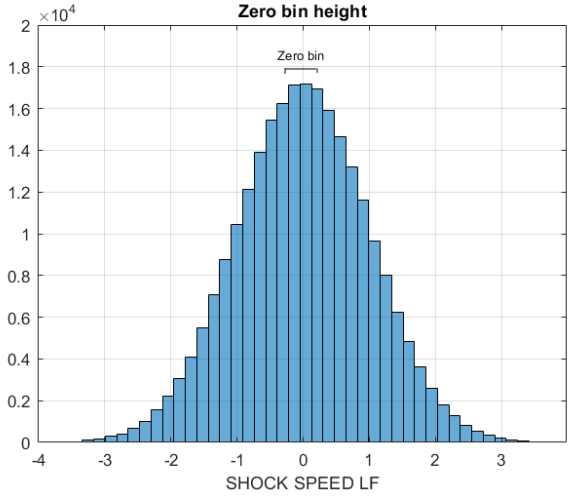

Figure 2.11: Zero bin height

The zero bin height, in general, tells about the relative suspension stiffness between the four corners of the vehicle. A stiff suspension would typically have a high zero bin height. To get the best performance, ideally, the zero bin height of all four corners should be the same as possible.

Median

Median returns the mid-value in the given dataset array. It is an objective measure of the symmetry in the damper histogram plots between bump and rebound. In the case of ideal shock absorber histogram, the median would be zero. If the median is zero, then it represents perfect symmetry in the histogram data. In case if the median value is greater than zero, then it signifies that the shock absorber is more oriented towards the bump/compression zone. The opposite is true i.e dampers are operated more towards the rebound zone if the median is less than zero.

Standard Deviation

This measures the deviation in the given dataset from the average value. Mathematically, the standard deviation is the square root of the average distance of each data points from their mean average value of the data. In discrete terms, the standard deviation is mathematically represented as,

$$\sigma = \sqrt{\frac{1}{N}\sum_{i=1}^{N}(x_i - \mu)^2} \tag{2.32}$$

Here, N = Total number of samples.
μ = Average values of the given data.

The standard deviation from the histogram conveys how much the data points have deviated from the average shock speed. A large standard deviation value indicates that the dampers are operated more in the high-speed regions, either in bump or rebound.

Skewness

Skewness measures the direction and magnitude of the asymmetry in the damper histogram plot. If the numerical value of the skewness is negative, then the damper speeds are oriented more towards the high speed rebound operating zones. And if the skewness is positive, then the damper speeds are oriented more towards the high-speed bump operating region. The two skewness case can be visually shown as below,

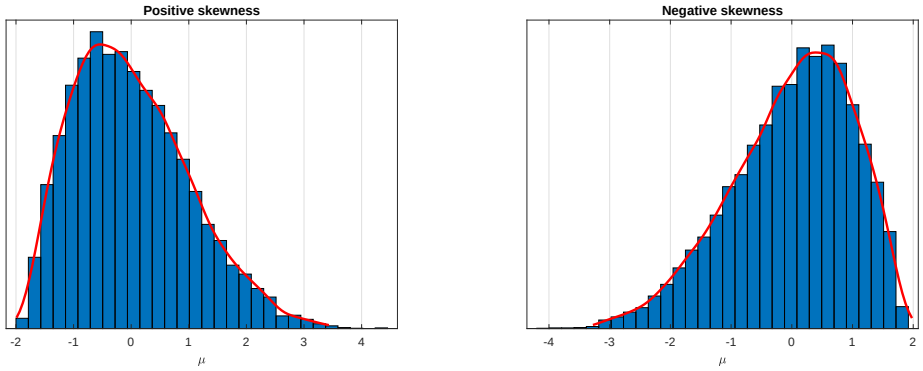

Figure 2.12: Skewness

Skewness is mathematically represented as follows [8],

$$A = \frac{N}{(N-1).(N-2)} . \sum_{i=1}^{N} \left(\frac{x_i - \mu}{\sigma} \right)^3 \tag{2.33}$$

Kurtosis

Kurtosis represents the magnitude of the peakedness of the histogram data. Kurtosis can be visualized in the histogram plots as follows,

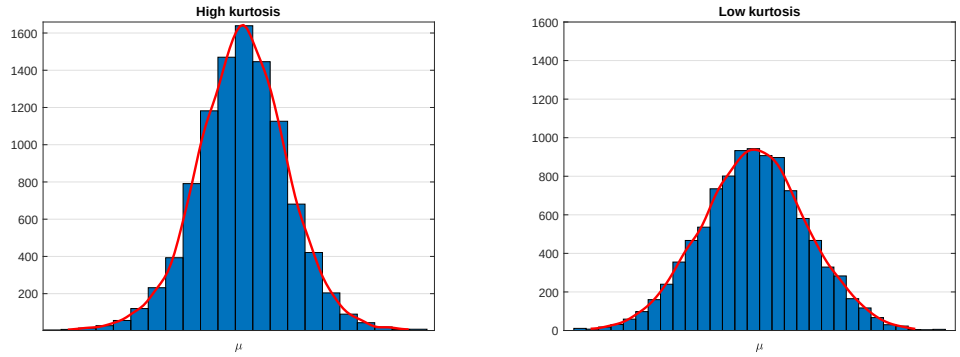

Figure 2.13: Kurtosis

A higher kurtosis signifies that the damper is operated more towards the low-speed friction region and less in the high-speed regions. Whereas the opposite is true for the lower kurtosis i.e the damper is operated more towards the high-speed friction region and less in the low-speed regions.

Kurtosis can be mathematically represented as [8],

$$K = \left[\frac{N.(N+1)}{(N-1).(N-2).(N-3)}.\sum_{i=1}^{N}\left(\frac{x_i-\mu}{\sigma}\right)^4\right] - \frac{3.(N-1)^2}{(N-2).(N-3)} \tag{2.34}$$

3

Vehicle model

To design and analyse the vertical dynamics of a vehicle, mathematical models have been developed from the first principle. Based on model complexity, there are different models. But in this thesis work, the three different mathematical vehicle models that were implemented are discussed in detail along with advantages and disadvantages.

In this chapter, first, a quarter car is discussed. The quarter car is the simplest mathematical vehicle model to represent the vertical behaviour of the vehicle, specifically targeting the heave motion. Then this model was extended to a full car vehicle model to capture the physics of roll, pitch and heave motion. Finally, a more detailed, high fidelity multibody dynamics model in IPG carmaker environment is discussed briefly. For the quarter car and full car model, the mathematical equation, model parameter and their respective state-space equation are given. And for the IPG carmaker model, a complete picture of the interconnection between each of the subsystems is shown.

3.1 Quarter car model

Quarter car model represents the physics/behaviour between the car body, wheel and road. Most often, quarter car models are 2 DOF as they have two mass bodies: sprung mass and unsprung mass. But they can have more degree of freedom, depending on the need and type of analysis. Here, the sprung mass comprises of the components above the springs like vehicle body, passenger etc and are lumped together. Whereas, components like brakes, wheels, parts of suspension kinematics etc are lumped together in the unsprung mass . A graphical representation of the model is shown in fig.

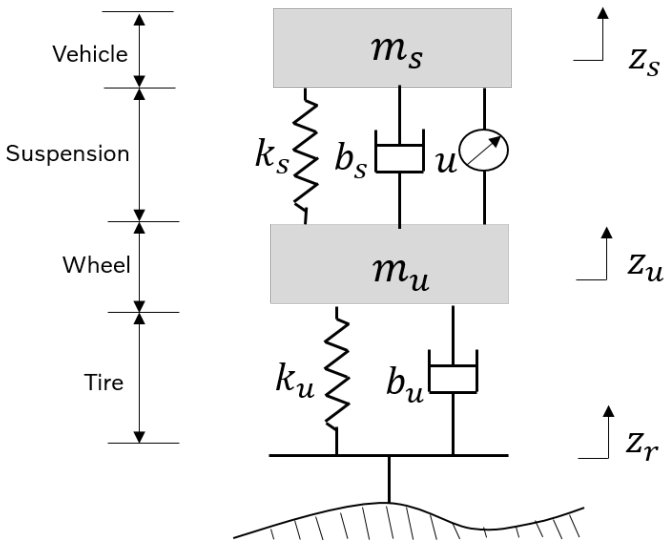

Figure 3.1: Quarter car model of active suspension

As it can be seen from the above figure , the sprung and unsprung masses are connected through spring and damper. Although in reality, these dampers and springs are nonlinear, for the sake of simplicity, they are linearized around an operating point. The unsprung mass is grounded to the road through another spring and damper. These spring and dampers represent the stiffness and damping of the tire model. The parameters used in the model are given in the following table,

Table 3.1: Parameters of the quarter car model

Symbol	Quantity	Unit
m_s	Sprung mass	kg
m_u	Unsprung mass	kg
k_s	Spring stiffness, Suspension	N/m
k_u	Spring stiffness, tire	N/m
c_s	Damping Coefficient, Suspension	Ns/m
c_t	Damping Coefficient, tire	Ns/m
z_s	Vertical displacement of sprung mass, heave	m
z_u	Vertical displacement of unsprung mass	m
z_u	Road height	m
u	Actuator force	KN

The equation of motion of the quarter car model around the equilibrium point is given by,

$$\begin{cases} m_s\ddot{z}_s = -k_s(z_s - z_u) - c_s(\dot{z}_s - \dot{z}_u) + u \\ m_u\ddot{z}_t = k_s(z_s - z_u) + c_s(\dot{z}_s - \dot{z}_u) - k_u(z_u - z_r) - c_t(\dot{z}_u - \dot{z}_r) - u \end{cases} \tag{3.1}$$

The state space representation of these equation of motion is given by,

$$\begin{aligned}\dot{x}(t) &= \begin{bmatrix} 0 & 1 & 0 & 0 \\ \frac{-k_s}{m_s} & \frac{-c_s}{m_s} & \frac{k_s}{m_s} & \frac{c_s}{m_s} \\ 0 & 0 & 0 & 1 \\ \frac{k_s}{m_u} & \frac{c_s}{m_u} & \frac{-(k_u+k_s)}{m_u} & \frac{-c_s}{m_u} \end{bmatrix} x(t) + \begin{bmatrix} 0 & 0 \\ \frac{-1}{m_s} & 0 \\ 0 & 0 \\ \frac{1}{m_u} & \frac{k_s}{m_u} \end{bmatrix} u(t) \\ y(t) &= \begin{bmatrix} \frac{-k_s}{m_s} & \frac{-c_s}{m_s} & \frac{k_s}{m_s} & \frac{c_s}{m_s} \\ 1 & 0 & -1 & 0 \end{bmatrix} x(t) + \begin{bmatrix} 0 & 0 \\ \frac{-1}{m_s} & 0 \end{bmatrix} u(t) \end{aligned} \tag{3.2}$$

Here the states of the system $x(t)$ are body deflection, body velocity, wheel deflection and wheel velocity. The input $u(t)$ to the system is the road input disturbance and actuator force. The output measurement $y(t)$ from the model is body acceleration and suspension deflection.

The advantage of the quarter car model is its simplicity and less computation time. This makes it a suitable model for concept simulation. Whereas the disadvantage of this type of model is that it won't be able to capture the transient behaviour and other body motions like Roll and pitch.

3.1.1 Pade appoximation

In general, delays are expressed as $e^{\tau t}$. This expression makes it difficult to analyse a control system with delays as this is an infinite-dimensional form. So to solve this problem using traditional control theory tools, this infinite dimension representation is approximated to a finite-dimensional one. And it can be done by approximating the exponential representing the time delay element with the ratio of two polynomials [28],

$$e^{\tau t} = \frac{Q_n(-s)}{Q_n(s)} \tag{3.3}$$

There are two possible definition for Q_n and they are given by,

$$Q_n(s) = \sum_{i=0}^{n} \frac{h^i(2n-i)!n!}{(2n)!(n-i)!i!} s^i. \tag{3.4}$$

$$Q_n(s) = \sum_{i=0}^{n} \frac{h^i}{2^i i!} s^i. \tag{3.5}$$

An example of the second order pade approximation of delay with 10ms is given by,

$$e^{-0.01s} = \frac{s^2 - 600s + 120000}{s^2 + 600s + 120000} \tag{3.6}$$

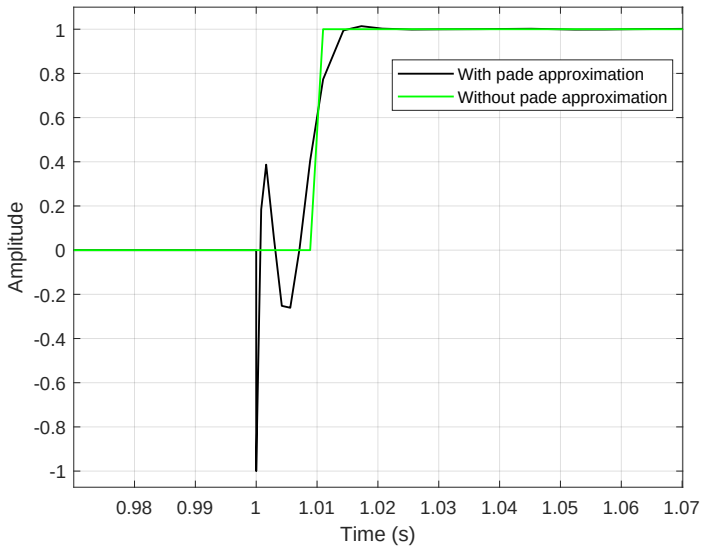

Figure 3.2: Pade approximation

3.2 Full-Car model

A full car model is an extension of the quarter car to the other three corners, and they are coupled together. This extends the 2 DOF model to a 7 DOF, with the degree of freedom motion being Roll, pitch, heave and displacement of the four suspension system. This extension makes it possible to simulate the behaviour of pitch and roll along with heave motion. The disadvantage of this type of model is the increased complexity and computation time. On the other hand, it can capture the behaviour of the vehicle more accurately. The graphical representation of the full car model is as shown,

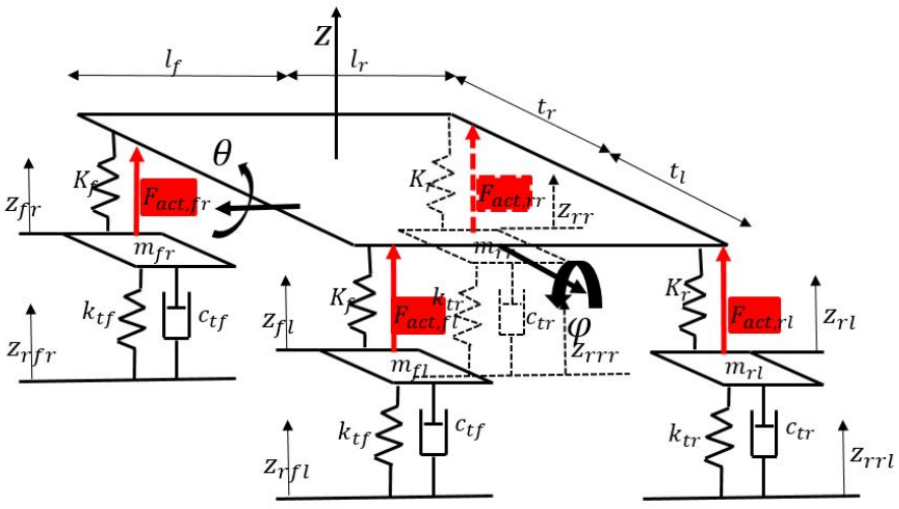

Figure 3.3: Full-Car model [12]

The parameters used in the model are given in the following table,

Table 3.2: Description of Parameters of full car model in Active suspension system

Symbol	Quantity	Unit
z	Body Vertical Displacement	m
θ	Body roll angle	rad
ϕ	Body pitch angle	rad
z_{fl}	Front left wheel vertical displacement	m
z_{fr}	Front right wheel vertical displacement	m
z_{rl}	Rear left wheel vertical displacement	m
z_{rr}	Rear right wheel vertical displacement	m
z_{rfl}	Road height at front left wheel	m
z_{rfr}	Road height at front right wheel	m
z_{rrl}	Road height at rear left wheel	m
z_{rrr}	Road height at rear right wheel	m
M	Sprung mass	kg
m_{fl}, m_{fr}	Front left and right unsprung masses	kg
m_{rl}, m_{rr}	Rear left and right unsprung masses	kg
k_f, k_r	Front and Rear suspension spring stiffness	N/m
k_{tf}, k_{tr}	Front and Rear tire stiffness	N/m
I_x, I_y	Longitudinal and lateral mass moment of inertia	Kgm^2
l_f, l_r	Front and rear coil spring longitudinal distance	m
t_l, t_r	Left and right coil spring lateral distance	m
$F_{act,fl}$	Front left sprung mass force	N
$F_{act,fr}$	Front right sprung mass force	N
$F_{act,rl}$	rear left sprung mass force	N
$F_{act,rr}$	rear right sprung mass force	N
F_{tfl}	Front left unsprung mass force	N
F_{tfr}	Front right unsprung mass force	N
F_{trl}	rear left unsprung mass force	N
F_{trr}	rear right unsprung mass force	N

The velocities and vertical displacement of the full car model is given as [9],

$$z_{fl}(t) = z(t) - l_f \sin(\phi(t)) + t_l \sin(\theta(t)) \tag{3.7}$$

$$z_{fr}(t) = z(t) - l_f \sin(\phi(t)) - t_r \sin(\theta(t)) \tag{3.8}$$

$$z_{rl}(t) = z(t) + l_r \sin(\phi(t)) + t_l \sin(\theta(t)) \tag{3.9}$$

$$z_{rr}(t) = z(t) + l_r \sin(\phi(t)) - t_r \sin(\theta(t)) \tag{3.10}$$

$$\dot{z_{fl}}(t) = \dot{z(t)} - l_f \cos(\dot{\phi}(t)) + t_l \cos(\dot{\theta}(t)) \tag{3.11}$$

$$\dot{z_{fr}}(t) = \dot{z(t)} - l_f \cos(\dot{\phi}(t)) - t_r \cos(\dot{\theta}(t)) \tag{3.12}$$

$$\dot{z_{rl}}(t) = \dot{z(t)} + l_r \cos(\dot{\phi}(t)) + t_l \cos(\dot{\theta}(t)) \tag{3.13}$$

$$\dot{z_{rr}}(t) = \dot{z(t)} + l_r \cos(\dot{\phi}(t)) - t_r \cos(\dot{\theta}(t)) \tag{3.14}$$

By using small angle assumption $\sin(\phi) \approx \phi$ and $\cos\phi \approx 1$, the full car model can be linearized to the following differential equations:

$$z_{fl}(t) = z(t) - l_f\phi(t) + t_l\theta(t) \tag{3.15}$$
$$z_{fr}(t) = z(t) - l_f\phi(t) - t_r\theta(t) \tag{3.16}$$
$$z_{rl}(t) = z(t) + l_r\phi(t) + t_l\theta(t) \tag{3.17}$$
$$z_{rr}(t) = z(t) + l_r\phi(t) - t_r\theta(t) \tag{3.18}$$
$$\dot{z}_{fl}(t) = z(t) - l_f\dot{\phi}(t) + t_l\dot{\theta}(t) \tag{3.19}$$
$$\dot{z}_{fr}(t) = z(t) - l_f\dot{\phi}(t) - t_r\dot{\theta}(t) \tag{3.20}$$
$$\dot{z}_{rl}(t) = z(t) + l_r\dot{\phi}(t) + t_l\dot{\theta}(t) \tag{3.21}$$
$$\dot{z}_{rr}(t) = z(t) + l_r\dot{\phi}(t) - t_r\dot{\theta}(t) \tag{3.22}$$

According to Newton's law, the following equations of motion is derived as follows:

$$M\ddot{z}(t) = -F_{fl}(t) - F_{fr}(t) - F_{rl}(t) - F_{rr}(t) \tag{3.23}$$

$$I_x\ddot{\theta}(t) = (F_{rr}(t) + F_{fr}(t))t_r - (F_{rl}(t) + F_{fl}(t))t_l + M_R \tag{3.24}$$

$$I_y\ddot{\phi}(t) = (F_{fl}(t) + F_{fr}(t))l_f(F_{rl}(t) + F_{rr}(t))l_r \tag{3.25}$$

$$m_{fl}\ddot{z}_{fl}(t) = F_{fl}(t) - F_{tfl}(t) \tag{3.26}$$
$$m_{fr}\ddot{z}_{fr}(t) = F_{fr}(t) - F_{tfr}(t) \tag{3.27}$$
$$m_{rl}\ddot{z}_{rl}(t) = F_{rl}(t) - F_{trl}(t) \tag{3.28}$$
$$m_{rr}\ddot{z}_{rr}(t) = F_{rr}(t) - F_{trr}(t) \tag{3.29}$$

The forces on the sprung mass can be represented as:

$$F_{fl}(t) = k_f(z_{fl}(t) - z_{tfl}(t)) - F_{act,fl}(t) \tag{3.30}$$
$$F_{fr}(t) = k_f(z_{fr}(t) - z_{tfr}(t)) - F_{act,fr}(t) \tag{3.31}$$
$$F_{rl}(t) = k_r(z_{rl}(t) - z_{trl}(t)) - F_{act,rl}(t) \tag{3.32}$$
$$F_{rr}(t) = k_r(z_{rr}(t) - z_{trr}(t)) - F_{act,rr}(t) \tag{3.33}$$

Similarly the forces on the unsprung masses can be represented as:

$$F_{tfl}(t) = k_{tf}(z_{tfl}(t) - z_{rfl}(t)) \tag{3.34}$$
$$F_{tfr}(t) = k_{tf}(z_{tfr}(t) - z_{rfr}(t)) \tag{3.35}$$
$$F_{trl}(t) = k_{tr}(z_{trl}(t) - z_{rrl}(t)) \tag{3.36}$$
$$F_{trr}(t) = k_{tr}(z_{trr}(t) - z_{rrr}(t)) \tag{3.37}$$

3.2.1 Actuator Model

The full car model consists of four individual active dampers in each side. These damper models are built with the assumptions that they are linear with no limitations on the bandwidth. Consequently, the actuators can provide the exact control force requested by the controller. Mathematically, the force generated by the active dampers is equal to the controller forces and represented as follows,

$$\begin{cases} F_{ctrl,fl}(t) = F_{act,fl}(t) \\ F_{ctrl,fr}(t) = F_{act,fr}(t) \\ F_{ctrl,rl}(t) = F_{act,rl}(t) \\ F_{ctrl,rr}(t) = F_{act,rr}(t) \end{cases} \tag{3.38}$$

3.2.2 State space model:

The state space representation of the mathematical model derived is written as,

$$\begin{aligned} \dot{x}(t) &= Ax(t) + Bu(t) + B_{\omega}\omega(t) \\ y(t) &= Cx(t) + Du(t) \end{aligned} \tag{3.39}$$

Here, u(t) is the input vector signal from the controller and $\omega(t)$ is the input vector signal from the road disturbance for all four corners.

The states of the system and input to the state-space model are given as follows,

$$x(t) = \left[z, \dot{z}, \phi, \dot{\phi}, \theta, \dot{\theta}, z_{fl}, \dot{z_{fl}}, z_{fr}, \dot{z_{fr}}, z_{rl}, \dot{z_{rl}}, z_{rr}, \dot{z_{rr}}\right]^T \tag{3.40}$$

$$u(t) = \left[u_1, u_2, u_3, u_4\right]^T = \left[F_{act,fl}, F_{act,fr}, F_{act,rl}, F_{act,rr}\right]^T \tag{3.41}$$

3.3 IPG Carmaker model

IPG carmaker is a virtual simulation environment that enables the simulation of complex vehicle behaviour in different scenarios. Similar to the mathematical models that is discussed before, the Carmaker also has the models based on a mathematical equation. But in previous cases, the models that were developed in Matlab were linearized at a particular operating point. Whereas the vehicle model in Carmaker is fully non-linear with multibody dynamics equations. Thus the IPG carmaker model can simulate the vehicle behaviour with a high degree of accuracy that can capture the non-linear, transient behaviour. This makes the model very much suitable for detailed nonlinear analysis. But the disadvantage of these higher fidelity model is the increased computation time.

The overall force interaction between different subsystem and environment of the carmaker model is as shown,

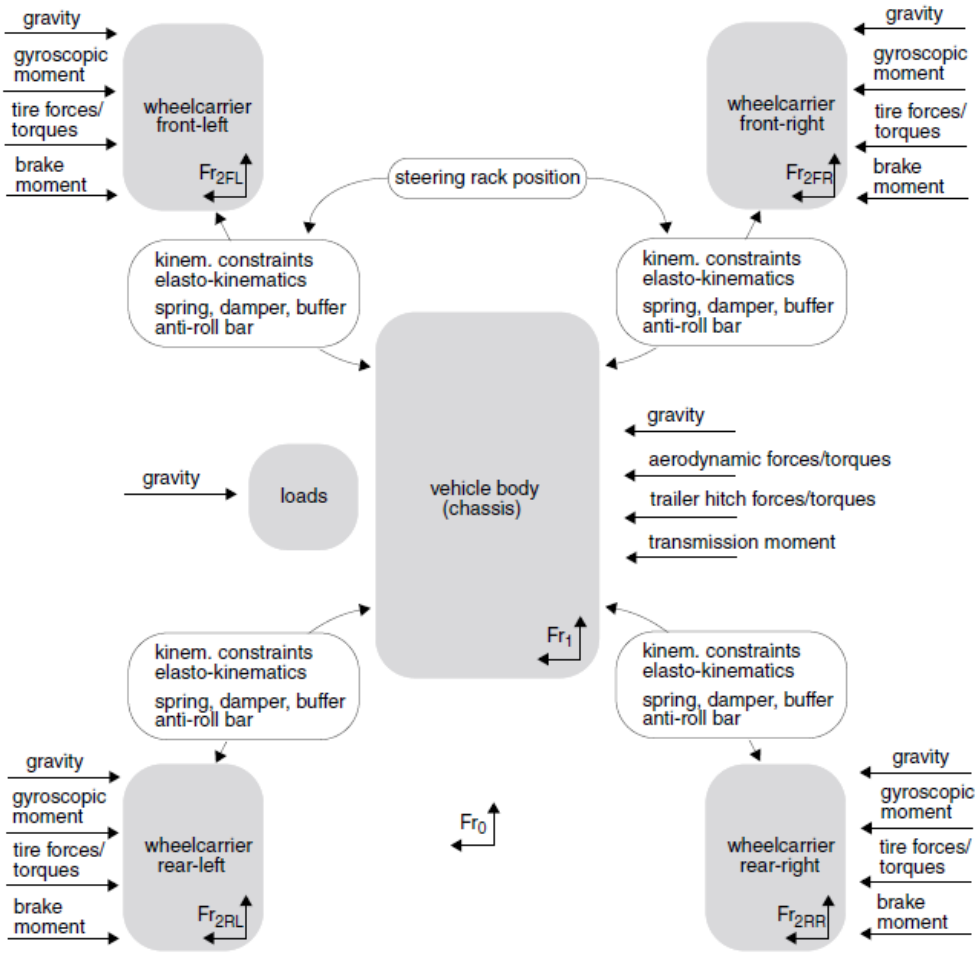

Figure 3.4: Force interaction in Carmaker model [10]

In this thesis work, this vehicle model from Carmaker was used in conjunction with the controller from the Simulink environment for the analysis purpose.

4

State of art controllers

Currently, there are several controllers to control the suspension system. In this thesis work, the three different controllers were analysed: Semi-active suspension with a simplified Skyhook controller, Active suspension with LQR controllers and semi-active suspension with a road preview functionality.

4.1 Semi-active system with skyhook controller

One of the most commonly used control algorithms for controlling the vertical dynamics of suspension is the skyhook controller. The skyhook controller is used widely to control and mitigate the main body motion: heave, pitch and roll. The fundamental logic of the skyhook control is quite simple.

Recall from chapter 2, the main objective in the design vertical dynamics essentially boils down to reducing the amplitude variation in both sprung and unsprung masses. So in the skyhook control, the controller generates forces in the opposite direction of the sprung mass motion to mitigate the amplitude variation in the body. So basically if the body moves up, the damper pulls it down and vice versa. But what separates this from the passive suspension is that the force at which it can pull the sprung mass can be actively varied. This is the fundamental principle of skyhook control. Now the skyhook that was evaluated in this thesis work is discussed.

Traditional skyhook controller controls only the heave motion through simple logic. The most common and simple one is on-off skyhook controller approach. But today this skyhook approach has been significantly improved with complex and very advanced functionality. One of the functionality includes their capability to control heave, pitch and roll motion of the vehicle simultaneously. Here, the simplified skyhook controller that was used in this thesis work is discussed [11]. The main overall structure in the simulation environment is as shown,

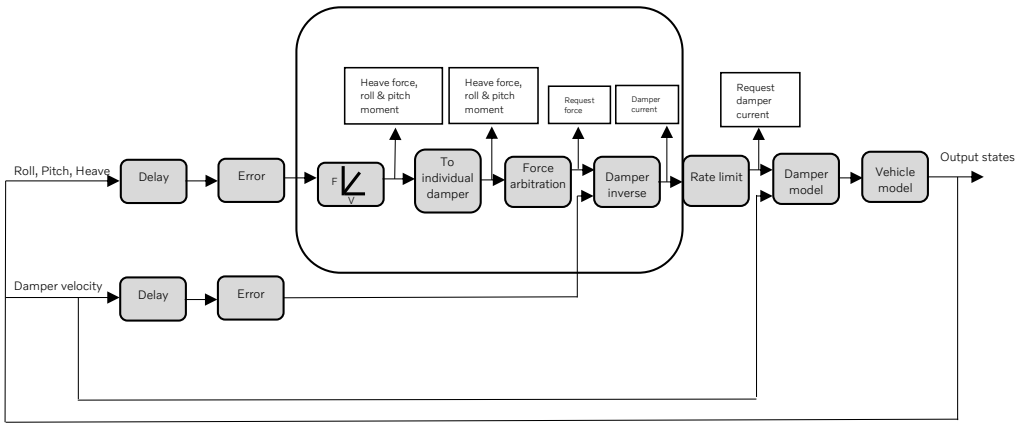

Figure 4.1: Sky-hook control strategy

From the figure 4.1, it can be seen that, first, the states of the vehicle model: heave, pitch and roll velocity, that is measured by sensor are provided as input to the Skyhook controller along with the damper velocity. The skyhook controller generates the target request current and sends it as input to the damper model. This damper model then generates the damper force to control the vehicle motion.

Within the controllers, first, there is a force/moment vs velocity lookup table. Based on the velocity signal, the output force signal is generated for the heave, and the moment is generated for the roll and pitch motion. The three signal represents the control force required to control the vehicle. To control the individual damper, the force and moments are split between the front and rear, to each wheel. In the end, at each corner, there will be three input request force signal for heave, pitch and for the roll. Then a force arbitration sequence is applied to these three signal to select one of those request force signal. This request forces, along with the damper velocity, is used by the damper inverse model. This damper inverse model then generates the target request current. This request current is further limited by its rate of change by a lower and upper limit before being sent as an input signal to the damper model.

4.2 Active suspension with LQR controller

As discussed previously, in the active suspension, the passive dampers are replaced by an electrohydraulic actuator. These actuators have the potential to add and dissipate energy from the system. In this thesis work, an LQR controller was used to control these actuator models to mitigate the discomfort [12].

The main objective of the LQR controller is to regulate the control signals to bring all the state variable to a setpoint value. In our case the setpoint here is Zero. The states that are regulated by these controllers are primarily the data from the accelerometer sensor like roll, pitch and heave acceleration and the data from the level sensor like shock displacement and velocity. The output from the controller is

the request force that is sent to the actuator model. This actuator then generates the target force to control the vehicle body motion. A simplified version of the complete working scheme of the simulation architecture is as shown,

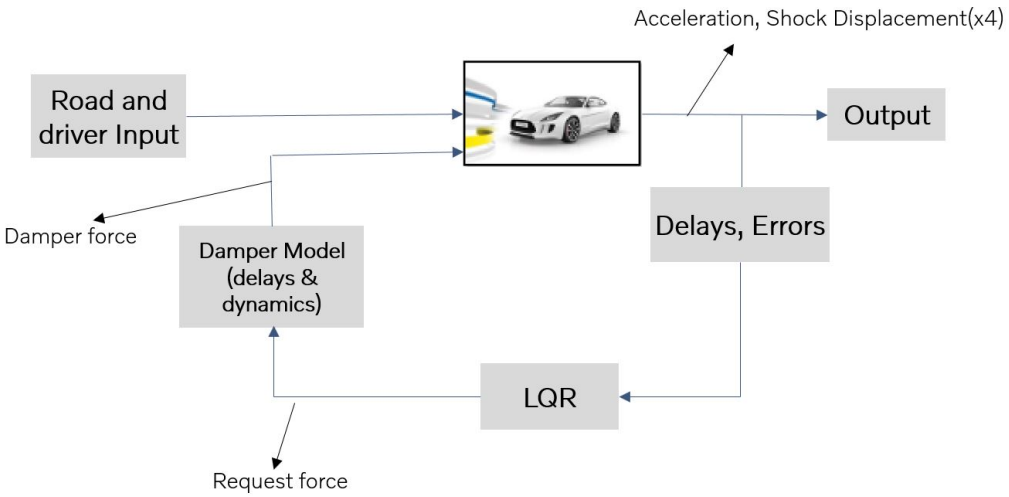

Figure 4.2: Active suspension Architecture

Here the input is the road disturbance and speed of the vehicle that is predefined in the IPG carmaker environment. Besides, there are two delays and error models. This work includes one of the mathematical delay models in between the sensor and the controller model for both level and accelerometer sensor. There is also a transport lag model in between the controller and the vehicle model, to represent the force build-up dynamics. This model is built within the damper, which is obtained from the supplier and is not modified. There is also a quantization error model in between the sensor and controller to induce error into the signals.

4.3 Semi active suspension with preview

In the semi-active suspension with the preview, an MPC controller [13] is used to control the damper motion by solving the optimization problem. The objective of this controller is similar to any other suspension control system, i.e to minimize the fluctuation in the states of the system. But the major advantages of the MPC is that it can provide the optimal solution given the future state and it can also be designed explicitly taking the constraint of the actuator, states and outputs into account.

The fundamental working principle of the MPC is that, given the future road disturbance and current states, the response of the vehicle model is predicted over a finite horizon using a mathematical vehicle model. Then an optimization algorithm is applied in this finite horizon over this predicted system response of the vehicle model, based on cost function subjected to constraints as mentioned above. At last,

the most optimal signal is chosen and is applied to the damper model. Then the rest of the signals are discarded. This is continued for the next sampling time and so on. The working schematics of the MPC controller is as shown,

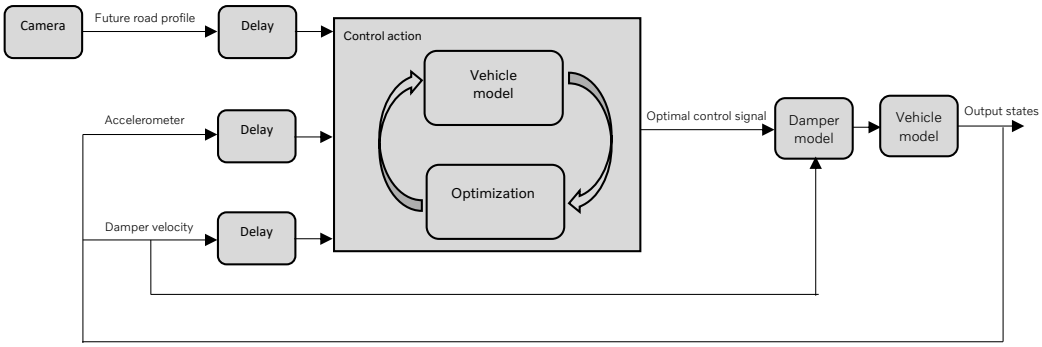

Figure 4.3: Operating region for Semi active suspension

In this thesis work, for the controller with the preview system, all three major sensor signals: road preview, accelerometer and level sensors are delayed as shown in figure 4.3.

5

Modelling of time delays and quantization errors

To analyse the system in the presence of delays and errors, it needed to be modelled first. Delays and errors, in general, are stochastic and random. They cannot be modelled physically but can be modelled mathematically using tools from probability. Different delays models have been developed till now [14], and in this thesis work, these models were employed based on the test cases and performance metrics. In this chapter, a brief explanation of the different delay and errors models that were implemented are discussed in details. The three different delay models that were used are,

- Constant delay model
- Delay based on gaussian distribution
- Delay based on markov jump system

5.1 Constant delay model

The constant delay is the simplest delay model. Adding this delay would just shift/delay the input signal by a constant magnitude before going to the controller. This model is most often used in this thesis work due to its simplicity. This delay is also referred to as the constant dead time delay. An example of this delay is graphically shown:

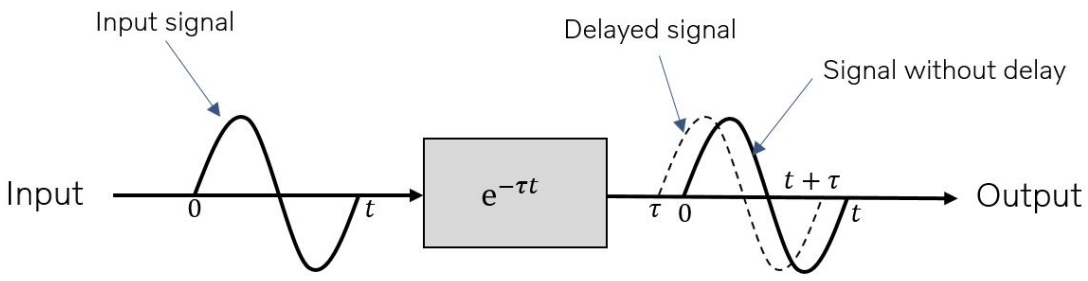

Figure 5.1: Constant time delay

5.2 Delay based on gaussian distribution

Delays are generally stochastic in nature, and they vary randomly over time [15–18]. This random nature could be due to the network load, message size and other external factors. But like any stochastic processes, this variation can be approximated to a model based on gaussian distribution with a particularly mean and variance. In this thesis work, three different gaussian based delay models are used to simulate the effect of the delays under different network loads. Each of these delay models has its own mean and variance. An example of the distribution is as shown.

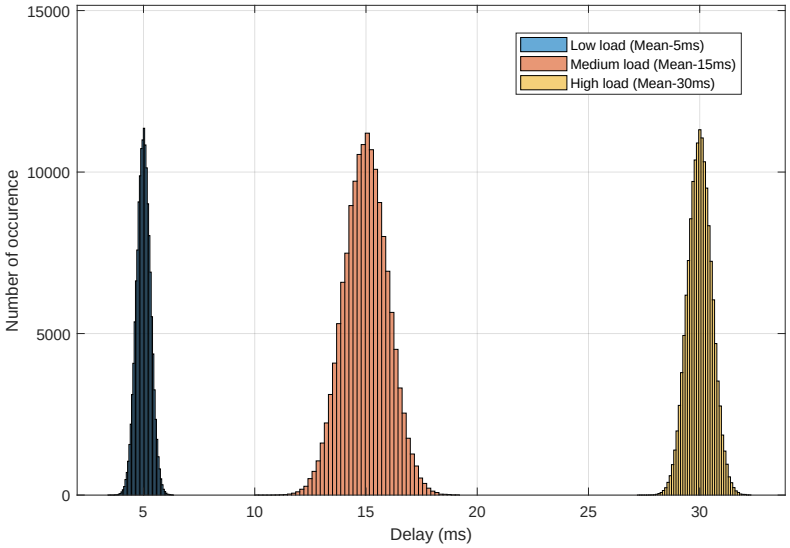

Figure 5.2: Delay based on gaussian distribution

It should be noted that the histogram of the three delay models is plotted together for convenience. But they are used individually in the actual simulation.

5.3 Delay based on Markov jump system

Most of the stochastics processes are entirely independent of each other and are equally distributed. According to [14], the delays in a network usually doesn't follow the bell curve/ Gaussian distribution curve. Instead, they would have two or three different histogram peak. This is due to the network queue, waiting time etc. To simulate this stochastic process, the mathematical model needs to have a memory/state. With this feature, the variable under study can switch between different states (or distribution) given the current state. This makes the model more accurate. Hence, a probability tool called the Markov chain was implemented to model the delay in the network.

This Markov chain model has different states based on the problem requirement. In this thesis work, three different states were chosen to simulate the network load: low, medium and high. This jump/switching between states depends on the current system state and the values in the state transition probability matrix. The states and the state transition pathway of the models are as shown,

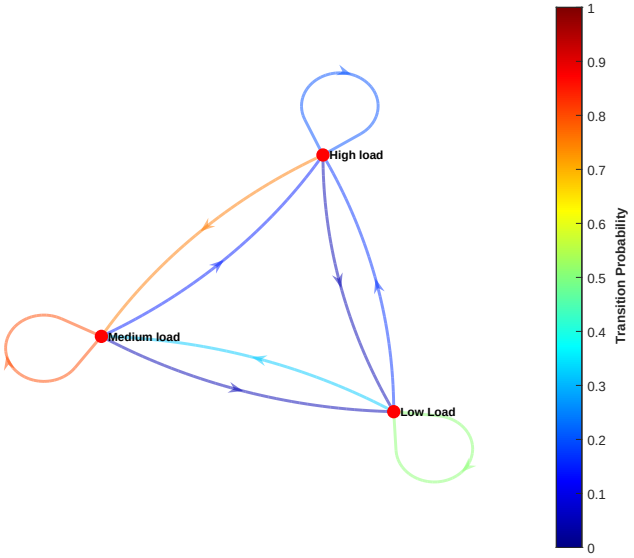

Figure 5.3: Markov Chain Modelling, L,M,H are the state of low, medium, high network loads which shows possible transitions

Then each of these network states is in turn modelled as a Gaussian distribution model. That means the network states, in turn, have their own mean and variance values just like in delay based on Gaussian distribution. Hence we can also say that the delay model based on Gaussian distribution is equivalent to the Markov model with a single state. These final distributions of the Markov delay model is shown in figure 5.4. This plot was obtained from one of the simulation run for the statistical analysis.

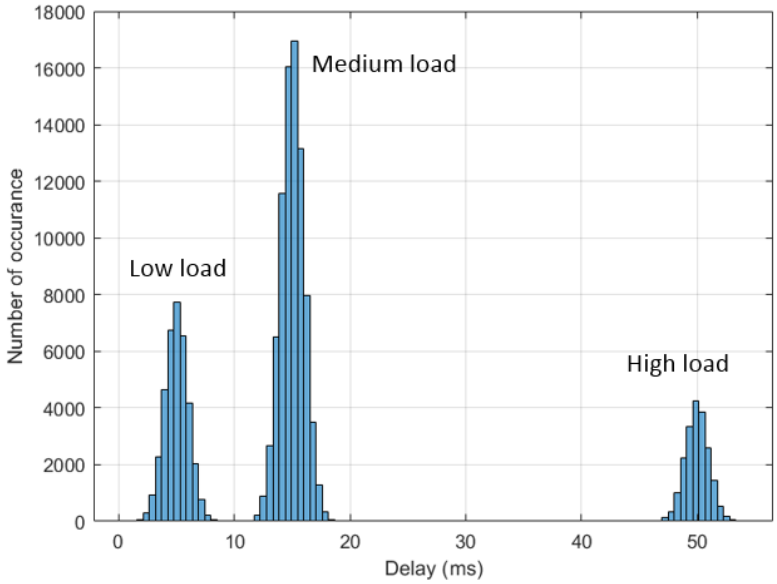

Figure 5.4: Delay distribution correspond to Markov chain modelling

Once the model is built, the inputs to the model needs to defined in the state transition probability matrix. This matrix defines the probability with which the

one system state jumps to another state. Mathematically this transition probability matrix is represented as,

$$q_{ij} = P\{r_{k+1} = j | r_k = i\}, \qquad i, j \in [L, M, H] \tag{5.1}$$

Due to lack of data, the values for these matrices were chosen iteratively such that medium load state has a high probability, and High load state has a lower probability. This choice of probability was based on [19].

5.3.1 Markov Communication Network

Let τ_k is a random variable, chosen with a probability distribution given by the state of Markov chain. This variable is used to collect the network delays and be a vector with the delays in the loop. When the random variable τ_k is generated, the Markov chain has the state $r_k \in \{1, ..., s\}$, the Markov chain represented with transition matrix is $\mathcal{Q} = \{q_{ij}\}, i, j \in \{1, ..., s\}$ where q_{ij} can be written as,

$$q_{ij} = P(r_{k+1} = j | r_k = i) \tag{5.2}$$

This equation represents Markov property, which conveys that the probability at which the future state, transition or switches to other state j, knowing only on the current state. Introducing the Markov state probability [14],

$$\pi_i(k) = P(r_k = i) \tag{5.3}$$

This has the state distribution vector,

$$\pi(k) = \begin{bmatrix} \pi_1(k) & \pi_2(k) & ... & \pi_s(k) \end{bmatrix}$$

The probability distribution function of r_k is given by,

$$\pi(k+1) = \pi(k)Q \tag{5.4}$$

5.4 Quantization

5.4.1 Sampling

The process of conversion of continuous-time signals to discrete-time signal is called sampling. The continuous analogue signal in the time domain in figure 5.5 is the function of both amplitude and time which is in continuous range where T_s is the sampling period, whereas the converted discrete signal is only the function of time and amplitude is in a continuous range. And also in discrete signal, at every instant of time, there is a sample value corresponding to the instantaneous amplitude of modulating signal $m(t)$.

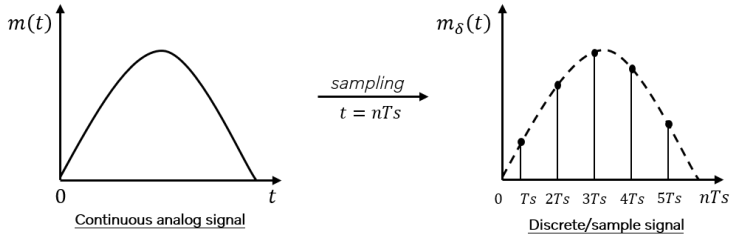

Figure 5.5: Sampling

5.4.2 Quantization process

Quantization is the process of delineating input values from a large set(infinite) to the output values in a smaller set(finite) with a finite number of elements. Quantization is also known as rounding off or truncation or approximation. In the quantization process, the converted discrete-time signal is again converted into a digital signal in which both time and amplitude are in discrete [20].

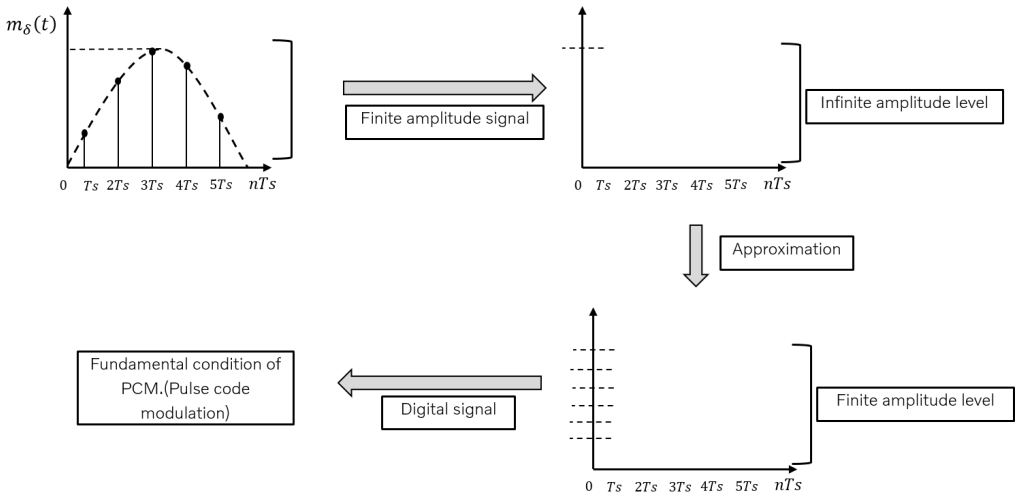

Figure 5.6: Quantization process

Since in discretized signal, time is discrete and amplitude is continuous with a finite amplitude range of the signal, it is possible to find the infinite number of amplitude levels. This is because, as the human eye or ear sense only finite-difference but having infinite capability. Therefore in the quantization process, the infinite number of amplitude level is approximated or rounded off to discrete amplitude levels, whereas the approximation is selected with minimum error within the available range of amplitude. This process of approximation results in a digital signal which has a finite number of amplitude levels [20]. And also the quantization process is the fundamental process for pulse modulation technique which is an irreversible process as seen from the figure 5.6.

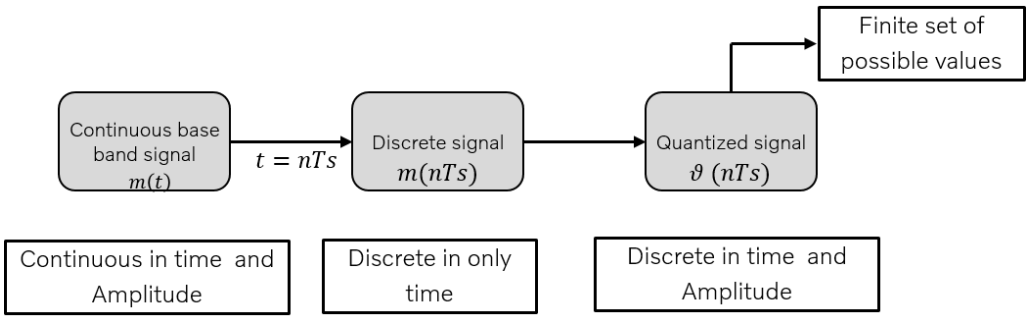

Figure 5.7: Quantization process in short

In both real-time system and simulation environment, the sensor signals that are measured are converted into continuous-time to discrete-time using Analog to Digital converter to represent the original signal in the form of finite discrete values before controller that sends control signals to the plant. During Conversion of continuous to discrete-time the signals were converted in the form of binary digits, which may results in the misplacement of binary digits compared to the original signal is called quantization. There are two types of quantization, In some quantization process where the quantization levels were uniformly spaced is called uniform quantization. Similarly, In some quantization process where the quantization levels are unequal and the relation between them is mostly logarithmic is called non-uniform quantization. The original signal can also be quantized using some algorithm or function, the component that performs those algorithms or logarithmic function to round of the value is called quantizer. Therefore the difference between the original signal and the quantized signal is called quantization error.

5.4.3 Signal to noise ratio

The noise introduced during the quantization process is called quantization noise to the sample signal. The resolution of ADC is inversely proportional both quantization error and noise. The higher the resolution of ADC is lower the quantization error and lower the quantization noise. Both resolution(in bits) and quantization error for an A/D converter can be expressed in terms of,

$$SQNR = -20 \cdot log\Big(\frac{1}{2^n}\Big) \tag{5.5}$$

where n is the resolution of A/D converter in bits.

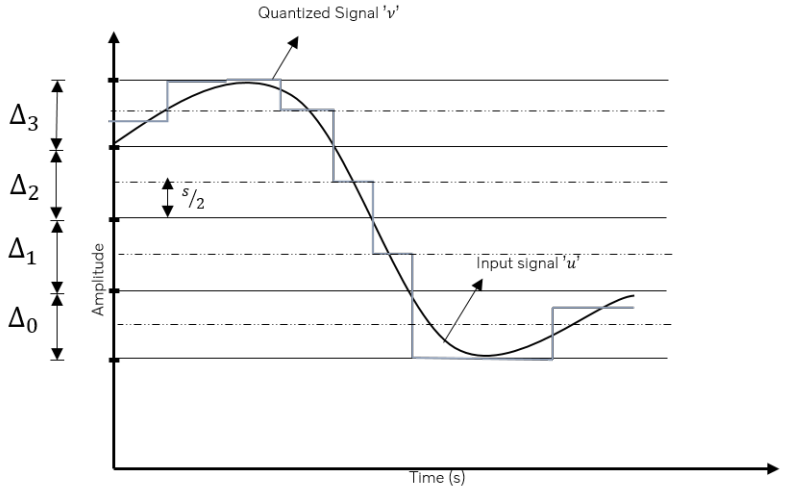

Figure 5.8: Quantization error

6

Methodology

In this chapter, the methodology that was adopted in the thesis work is discussed. The results from these analyses are then shown in the next chapter. The two main objectives in this work are, first to study and analyse the influence of the signal delays and errors on the performance of the system. Then the second part of the work is to implement a controller to compensate for the delays in the system. Due to the broad nature of the project, the methodology is broken into a structured way as shown,

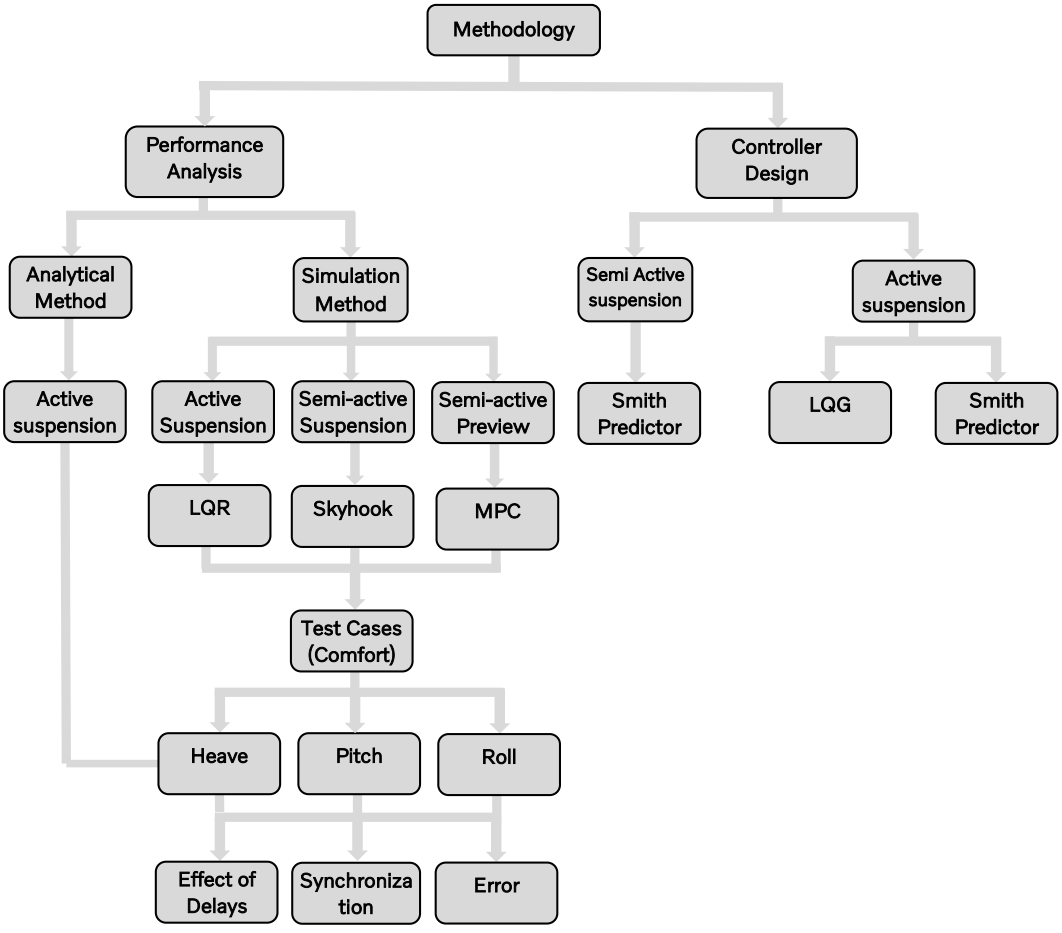

Figure 6.1: Methodology

At first, the performance analysis of the suspension system is discussed in brief.

6.1 Performance analysis

In the performance analysis, different suspension controllers and models are analysed in details under the influence of signal delays and errors. The performance analysis was carried out in two different ways. At first, the influence of delays was studied in detail using the analytical approach using a mathematical quarter car with fully active suspension system. Then a detailed analysis was carried out it in the simulation environment using IPG carmaker vehicle for three different systems/-controllers: Semi-active suspension with skyhook controllers, active suspension with LQR controllers and semi-active suspension with road preview functionality.

Before moving on to the analytical and simulation approach, the main simulation architecture, that was used in both analytical and simulation approach is discussed.

6.1.1 Simulation architecture

In chapter 2, the complete system architecture of the electronic wheel suspension system, along with the sources of delays and errors, were discussed. As was shown, there are multiple origins of delays and signal errors, and this makes the problem more complex and difficult to study. Hence the simulation architecture, along with the source of delays and signal errors, was simplified in this thesis work.

The final simplified version of the system architecture, along with delays and errors, are as shown.

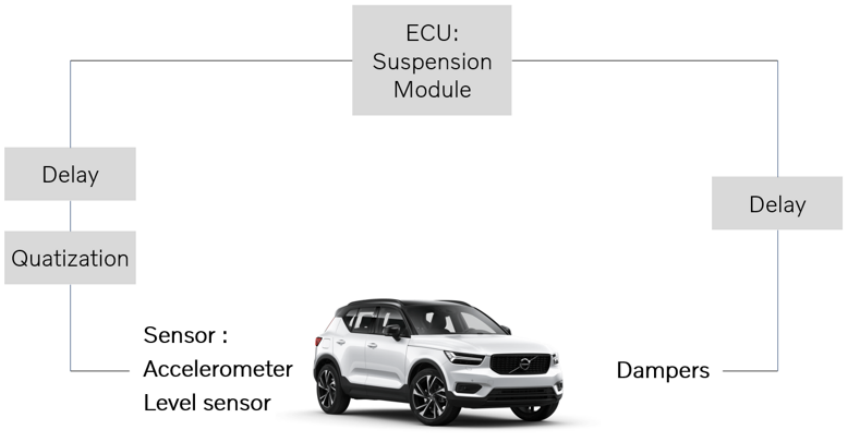

Figure 6.2: Reduced model

As can be seen from the above figure, the delay and error sources are reduced to these two locations: from the sensor to controller and controller to the actuator. The main reason for this simplification is as follows,

- The more complex the model is, the need for validation of these delays and errors models become essential.

- The study of each of the error and delay sources is time-consuming and resource-intensive.
- In most of the literature [14], [21], [22], the authors have concluded that delays in these two positions are the most important and enough to study the system.
- Plenty of research works and analytical tools are available for problems of this sort, whereas not many research work has been carried out in such a broad structure.

6.1.2 Analytical approach

The analytical approach gives a greater flexibility in analysing the system stability and performance under the influence of delay, with plenty of control theory tools. In this method, a mathematical quarter car was developed, which was discussed in detail in the third chapter. This model is then equipped with a fully active LQR controller,constant delay and a first-order lag dynamics model to mimic the actuator force dynamics.

The methodology utilized for the analytical approach is as shown below,

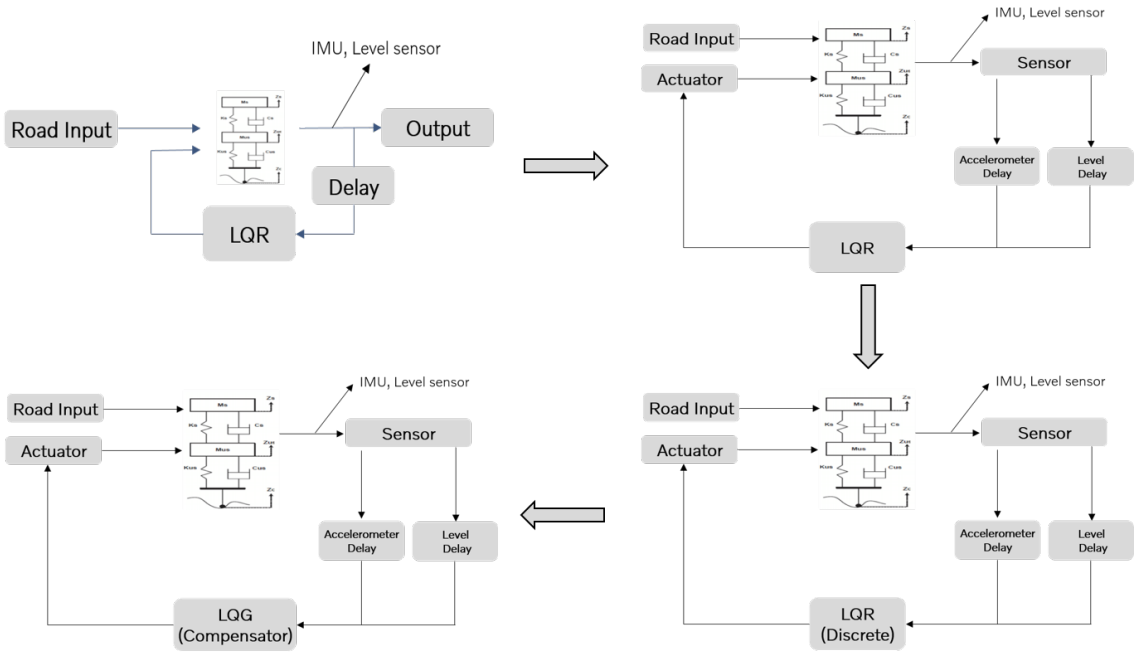

Figure 6.3: Reduced model

6.1.2.1 First model

As shown above, in the figure 6.3, it has a quarter car model as the main plant. Two state: vertical acceleration and suspension displacement are measured. Then only one of this signal is delayed, and then these signals are sent to the LQR controller, and the control force which is calculated by this LQR is sent to the actuator model. Here a simple first-order dynamics block is used to simulate the dynamics of the

actuator. Then finally, this force goes to quarter car model to control the model. This model is used to gain insight into the effects of delays on one of the sensor delay at a time. The system equation of this model is given by,

$$\begin{aligned} \dot{x}(t) &= Ax(t) + Bu(t-\tau) \\ y(t) &= Cx(t) \end{aligned} \tag{6.1}$$

6.1.2.2 Second model

In the second model, both level and accelerometer sensor were delayed. This was done to study the influence of the delays on each other and how the unsynchronized signals affect the system performance.

6.1.2.3 Third model

In the third model, the controller was discretized to study the effects of delays and sampling time. Three different test cases were developed: sampling time less than delay, equal to delay and finally sampling time greater than delay. The system equation for this discrete model with delay is given by,

$$\begin{aligned} \dot{x}(k+1) &= Ax(k) + Bu(k-\tau) \\ y(k) &= Cx(k) \end{aligned} \tag{6.2}$$

6.1.2.4 Fourth model

Finally, a delay compensated LQG controller is developed to compensate for the delayed system and was simulated for different test cases. The result from this system is not shown in this thesis report, as the quarter car model was only used as a concept check. But the final results with the IPG carmaker model is shown in Chapter 7.

6.1.3 Simulation approach

The controller and damper models in general for the semi active system are highly non-linear. This makes it difficult to analyse the system analytically. Hence the analysis was carried out in the simulation environment using higher fidelity vehicle, controller and damper model. Here, all three different controllers: semi-active, active and semi-active system with road preview are analysed. The main simulation architecture with the carmaker model is as shown,

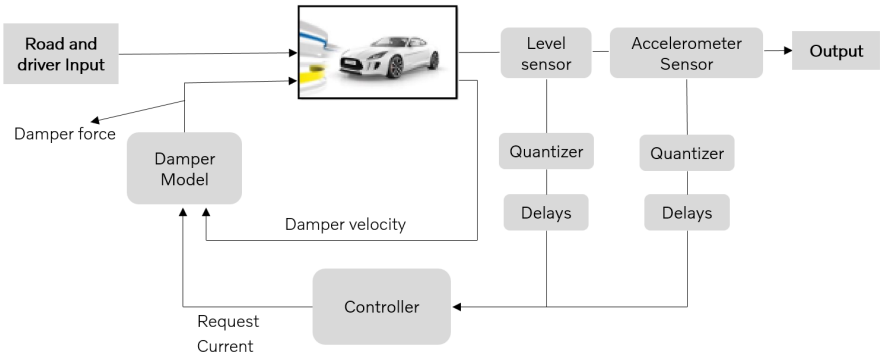

Figure 6.4: Simulation structure

Even though different controllers are simulated and studied, the main structure in the simulation environment is very much similar to the figure 6.4. As can be seen in the figure, a vehicle model in IPG carmaker was used. The controllers, delay and quantization models that were used in the simulation are explained in the previous Chapters. The damper model is obtained from Volvo cars, which is a lookup based model. The model has two first-order dynamics block to represent the force and current build-up dynamics, to simulate the exact behaviour of the dampers.

6.2 Testcases and metrics

Performance of a suspension is very important in terms of both comfort and road hold. But in this thesis work, the performance analysis is limited to comfort with a focus on heave, pitch and roll body motion. First, the main structure/ methodology of the test cases and metrics used in the thesis work for the analytical approach is discussed.

6.2.1 Analytical approach

In the analytical approach, only the heave motion of the vehicle is studied. The main interest of the study is the influence of delays, synchronization and signal errors. Output metrics that were chosen for this study are time-domain plots, frequency domain plots and different sweeps. The structure for the performance analysis using the analytic model is as shown,

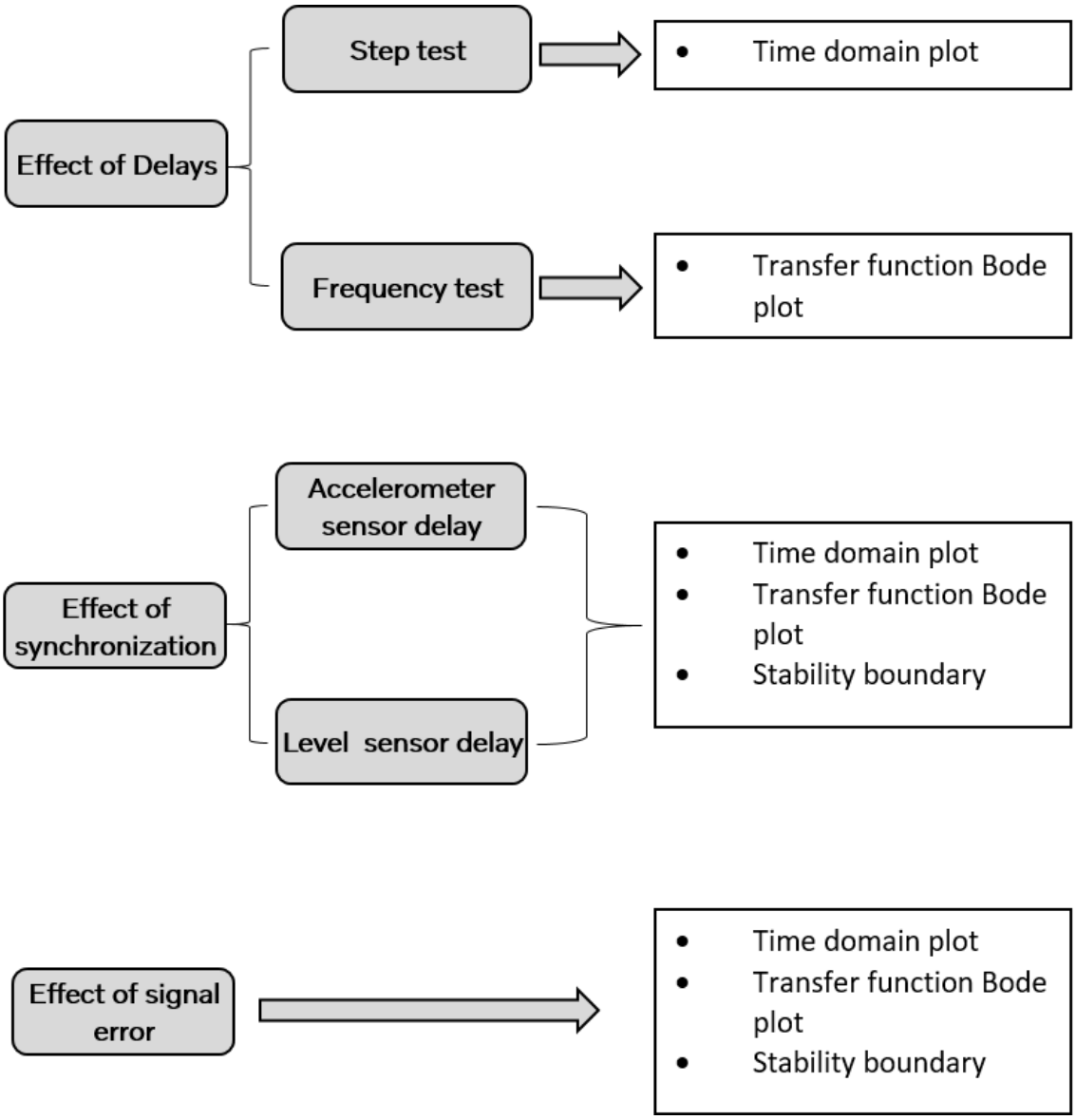

Figure 6.5: Performance evaluation structure for Analytical model

6.2.2 Simulation method

Three different controllers are analysed here: Semi-active system with preview, active suspension and semi-active with preview system. The main interest of study here is the influence of the delays, synchronization and errors. Different metrics and test cases were utilized to study the system in detail. The main structure for the performance analysis for the three controllers is as shown,

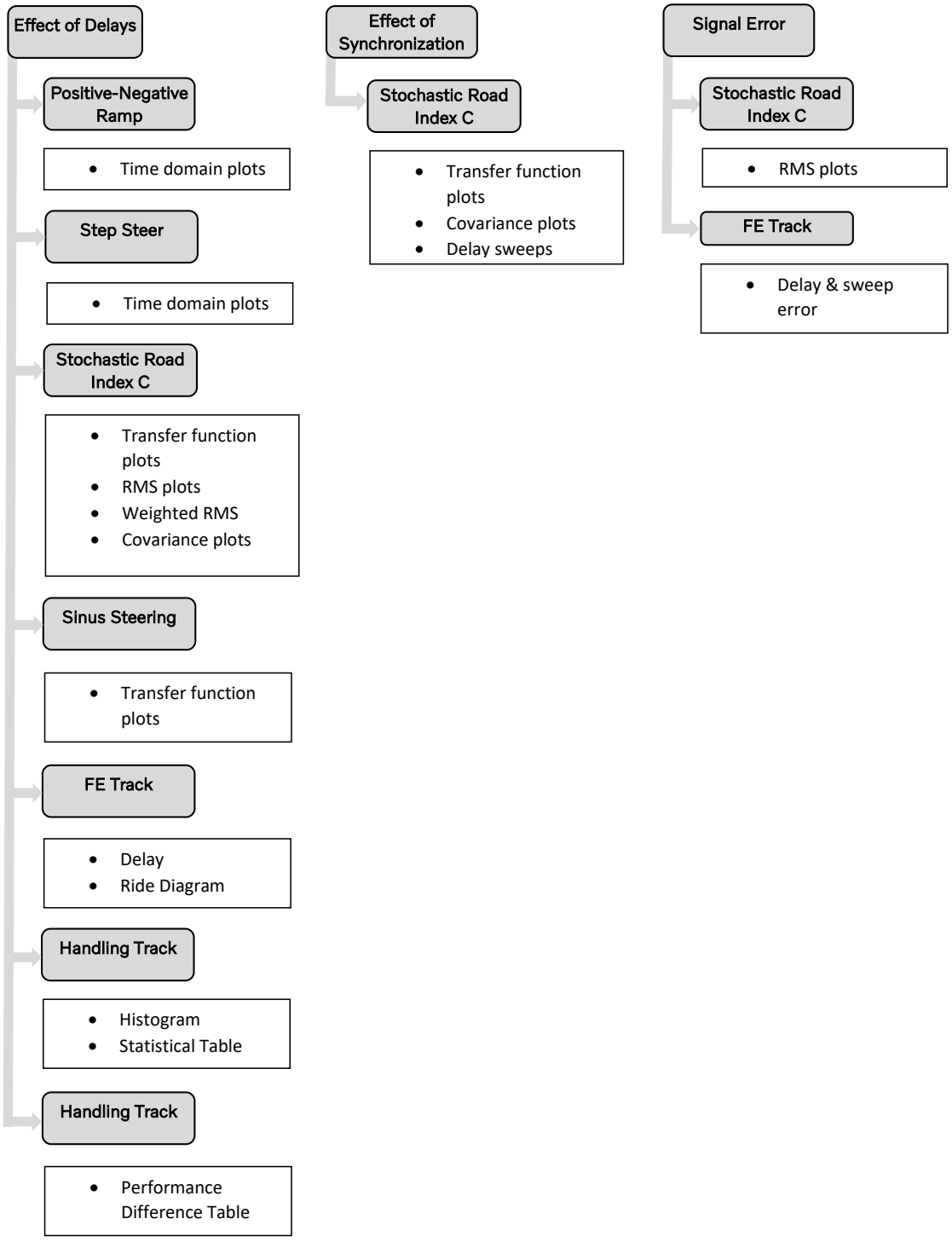

Figure 6.6: Performance evaluation structure

As can be seen from the figure 6.6, several test cases and metrics were implemented to evaluate the system under the influence of the delay, synchronization and errors. A brief description of these test cases and metrics are given in the following section.

6.2.2.1 Test cases

Positive-negative bumps

The objective of this test case is to evaluate and compare the system performance in the time domain. The parameters of the profiles were chosen such that they excite the damper speed to a high speed both in bump and rebound motion. The profile of this test case along with the dimension is as shown,

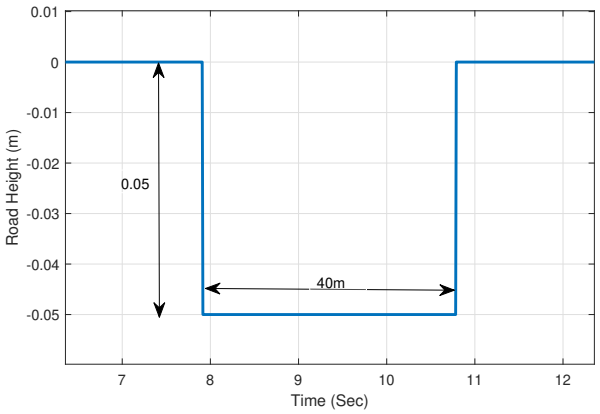

Figure 6.7: Positive negative bumps

The output quantities of interest are mainly the heave motion, but signals from damper velocity, requested damper force and actuator force are logged and compared as well.

Step steer:

The objective of this test case is similar to that of a positive-negative bump, but this test case is specifically chosen to excite the roll motion of the vehicle. So here the vehicle is simulated in a flat road, and only the steering wheel angle is changed. The profile for the steering wheel angle is as shown,

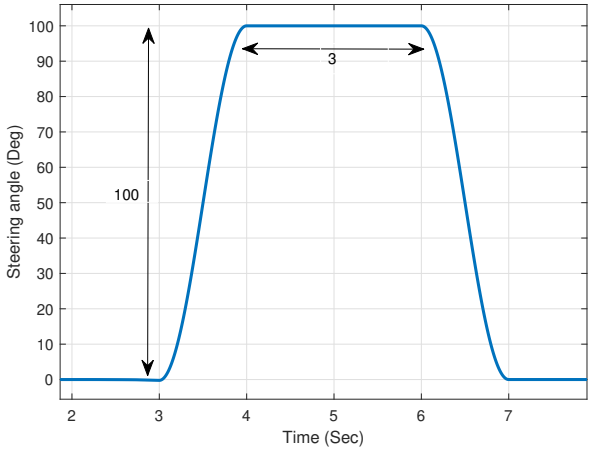

Figure 6.8: Step steer

Here the output quantity of interest is primarily the roll velocity of the vehicle. But other signals of interest that were logged are damper velocity, requested damper force and actuator force.

Stochastic road: Index C

The stochastic road is one of the road profiles that are generated based on parameters like the waviness, frequency range, vehicle speed etc. According to [23], these roads are classified into five different types, based on their magnitude and waviness. In this thesis work, the road profile with Index C is predominantly used in most of the evaluation as it offers a good balance between soft and extreme rough roads.

The profile of the road height is as shown,

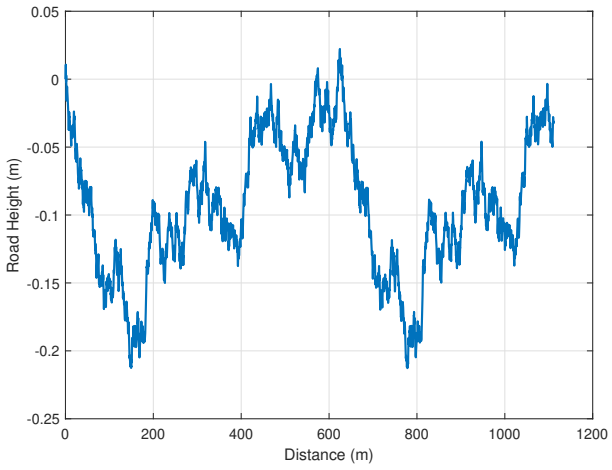

Figure 6.9: Stochastic road: Index C

It should be noted that the profile varies only in the z-direction. So only the heave and pitch motion is excited. The roll motion is not excited in this case, hence the main output quantities of interest are only the heave and pitch motion.

Sinus steering

In this test case, a sinus swept motion of increasing frequency is given as input to the steering angle. Here, the frequency of the steering angle input is varied from 0 to 4 Hz. This covers the operating range where the steering angle of the vehicle would be operated in. The final profile of the steering angle is as shown,

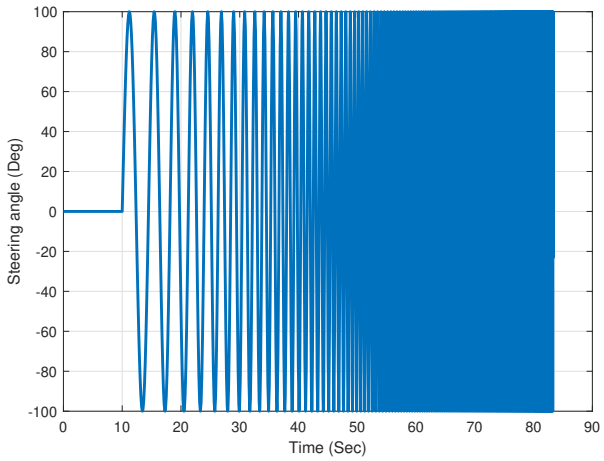

Figure 6.10: Sinus steering

The main output of interest here is the steering and roll angle for the transfer function plots.

FE Road

FE road is part of the test track at Hällered proving ground. This road is used in comfort analysis as it excites the vehicle in a wide operating range. The test track here is an unsymmetric road, so here, all the three motions: roll, heave and pitch motion are excited. The road height profile of the test track is as shown,

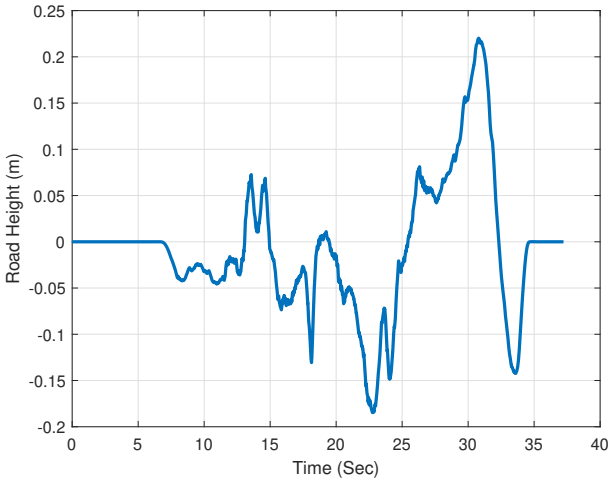

Figure 6.11: FE road

All three vehicle motion: heave, pitch and roll are taken as output measure of interest in this test case.

Handling track

The handling track is also part of the test track at Hällered proving ground. This track represents a typical country road in Sweden, making it a perfect test case to analyse the suspension system statistically. The only parameter in the test cases is the vehicle speed and is chosen such that the damper velocity is excited to cover a wide operating region. The top view of the test track is as shown,

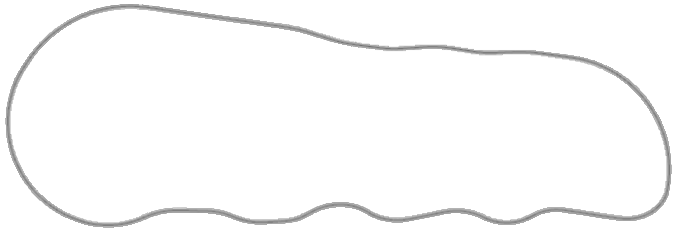

Figure 6.12: Hällered proving ground

The main signal of interest in the test case is the Damper velocity signal of all the four corners.

6.2.2.2 Performance metrics

Throughout the thesis project, several metrics and plots were used to assess system performance. In this section, a brief description of some of those metrics and plots are discussed in detail.

Covariance analysis

This method measures the performance of the control system in terms of their standard deviation from the state variable, provided that the closed-loop system is stable and the ground road velocity is a zero-mean, Gaussian white noise.

In [24], a numerical procedure is proposed for obtaining a covariance analysis-aimed result for a non-linear system. This procedure for this particular analysis is listed as follows,

- The vehicle is simulated with a ground velocity of zero-mean and normally distributed white noise.
- The duration of the simulation is set to be greater than K multiplied by the reciprocal of the sprung mass natural frequency of ω_n. Here K is set to be 500.
- Finally, the RMS values of Heave acceleration, tire deflection and suspension deflection are normalised with respect to the power spectral density of the simulate road profile. Mathematically this can be represented as,

$$\text{Normalized } RMS_{\ddot{Z}_s, Z_s - Z_u, Z_u - Z_r} = \frac{RMS_{\ddot{Z}_s, Z_s - Z_u, Z_u - Z_r}}{\sqrt{2\pi AV}} \tag{6.3}$$

The final result from this equation is then plotted with respect to each other.

Weighted RMS plots:

In general, it is accepted for stationary vibrations, that humans are sensitive to the RMS value for the acceleration in which the sensitivity is frequency dependant where the highest discomfort occurs in the certain range of frequencies. The frequencies from 4-8 Hz is suggested by the SAE to be the most sensitive frequencies, and acceleration should not be more than 0.025 g(RMS). So it is important to check the Influence of delays inv active and semi-active suspension with ISO2631 standard curves. In weighted RMS, RMS of acceleration at multiple frequencies can be calculated. Since humans are sensitive to the acceleration it would give one measure of human discomfort. The weighted RMS of the acceleration a_w can be calculated by,

$$a_w = \sqrt{\int_{\omega=0}^{\infty} (W_k(\omega))^2 \cdot G_{\ddot{z}}(\omega) \cdot d\omega} \tag{6.4}$$

where W_k is vertical human body vibration sensitivity and $W_k(\omega)$ is a human filter function.

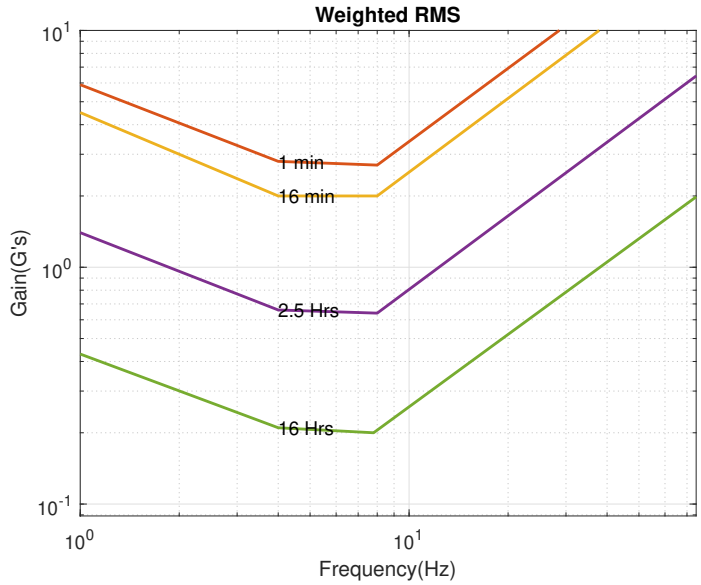

Figure 6.13: Weighted RMS

Ride diagram:

Most commonly used ride evaluation measures are RMS and PSD. While both of them are a good measure, the problem is that they smooth out the transient events by averaging. This is undesirable [25]. According to [25], humans react negatively to changes in the vibration character, rather than the absolute amplitude value alone. So a new method is proposed in the [25], a ride diagram, that measures both the changes in the intensity as well as the character of the amplitude profile. The description of the ride diagram is as follows.

To generate a diagram is a three-step process given the heave acceleration data. The first step in ride diagram is to divide the signals into segments separated by sign changes in the derivative of acceleration as in the figure. The second step is to classify each segment as either 'transient' or 'stationary' signal depending on its peak to peak values that are limited based on suspension travel. The limit that determines whether the peak to peak value falls under the category of "transient" or "stationary" is given by,

$$T_{limit} = 2\sqrt{2}RMS(a) \tag{6.5}$$

So based on this limit value, if the peak to peak value is less the T_{limit} then is classified as a "stationary" component and if its greater than the T_{limit}, then classified as "transient" component. Finally, the mean square of these two datasets is calculated.

Once these two values are computed, they are plotted according to their corresponding vehicle speed. The mean square of the transient signal is plotted on the left side and mean square of the stationary signal is plotted on the right side. In this thesis work, this procedure for carried out for three multiple delay values and the results are as shown,

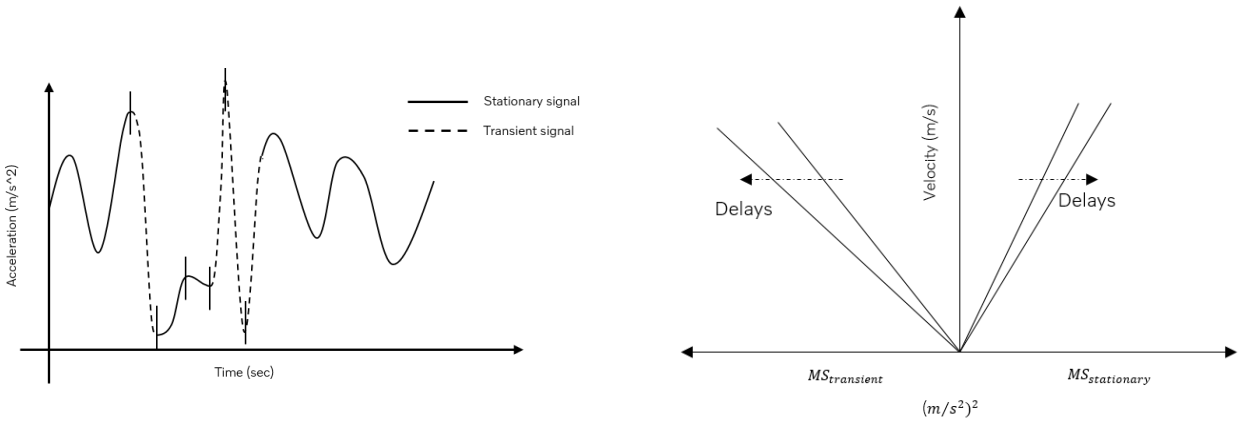

Figure 6.14: Output of vertical acceleration with classification as a stationary and transient signal on left and Example of ride diagram on right

7

Results and inference

In this chapter, the results from analytical and simulation studies are shown and discussed in detail. The main interest of the study here is the influence of delays, synchronization and errors. As discussed in the previous chapter, at first, the results of the Analytical approach is discussed in detail. Then the results of the simulation approach are shown. Furthermore, the results from the experimental data which was conducted in hällered proving ground are then presented in the appendix and are not available for public. Finally, the results obtained from the delay compensated controllers are presented.

For some of the results, an objective performance difference value is also presented. The mathematical representation of this performance difference measure is given by,

$$\text{Performance degradation}(\%) = \frac{RMS_{\text{with delay}} - RMS_{\text{without delay}}}{RMS_{\text{without delay}}} \tag{7.1}$$

7.1 Analytical results

The results of the quarter model with a fully active suspension and LQR controller is presented here. The entire work was carried out in the Matlab environment.

7.1.1 Effect of signal delay

In this section, only the effect signal delay is presented, assuming that both the level and accelerometer sensor delays are constant. Hence, in this case, the signals are delayed and synchronized.

Time domain

The mathematical quarter model was simulated over a small bump with an amplitude of 2.5 cm. It should be noted that both the accelerometer and level sensor are delayed by the same value. And the test was carried out for four different delay values: 0, 16.66,33.3 and 50 ms. The final results are as shown,

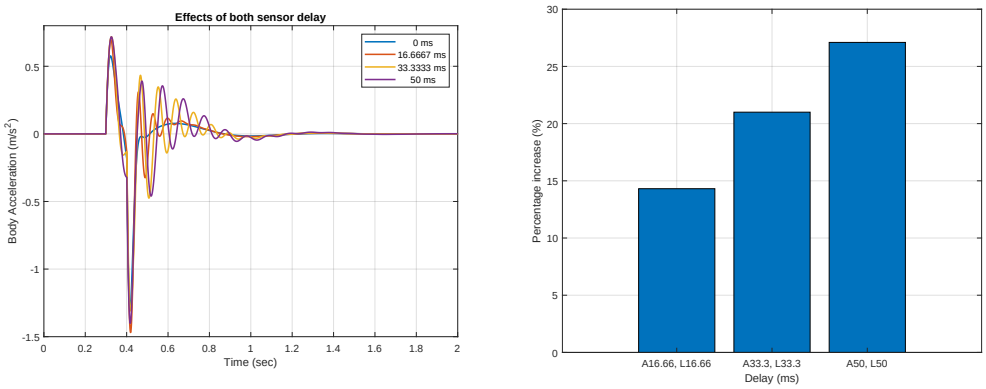

Figure 7.1: Effect of both sensor delay in time domain and percentage difference

As can be seen from the figure on the left is the time domain. As we add delays into the system, the amplitude and the oscillations start to drastically increase. This type of behaviour is not tolerable in terms of comfort, causing discomfort to the passenger. The figure on the right side is the bar chart of the percentage RMS acceleration increase. Here it starts with a value of 15% difference in comparison to the result with no delay and increases until 28% which signifies a severe performance degradation in the system.

Frequency domain

The mathematical model was converted to its transfer function form, from road displacement to heave acceleration. Then a bode plot was taken for this transfer function to analyse the system in the frequency domain. Here the mathematical model was evaluated with three different delay values: 0, 25 and 50 ms. The magnitude of the bode plot is as shown,

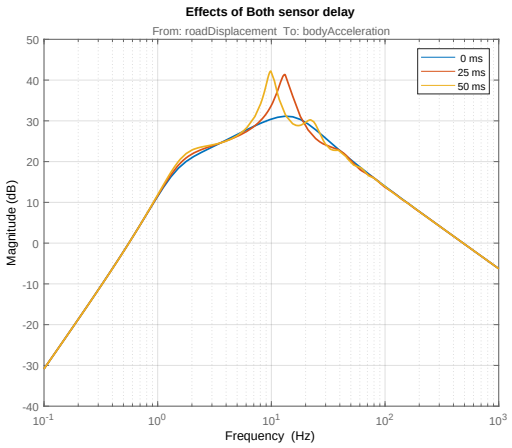

Figure 7.2: Effect of both sensor delay in Frequency domain

From figure 7.2, it can be noted that the amplitude increases in both primary and secondary ride frequency. But in comparison to the primary ride, the performance degradation at the secondary ride has been affected the most at around 10 Hz.

7.1.2 Effect of unsynchronized delays

In this case, the mathematical model is evaluated with different delay values for both accelerometer and level sensor. So here the signals are delayed and are also unsynchronized. The number of test cases and values for the delays are similar to the last section. The only change here is that the accelerometer and level sensor delays are separately analysed.

Effect of accelerometer delay

Similar to the test case in figure 7.1, the mathematical model was simulated with a bump profile of 2.5 cm. But in this test case, the level sensor delay is kept zero, and the accelerometer sensor varied from 0 to 50 ms with four steps. The final results in the time domain and their percentage performance difference are as shown.

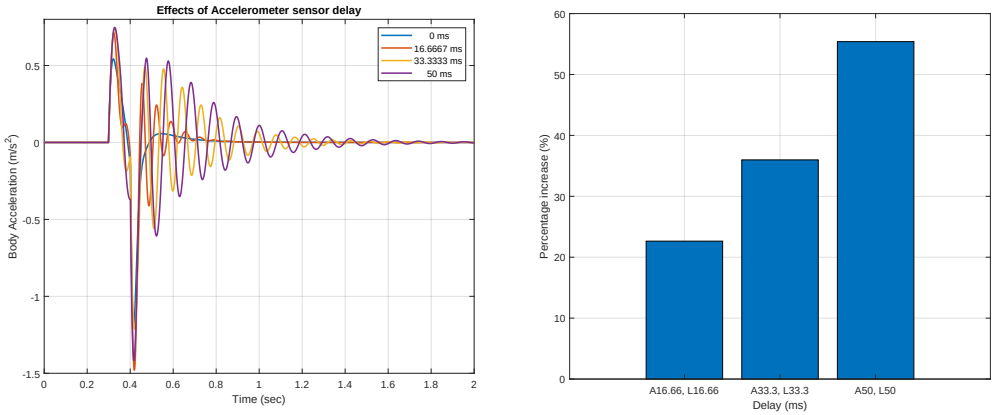

Figure 7.3: Effect of accelerometer sensor delay in time domain and percentage difference

From figure 7.3, it can be noted that the amplitude and oscillation are very worse in comparison to the result in figure 7.1, where both the signals are delayed. From the percentage difference in the performance, it can be noted that it starts with a value of around 22% and it increases up to 58%. This is almost twice the test case where both the sensors are delayed.

Frequency domain

Similarly, a bode plot was taken for the transfer function from road displacement to heave acceleration for three different accelerometer delay: 0,25 and 50 ms. The level sensor delay is kept zero. The result from the bode plot in the frequency domain is as shown,

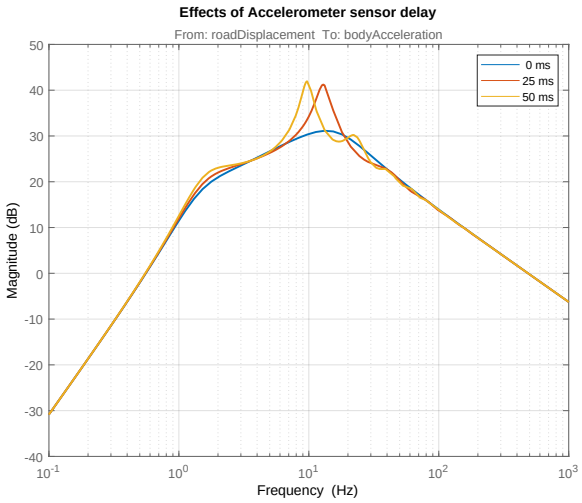

Figure 7.4: Effect of accelerometer sensor delay in Frequency domain

As can be seen from the above figure, the effect of the accelerometer delay is quite similar to the results for both the sensor delay. However, it should be noted that the magnitude in the primary ride is slightly higher in comparison to the other case with delays on both the sensor.

Effect of level sensor delay

Similarly, in this case, the level sensor delay is varied from 0 to 50 ms with four steps, whereas the accelerometer sensor signals is not delayed in this case. The results from the simulation are as shown,

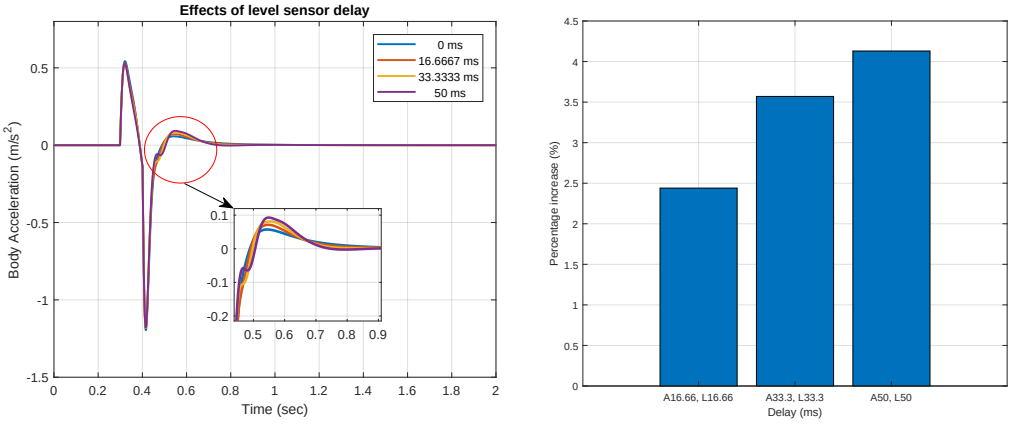

Figure 7.5: Effect of level sensor delay in time domain and percentage difference

As can be seen from the figure, there is no major difference in the heave acceleration plot, when the level sensor signals is delayed alone. This is due to the formulation of the LQR controller. A feedback controller like LQR regulates the system based on the magnitude of the error signal. Since the magnitude of the displacement is

very small in comparison the acceleration value, the magnitude of the level sensor error would also be very low in comparison to the accelerometer sensor error signal. Thus making the controller less sensitive to level sensor signal.

On the right, it can be noted that the performance difference in percentage in the bar chart. It is very clear that the performance difference for level sensor delay is order of magnitude smaller than the other test cases.

Frequency domain

Now, a bode plot was taken for the transfer function from road displacement to heave acceleration for three different level sensor delay: 0, 25 and 50 ms. Here, the accelerometer sensor signal is not delayed. The result from the bode plot in the frequency domain is as shown,

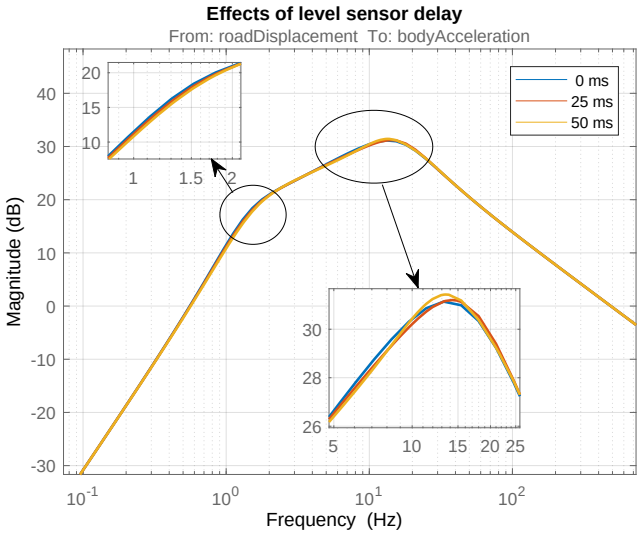

Figure 7.6: Effect of level sensor delay in Frequency domain

Similar to the time domain, the frequency plot also shows less sensitivity to performance change. But still,it can be noted from the two zoomed plot that there is slight change in performance degradation as we add delays into the system.

Sensor delay sweep

In this analysis, both the accelerometer and level sensor delays are swept from 0 to 100 ms in loops. Within this main loop, the control weights are varied between a particular range and tested for the maximum possible control gain that the controller can have before the system gets unstable. Finally, the accelerometer and level sensor delays are plotted against this maximum control gain. The final plots are as shown,

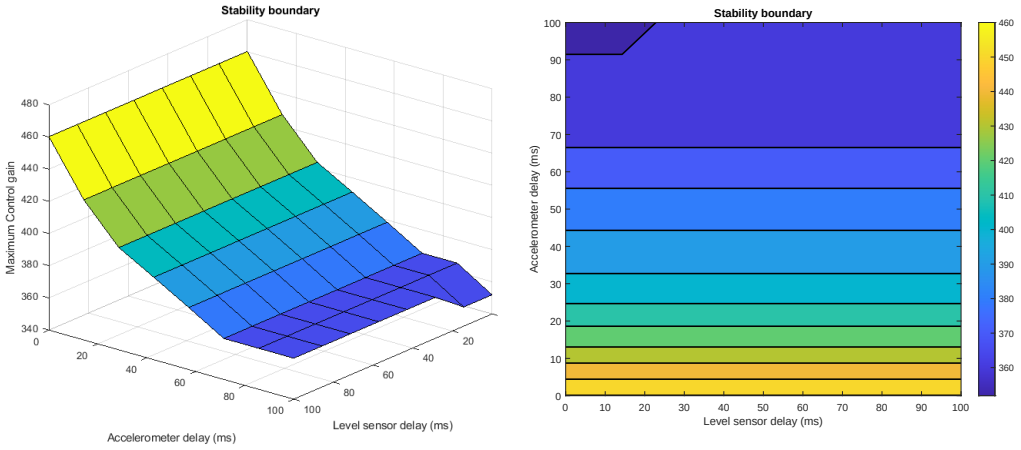

Figure 7.7: Stability boundary

As can be seen from the above figure, as we add the accelerometer sensor delay, the maximum allowable control gain starts to decrease. This essentially makes the controller slow and causes performance degradation, whereas this is not the case with level sensor delays. The level sensor delays shows almost zero sensitivity. But in the extreme case, it can be noted that simulating the system with 100ms delay on both sensor is slightly better than the case with delay on only the Accelerometer sensor.

7.1.3 Effect of signal errors

In this section, the influence of the signal errors on the performance of the suspension system is studied. The input to the system for this test case is a step input. Here the sampling time is intentionally modified to induce errors into the sensor signals. This results in a discrepancy in the original signal and the signal that is used by the controller. The difference between the two is the signal error. In this analysis, three test cases are assessed. They are, sampling time less than delay, sampling equal to delay and sampling time greater than delay. The results from the time-domain analysis are discussed first.

Time domain

The mathematical quarter model was simulated over a Bump for three different sample time case and with a constant delay on both accelerometer and level sensor. The objective is to see the effects of the sampling time and delays on each other. The final results are as shown,

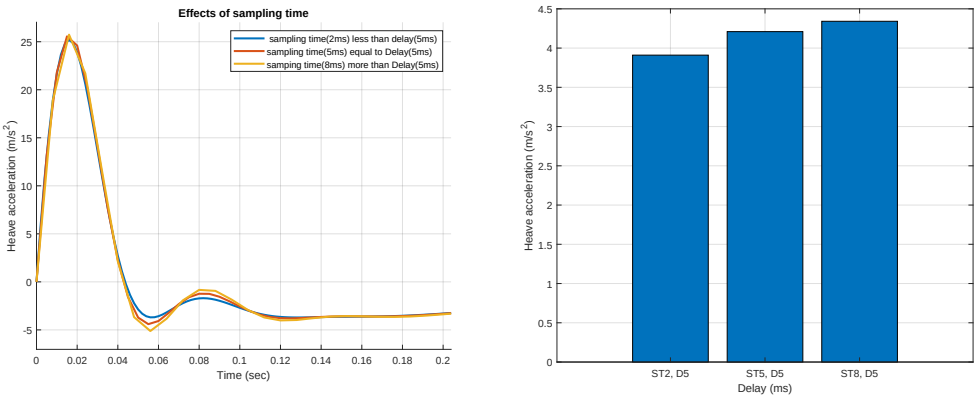

Figure 7.8: Effect of different sampling time in Time domain

The figure 7.8 on the left is the measure of heave acceleration with respect to time. it can be noted that the case with sampling time more than delay results in performance degradation. Whereas, having a lesser sampling time compared to the delay results in better performance. The case with equal delay and sampling time is in between the other two extreme cases. We can also see a similar trend in the RMS bar plot on the right.

Frequency domain

There are two frequency plots obtained for this test case. In the first test cases, the values of the sample time and delay are relatively small, and in the second case, the amount of the sampling time and delays are relatively higher. This was done to effectively see the influence of the signal errors on the performance of the system in the extreme cases. The results form the bode plot in the frequency domain are as shown,

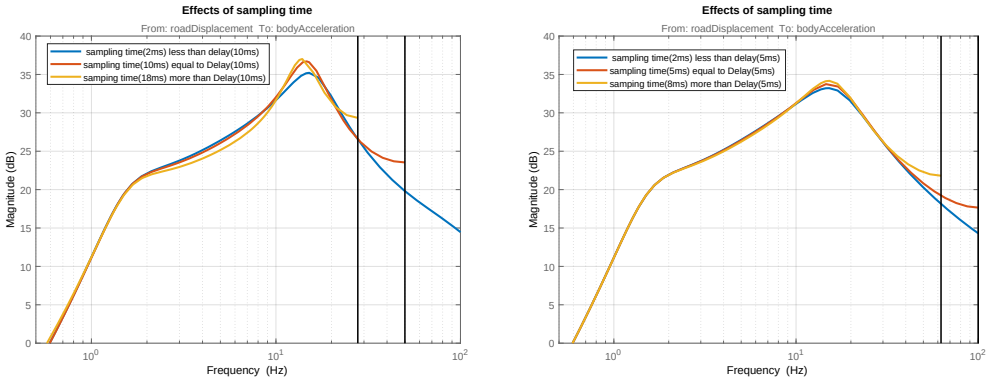

Figure 7.9: Effect of different sampling time in frequency domain

As we can see from the figure on the left, the scenario with sampling time less than the delay shows poor performance in comparison the other two cases, in the frequency range from 1.2 to 10 Hz. This behaviour could be due to loss of complete data as the delays are greater than the sampling time.

But in the secondary ride frequency, the test case with sampling time greater than the delay results in poor performance in comparison to the other two test cases. An interesting pattern to note here is that the test case with a sampling time equal to the delay value results in poor performance throughout the frequency range.

Stability boundary

Similar to the results from figure 7.7, a stability boundary has been formed for the sampling time and delay. Here, the delay on the sensor is swept from 0 to 100 ms and sampling time is swept from 1 to 20 ms in eight steps. Finally, the sensor delays and sampling time are plotted against maximum possible control gain without making the system unstable. The results are as shown

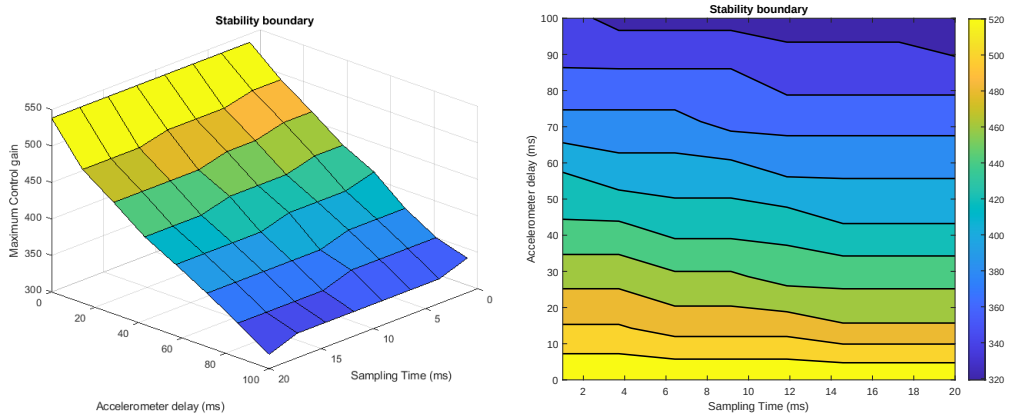

Figure 7.10: Stability boundary considering delays and sampling time

There are two plots in the figure 7.10, the figure on the left is the three-dimension plot that was mentioned before and the figure on the right is a contour version of the same plot. Both the plot shows the maximum control gain boundary that we can have for a particular combination of delay and sampling time before the system gets unstable. So, we can say that having any control gain value above the surf plot destabilizes the system whereas, having it below the surface can guarantee system stability.

From the plot on the right side, we can see each region separated by a lines and the slope of these lines shows the sensitivity of delays to the sampling time and vice versa. Here we can see that the delays are much more sensitive to performance than sampling time. Also we can see here that the sensitivity of sampling time starts to increase at higher delay value.

7.2 Simulation results and inference

In this section, results from the simulation using IPG Carmaker and Matlab/Simulink are shown and discussed in detail. Among the three controllers: Skyhook, Fully active LQR and System with Road preview, only the skyhook and some important results of the LQR are discussed here. The results from the preview system and

remaining results of the LQR controller are presented in the final Appendix.

The order at which the results are presented is as shown in the methodology section, in figure 6.4. First, the results of the effect of delays are analysed. Here, both level and accelerometer sensors are delayed by the same magnitude. The analysis was carried out for both active and semi-active suspension system. Next, the effect of signal synchronization is studied. In this case, both the level and accelerometer sensor signals are delayed with different values. Thus, the signals are delayed and unsynchronized. Finally, the effects of signal errors/inaccuracy of the performance of both the system are studied in detail.

7.2.1 Effects of signal delays

Here the simulation was carried out with delays on both accelerometer and level sensor. The simulation results for both semi-active with skyhook controller and LQR active suspension is presented in this section.

7.2.1.1 Positive-negative ramp

This test case was generated to excite the damper speed to high speed and analyze the effects of delays in the time domain. Here both level and accelerometer sensors are delayed by 100 ms for the semi-active suspension and 30 ms for the Active suspension. The magnitude of the delay values were chosen to show a clear difference in the system with and without delay.

The figure 7.11 shows the final result from the Positive-negative ramp test case. Here the results of the semi-active suspension are plotted on the left side and result of the active suspension is plotted on the right side.

The subplots in the figure 7.11 below are plotted in an order starting with road impact on the wheels. This in turn directly translates to damper velocity. This plot of damper velocity is plotted in the first row. Due to this impact, there will be vehicle motion in heave and pitch. Both the vehicle motion: heave and pitch, along with damper velocity that is measured by the sensor are delayed before they are sent to the controller to generate the request force. This request force is then is plotted in the second row. This request damper force is converted to damper current within the controller and is plotted in the third row in the case of semi-active suspension. This current signal is then sent to the damper model to generate the damper or actuator force. The damper force is then plotted in the third row for the active suspension. Finally, the forces that are generated by the dampers then control the vehicle motion to mitigate the heave, pitch and roll motion. The results of the heave and pitch velocity signals are plotted in the 4th and 5th row.

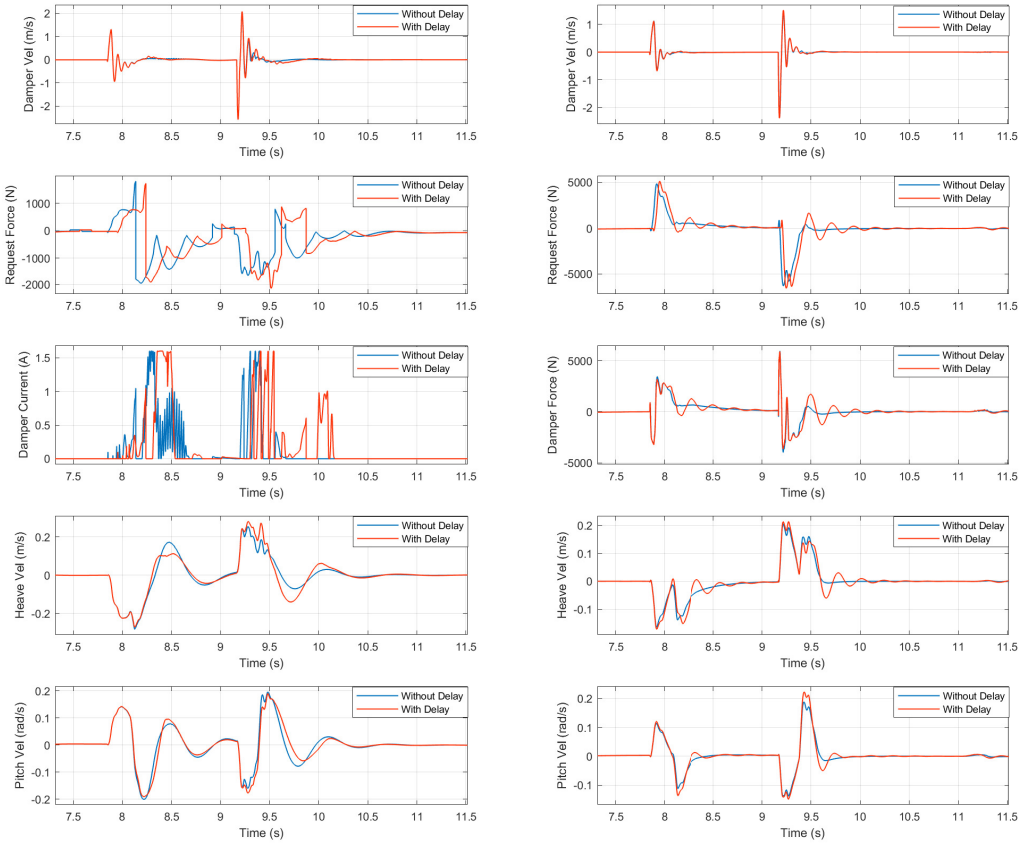

Figure 7.11: Comparison of Semi-active and Active suspension with and without delays(100 ms for semi-active and 30 ms for active suspension).

Inference: Two main inference can be drawn from the results. The difference in the semi-active suspension with and without delay is only visible in high damping speed around 2 m/s with an increase in amplitude. Whereas the difference is less in the lower damping velocity range. Similarly for pitch, the effect is very much visible in the high damping speed whereas not so much difference in the low speed. On the other hand, it can be noted that there is a clear difference in the active suspension case. The active suspension system with delay is highly oscillatory in comparison to the case withoutdelay.

7.2.1.2 Step steer test

The objective of this test case is similar to that of the positive-negative step road, but here we are specifically targeting to excite the roll motion of the vehicle. Similarly, here both level and accelerometer sensors are delayed by 100 ms for the semi-active suspension and 30 ms for the Active suspension.

The description of the figure is similar to that of the positive-negative ramp profile, Except the roll velocity is plotted in the fourth row instead of heave and pitch motion.

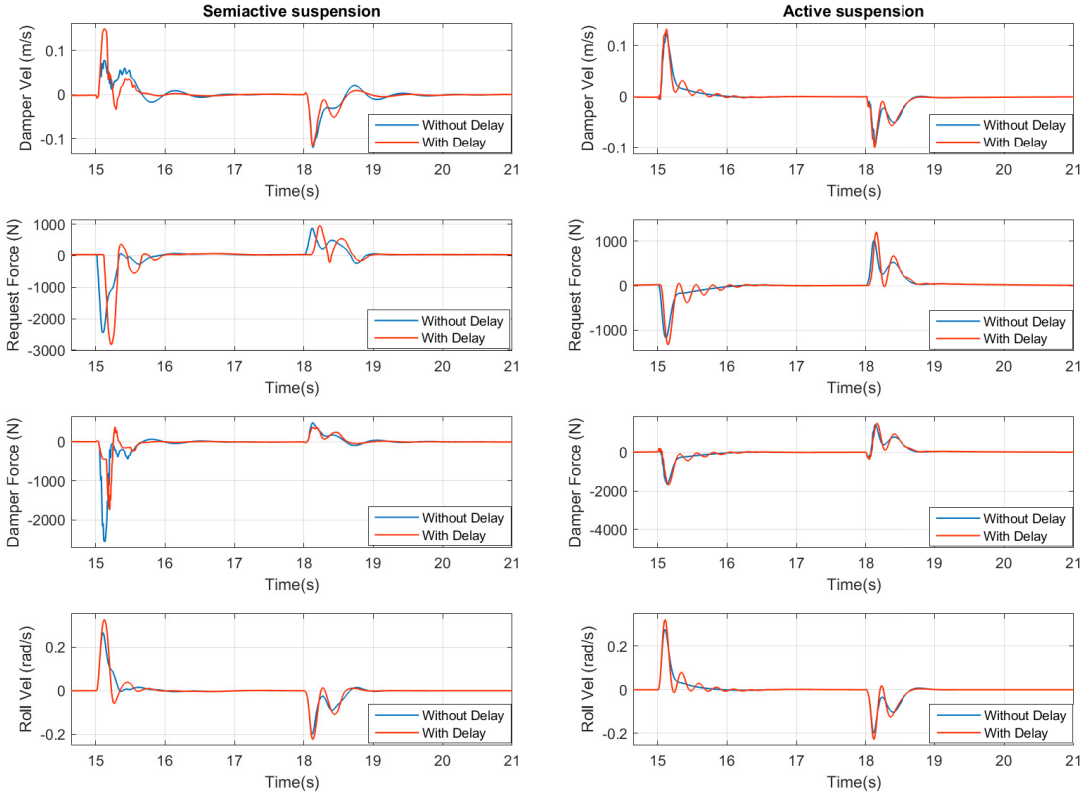

Figure 7.12: Comparison of Semi-active and Active suspension with and without delays(100 ms for semi-active and 30 ms for active suspension).

Inference : The performance degradation caused by the delays on the roll motion of the vehicle seems to be quite high in comparison to the heave and pitch motion. This is the case in both active and semi-active system. Another important point worth noting is that roll velocity on the positive magnitude is affected more than the negative roll velocity, even though the magnitude of the step input is the same in both directions.

7.2.1.3 Stochastic road: Index-C

The stochastic road with index C offers a better trade-off between too soft and extreme rough road. This makes this test case suitable for analysing comfort. The output plots that were obtained from this test case are transfer function, RMS, Weighted RMS and Covariance analysis plots.

Transfer function plot

Time-domain plots are intuitive in analysing the performance of the vehicle than other metrics. But analysing the system in time domain doesn't give complete information about the system. Hence the system was examined in the frequency domain, to visualize the effects of the delays at different frequencies.

The objective in this analysis was to get the results of the transfer function from

road displacement to heave acceleration of the vehicle at different frequencies. Here both the active and semi-active system was simulated in the stochastic road of index C. For this road condition, the simulation was carried out for three different delays values: 0, 30 and 100 ms for the semi-active system, and 0, 20 and 40 ms for the active suspension.

The final results of the semi-active suspension are presented on the left, and that of the active suspension is shown on the right in figure 7.13.

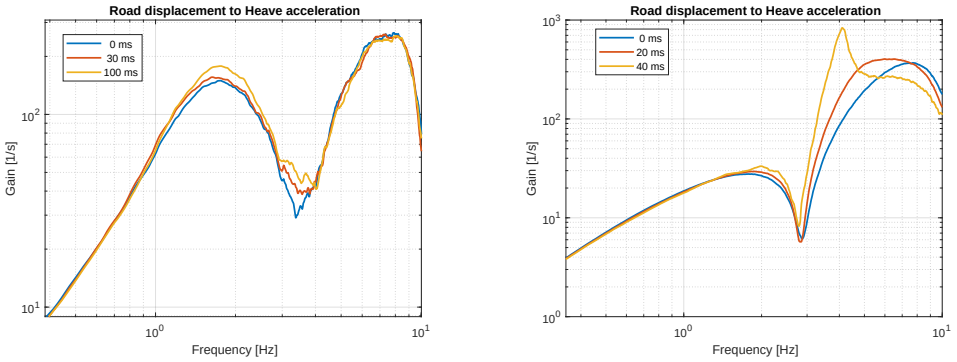

Figure 7.13: Transfer function plot from road displacement to heave acceleration for different delay (0, 30 and 100 ms for semi-active on left and 0, 20 and 40 ms for active suspension on right)

Inference : As can be seen from the figure 7.13, on the left, the transfer function gain increases for the semi-active suspension system as we add delays into the system, specifically in the primary ride frequency range 0.01 - 5 Hz. Whereas from the right side of the figure in 7.13, it can be noted that for an active suspension system, the gain increases in both primary ride and secondary ride. But the magnitude of gain in the secondary ride frequencies is significantly higher than the primary ride frequency range. The plot also shows how sensitive the system is in the presence of delays in the system. In comparison with each other, it can be concluded that the active suspension is more sensitive to the presence of delays, whereas not so much in the semi-active system.

RMS Plot

The previous plots were to get an insight in into the system behaviour. But, to get an objective value so a comparison can be made in terms of the performance difference, the RMS measure is taken for the acceleration signal for different delay values.

In this analysis, the vehicle was simulated in the stochastic road with Index C. This track was chosen as it shows a good performance difference in comparison to other test tracks. Here, the simulation was carried out by sweeping the magnitude of delay for both the level and accelerometer sensor from 0 to 200ms for the semi-active suspension, and 0 to 60 ms for the active suspension.

For both the semi-active and active, three different plots were obtained. In figure 7.14, the first plot is a direct plot of RMS heave acceleration and different delay values. The plot in the second row shows the sensitivity of the performance difference in percentage. Finally, in figure 7.15, the overall performance degradation in comparison to the system without delay is presented.

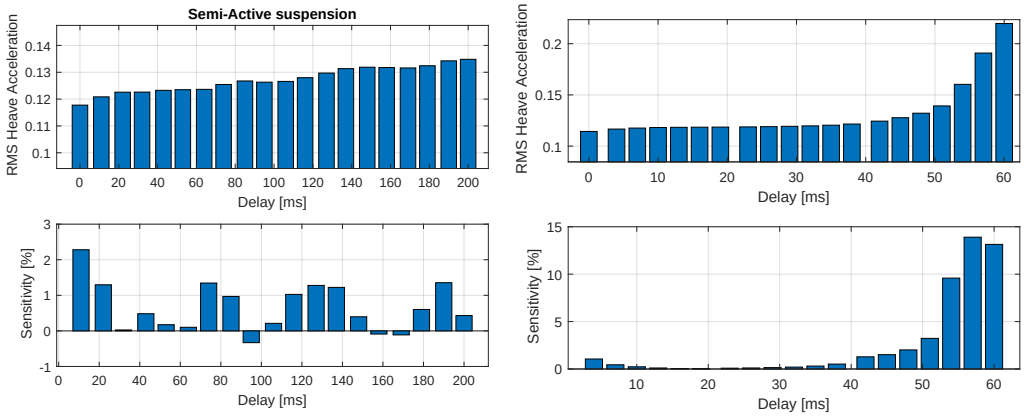

Figure 7.14: Root mean square of heave acceleration for different delays

Inference : The results from the performance analysis of active suspension are quite straightforward, as can be seen in both the figure 7.14 and 7.15. As we add delays into the system, the performance gets exponentially worse. It should be noted that the simulation was carried out until 60ms as the system starts to get unstable beyond that value. As for the semi-active system, performance difference sensitivity is less in comparison to the active suspension system. Nevertheless, as can be seen from figure 7.15 that performance degrades as we add delay into the system from 3% at 15ms delay and increases to 15% at around 200 ms delay value.

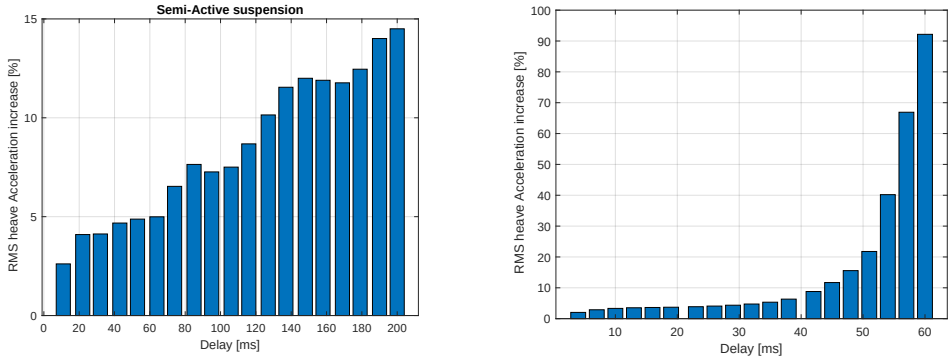

Figure 7.15: Percentage increase in Root mean square of heave acceleration for different delays

Weighted RMS plot:

The weighted RMS plot shows how much acceleration that can be tolerated by a human being. The description of this particular evaluation method is given in the methodology section.

In this test case, the active suspension was evaluated for three different delay values: 0,20 and 40 ms. Whereas the semi-active suspension was evaluated for 0, 67, 134 and 200 ms. The final results are as shown,

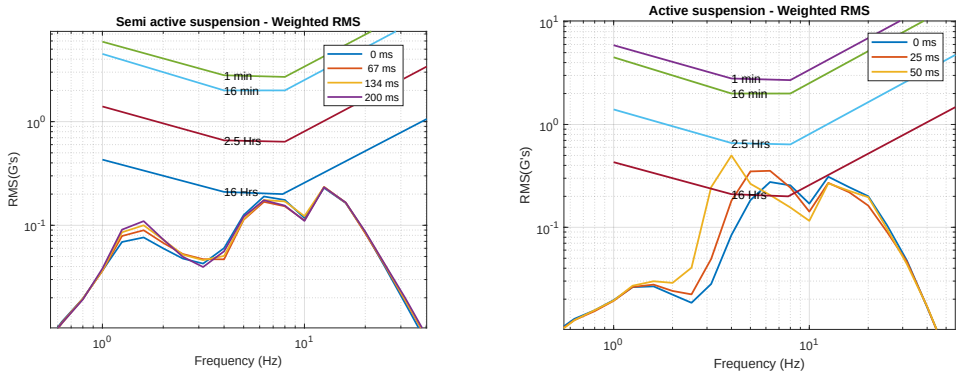

Figure 7.16: Weighted RMS plot for different delays(for semi-active on left and for active on right)

As can be seen from figure 7.16, the result of the semi-active suspension on the left side and the result for the active suspension on the right side. In the case of semi-active suspension, the frequency weighted RMS in Gs are less than the maximum tolerable limit. And it can be noted that there is a major difference in the performance, mostly in the primary ride frequency zone and not any significant difference in the other frequency regions.

In the case of the active suspension, all the three test cases cross the "16 Hrs" threshold. This happens around the secondary ride frequency zone. But the case with 50ms delay is very close to "2.5 Hrs" threshold, slightly below the secondary ride frequency zone and is not tolerable.

Covariance analysis

In this test case, the analysis was carried in loops from 0 to 200 ms in twenty steps for the semi-active system, and 0 to 60 ms in twenty steps for the active suspension system. The simulation was carried out in the Stochastic road with Index C.

The final results are plotted in figure 7.17. Here the result of the semi-active suspension is plotted on the left, and that of the active suspension is shown on the right. They are two subplots in the figure. The result of normalized suspension deflection and normalized heave acceleration is shown in the first row Whereas the normalized tire deflection and heave acceleration are shown in the second row. And ideally, lower values in these normalized data signifies the better performance of the system.

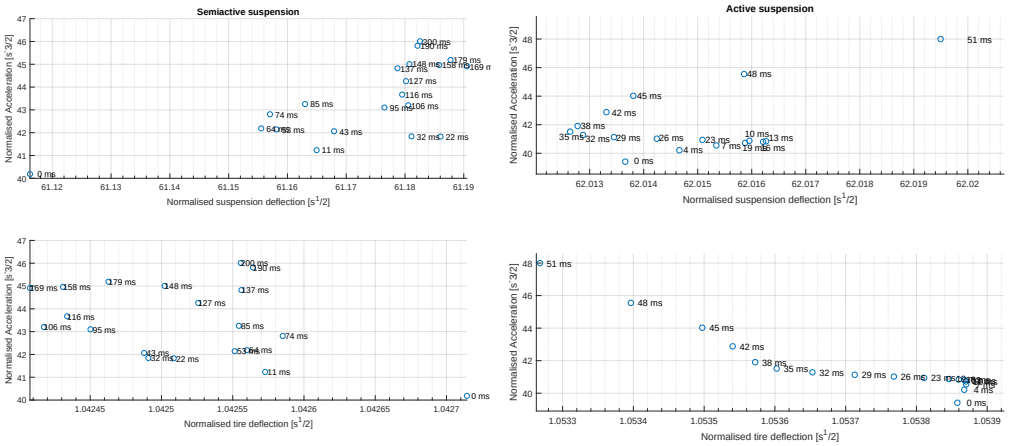

Figure 7.17: Covariance analysis of Normalized acceleration against tire deflection for different delays

Inference : From the figure 7.17, it can be noted that as we add delays into the system, the performance gets worsen overall for heave acceleration, but drops in some cases for the semi-active system. It should also be noted that the suspension and tire deflection are more oriented towards the decreasing side as it can be noted in the x-axis. But since their magnitude is very small, it is neglected in the study. On the other hand, for the active suspension system, the performance clearly drops as we add delays, but the tire deflection drops in non-linear curve pattern. But since the magnitude is very small, it can be neglected here as well.

7.2.1.4 Sinus steering

Next, the performance of the vehicle in Roll direction is evaluated. The effects of delays on the controller in the time domain were evaluated in section 7.2.1. In order to analyse the system in the frequency domain, the vehicle is simulated with sinus steering with frequency from 0-4Hz. Here the semi-active skyhook controller was simulated for three different delay values: 0, 30 and 100 ms and the active suspension LQR controller was evaluated for 0, 20 and 40 ms. The final results are as shown.

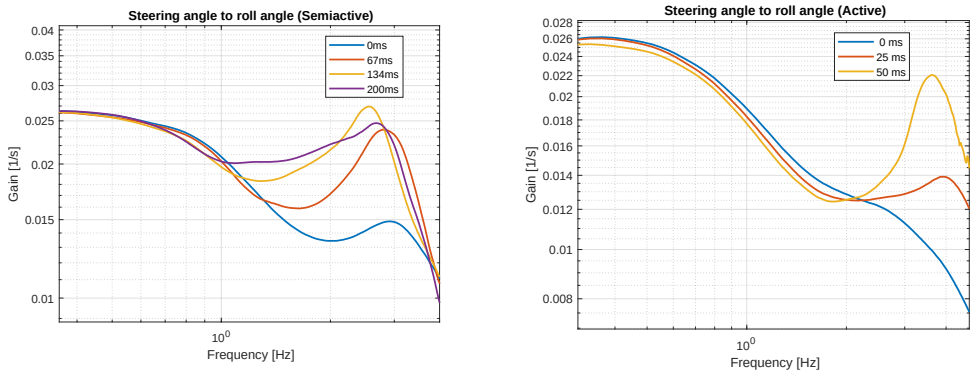

Figure 7.18: Transfer function plot from steer angle to roll angle for different delays

Inference: As can be seen from the figure 7.18, when the delays were added into system, the performance get worsen as the frequency is increased and then drops around the 4 Hz. This the case for the semi active suspension system. In the case of the active suspension, the amplitude is less up to a frequency range of 2 Hz and then it starts to increase significantly as the frequency is increased.

7.2.1.5 FE Road

FE road is part of the HPG, and the description of the track is given in the methodology chapter.

Ride diagram:

The ride diagram shows are good difference in terms of performance even for a smaller delay value. Thus for this test case, the analysis for both the controllers was carried out with three different delay values: 0,10 and 20 ms. The final results from the simulation are shown in 7.19. Here the result of the semi active suspension is plotted on the left side and that of the active suspension is plotted on the right side.

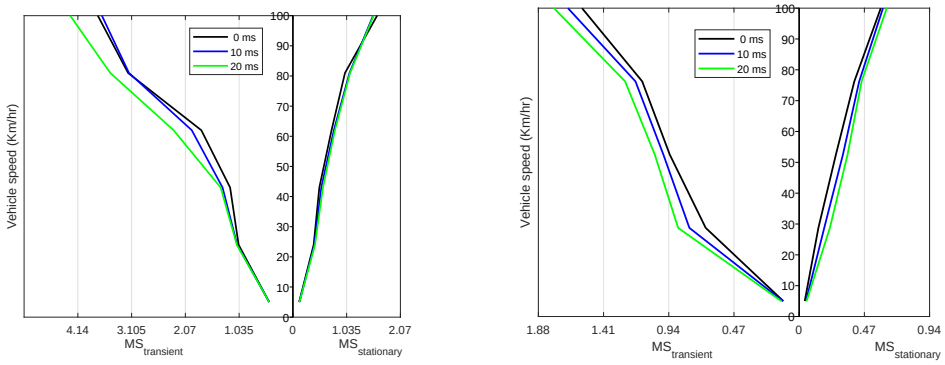

Figure 7.19: Ride diagram for both semi-active and active suspension

Inference : From figure 7.19, it can be noted that there is a better performance degradation difference for both active and semi-active suspension even for a small delay magnitude in the transient side. This is especially true as the vehicle speed is increased. Not much significant difference is noticed on the stationary side of the analysis.

7.2.1.6 Handling track

Histogram:

The histogram shows the number of occurrence of numerical data in the signal. In this thesis work, the histogram of all the four damper velocity is taken for the analysis, for the test case with and without delay. Here a delay model based on the Markov chain is implemented for the test case with delay. The final results for the semi-active suspension are as shown,

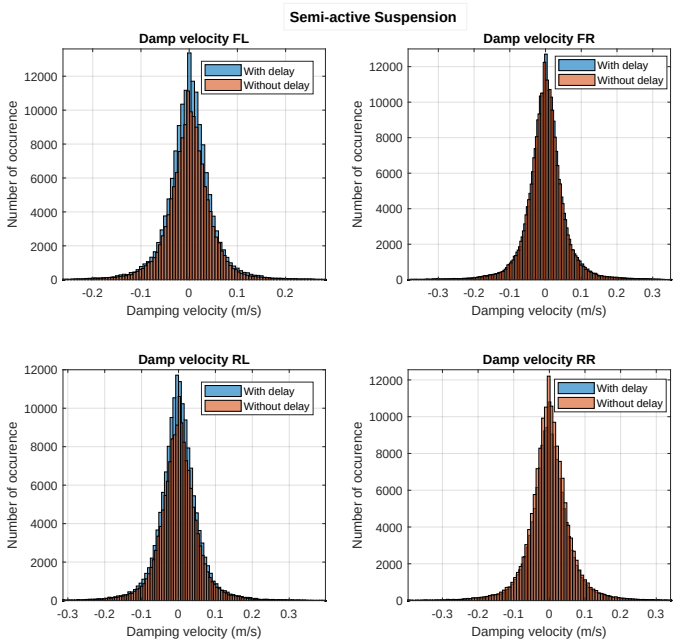

Figure 7.20: Histogram data for Semi-active suspension for both with and without delay

Inference: From the figure above, for the semi-active suspension, the number of occurrences increases in the low to medium speed region, for the case with delay as compared to the case without delay. It should also be noted that this behaviour is highly predominant in the left side.
The histogram plot for the active suspension system is as shown,

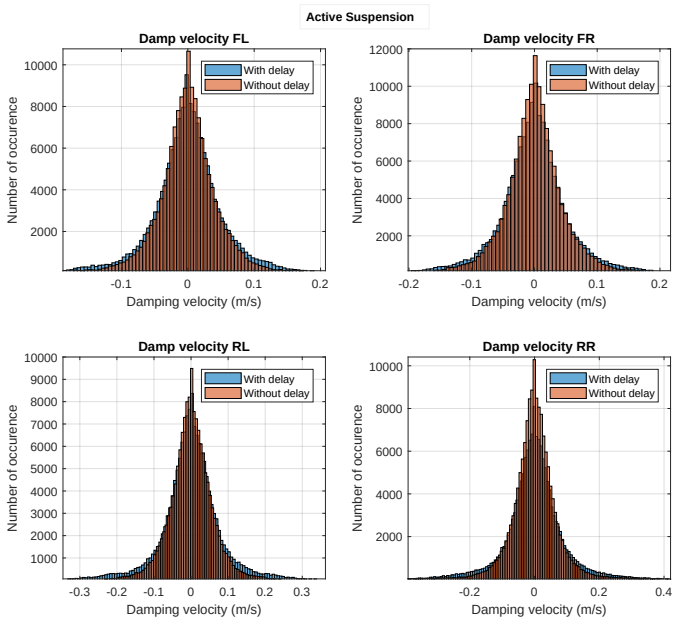

Figure 7.21: Histogram data for active suspension for both with and without delay

Inference: For the active suspension, the number of occurrences of damper velocity decreases in the low-speed range and moved more towards the high-speed range. This increased number of occurrences of the high-speed damping velocity leads to high body oscillation, thus resulting in performance degradation.

Statistical results:

The graphical representation of the histogram provides a good insight by visualization, but there are a lot of other numerical values that can be extracted from the histogram for analysis of the suspension system. The table below represents the statistical parameters and their values of the front left damper histogram for both semi-active and active suspension system.

Parameters	Without delay	With delay
Zero bin height	20435	23597
Percentage low-speed bump	48.817	48.493
Percentage low-speed rebound	45.571	45.738
Percentage high-speed bump	2.5784	2.7324
Percentage high-speed rebound	3.0334	3.0363
Average damper speed in bump	0.034845	0.035349
Average damper speed in rebound	-0.036882	-0.037162
Median	0.00053076	0.00036857
Standard deviation	0.054258	0.055339
Skewness	-0.10828	-0.21456
Kurtosis	13.506	16.257

Table 7.1: Statistical data for semi-active suspension

Parameters	Without delay	With delay
Zero bin height	19812	17436
Percentage low-speed bump	48.242	46.221
Percentage low-speed rebound	46.748	45.281
Percentage high-speed bump	2.3898	4.2568
Percentage high-speed rebound	2.6206	4.2409
Average damper speed in bump	0.033609	0.040005
Average damper speed in rebound	-0.034505	-0.040727
Median	0.00017049	0.00015077
Standard deviation	0.049558	0.058065
Skewness	-0.21176	-0.11328
Kurtosis	10.403	7.51

Table 7.2: Statistical data for active suspension

Inference: Some of the interesting parameters from the table for studying the effects of the delays are the average damper speeds, percentage in rebound and skewness. In the case of the semi-active suspension system with delay, the occurrence percentage in rebound is increased in both high and low speed. The average

damper speeds for both bump and rebound are increased as well. Finally, from the skewness value, it can be inferred that the histogram of the case with delay has skewed more towards the rebound side in comparison to the case without delay.

In the case of the active suspension, similar trends can be seen. Except, the magnitude of difference in the percentage of occurrence, damper speeds etc are much higher in comparison to semi-active suspension.

7.2.1.7 Multiple test track

Table 7.3 is the performance difference table, that shows the RMS of heave, pitch, roll and jerk difference calculated for different test cases which is based on the markov delays with three different network loads that has mean of 10ms and variance of 1 for low load state, 50ms for mean and 10 for variance in medium load state, and finally 100ms for mean and 5 for variance in high load state.
The heave, pitch, roll and jerk difference is calculated as

$$\text{Difference} = |RMS_{\text{with delay}} - RMS_{\text{without delay}}| * 100 \tag{7.2}$$

The minimum and maximum value of heave, pitch, roll and jerk difference is highlighted with green and red colour respectively.

Test Cases	Heave Difference	Pitch Difference	Roll Difference	Jerk Difference
FEC Road	0.95744	0.69632	4.1237	70.812
FE Road	2.0066	0.2198	2.0491	130.29
Lane Groove	0.14518	0.20745	1.2592	117.98
LD Innerlane	1.5564	1.0387	8.0754	45.206
LD Road	0.7294	0.13365	3.8229	110.38
Neg-positive ramp	0.59411	0.11492	1.2592	117.98
Positive ramp	6.9397	3.7292	7.2113	888.74
SB Road	1.3845	2.1672	8.0318	389.78
SH Road	0.94755	1.421	2.1574	188.6
Sinus steer	1.3503	1.227	25.748	121.24
Step steer	0.80214	0.30434	4.2609	31.799
Stochastic A	1.5726	1.695	1.506	398.52
Stochastic B	0.93663	1.9823	0.89266	239.89
Stochastic A	0.41899	5.2726	0.16132	281.86
HPG	0.59419	0.40025	4.1381	53.287
Sine road	0.70152	4.3939	2.9706	68.518
Wavy step road	1.565	8.2208	9.342	854.13
Pot hole	0.94977	0.65317	1.1103	178.92

Table 7.3: Performance difference table of different test cases for heave, pitch, roll and jerk

Inference: As can be seen from the above table 7.2 , For heave difference, Lane groove results in better performance than other test cases whereas the positive ramp

results in worst performance. For pitch difference, negative-positive ramp results in better performance than other test cases and wavy step road has the worst performance. Similarly, for roll difference, stochastic road index-A has better performance and sinus steer results in worst performance compared to other test cases. Finally, for jerk difference, step steer has better performance and positive ramp has worst performance compared to other test cases.

7.2.2 Effect of synchronization

Until now, in all the test cases both the accelerometer and level sensors were delayed by the same magnitude. Now, in order to study the effects on signal synchronization, the level and accelerometer sensors are delayed by a different value. In this analysis, only the results of the semi-active suspension are shown and discussed. The results of the active suspension system are added in the final Appendix as it was previously concluded from the analytical results they not so sensitive to synchronization.

7.2.2.1 Stochastic road: Index-C

Transfer function plot

The objective in this analysis was to get the results of the transfer function of the road displacement to heave acceleration of the vehicle at different unsynchronized delays for both accelerometer and level sensor delay. Here the semi-active suspension system was simulated in the stochastic road of index C. For this test case, the simulation was carried out for four different unsynchronized delay values for both accelerometer and level sensor. The final results are shown in figure 7.22. The results from the semi-active suspension when accelerometer delay is higher than level delay is shown in the left side, and the final results where level sensor delay is higher than accelerometer sensor delay is plotted on the right side.

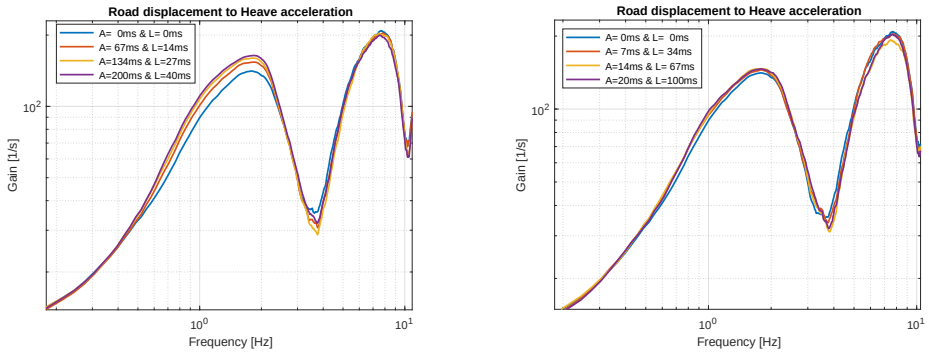

Figure 7.22: Transfer function plot of unsynchronized delays for semi-active suspension

Inference: As can be seen from the figure 7.22, the performance of the system gets worsen specifically in the primary ride frequency range 0.01 - 5Hz for the case when accelerometer delay is higher than level sensor delay (plot on the left). Whereas from the right side of the figure 7.22, the test case with level sensor delay higher

than accelerometer sensor delay, the performance degradation is not so significant and is almost negligible.

Covariance plot

Here the result from the covariance analysis for unsynchronized delays cases is shown. The simulation was carried out in the Stochastic road with Index C. The final results are shown in figure 7.23. Similar to the previous transfer function plot, there are two cases in this analysis as well. The orange circle data in figure 7.23 represents the case where the level sensor delay is higher than the accelerometer sensor delay. And the blue square box represents the data where the accelerometer sensor delay is higher than the level sensor delay.

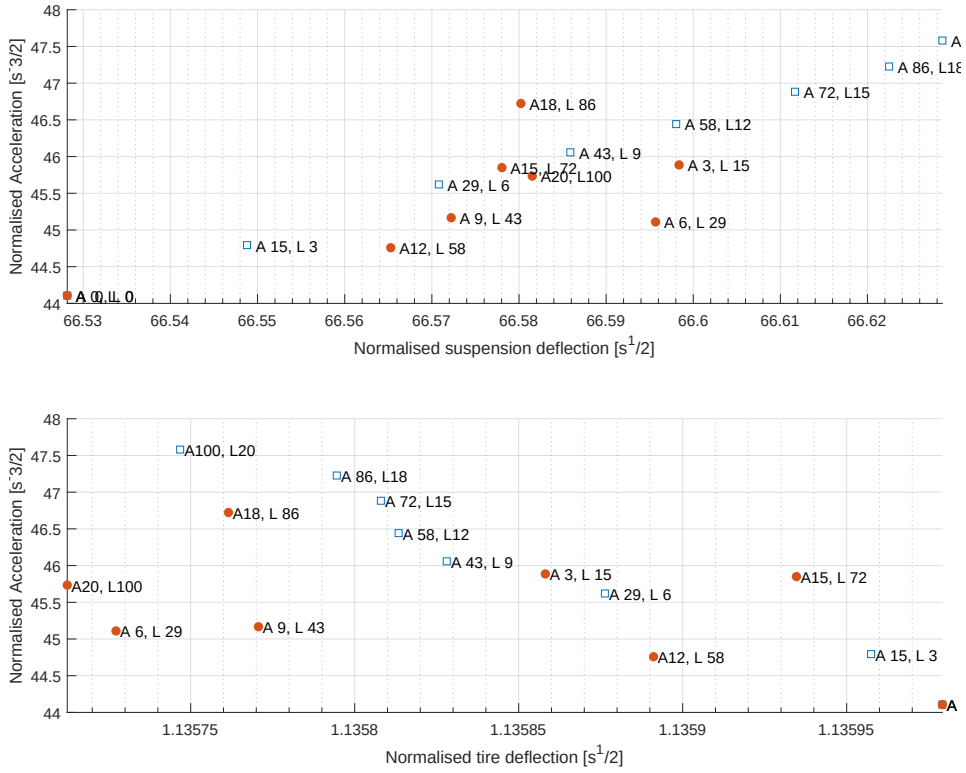

Figure 7.23: Covariance plot of unsynchronized delay for semi-active suspension

Inference: From the first subplot in the figure 7.23, the suspension deflection increasing linearly with increasing heave acceleration when accelerometer delay is higher than level delay. But the case with level sensor delay higher than accelerometer sensor delay doesn't follow any pattern. It increases and decreases randomly in both suspension and tire deflection. From the second subplot in the figure 7.23, the tire deflection decreases and heave acceleration increases when accelerometer delay is higher than level delay. But this decrease in tire deflection is very small and negligible.

Delay Sweeps

In this analysis, the magnitude of delay of the two sensors: level and accelerometer sensor are swept from 0 to 100 ms in 10 different steps. The performance index was evaluated for each combination of the delay value. Here the performance index is the combination of RMS of heave, pitch and roll motion with different weights. Therefore smaller the value of performance index, better is the system performance. Finally, the level sensor and accelerometer sensor delay are plotted against their respective performance index. The contour version of the plot is shown in figure 7.24.

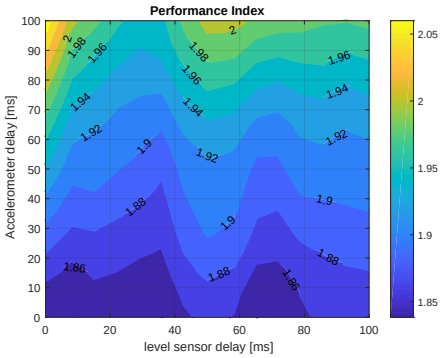

Figure 7.24: Effect of synchronization of accelerometer and level sensor for both semi-active suspension by sweeping the delays

The results are interpreted with three different extreme cases. The first test case, in which accelerometer delay is 100ms and level sensor delay is 0 ms results in the performance index value of approximately 2.05. This is a case with signals unsynchronized. Next, the performance index is evaluated for the second extreme case in which the accelerometer sensor delay is 0ms, and the level sensor delay is 100 ms. The value is found to be around 1.88, which is quite low compared to the previous case. Finally, in the third case, the performance index is evaluated, keeping both accelerometer and level sensor delay to 100 ms. Here the value of performance index is around 1.98, which is intermediate between the maximum and minimum range. So having 100 ms delays on both the sensor signal is better than having 100 ms delay only on the accelerometer sensor signals. From these analyses, it can be concluded that having the signals synchronized can significantly help in improving the performance in the system.

7.2.3 Effects of Signal errors

Signal errors are another common issue within the network control system, and in the following section, its influence on the performance of the semi-active suspension is studied in detail.

7.2.3.1 Time domain

In this analysis, the semi-active suspension with skyhook controller was simulated in the stochastic road profile with road index C, for three different bit values. A portion of the final analysis is shown in figure 7.25.

There are two subplots in the figure. The first subplot is a plot of heave velocity signal that was quantized before going to the controller, and the second subplot shows the figure of the true heave velocity of the vehicle body.

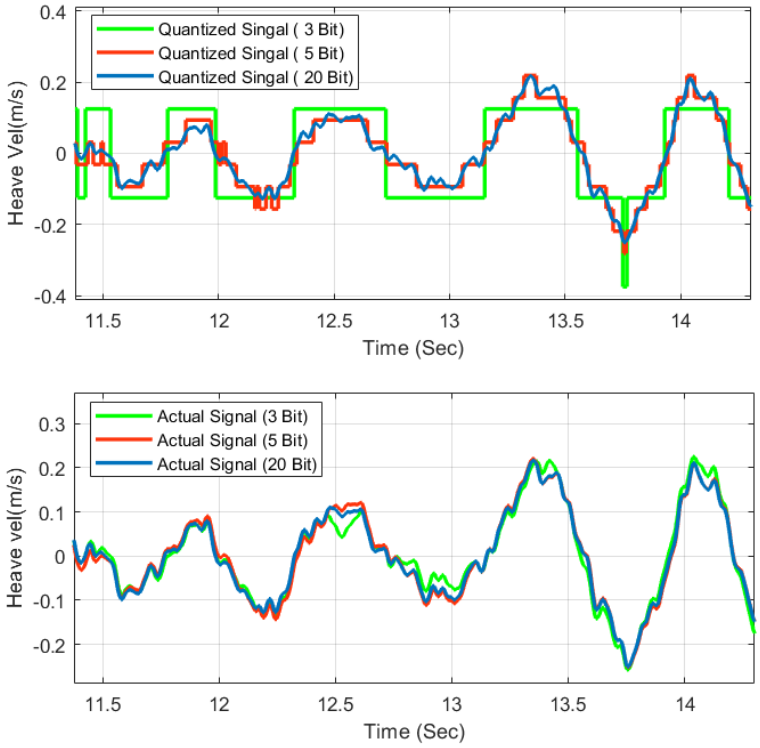

Figure 7.25: Time domain

Inference: As can be seen from the above figure, the performance drops for the case with 3 Bits, although not as significant as delays. And the case with 5 and 20 bits seems quite similar but with 5 bits showing slight performance degradation at certain situation.

7.2.3.2 RMS Difference

In this analysis, the vehicle was simulated with stochastic road profile as well. Here the RMS of the heave acceleration was computed for bit size from 0 to 20. In the case with zero bit size, the input to the controller is just constant zero, making it inactive. The final results are as shown,

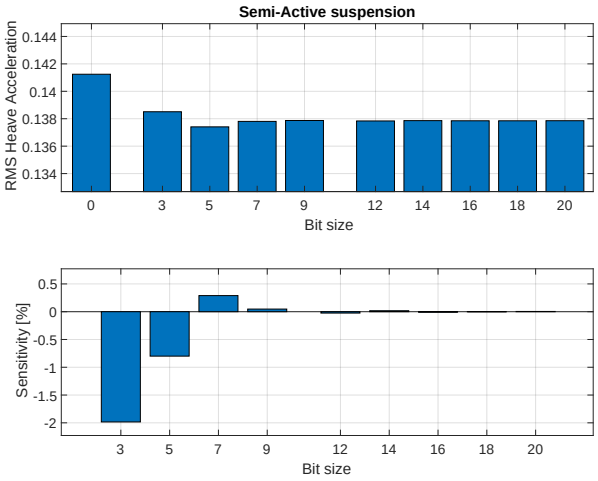

Figure 7.26: RMS bar chart

Inference: From the figure, it can be noted that the performance difference is quite low for the different magnitude of signal errors. A similar effect can be seen in the performance sensitivity plot as well.

7.2.3.3 Quantization and delay sweep

This analysis was carried out to study the effect of both delays and errors. In this, the magnitude of both the sensor delays is swept from 0 to 100 ms in ten steps and its errors is swept by changing the bit size from 4 to 14. The performance index was evaluated for each combination of the delay and error value. Here the performance index is the combination of RMS of heave, pitch and roll motion with different weights. Therefore smaller the value of performance index, better is the system performance. Finally, the sensor delays and bit size are plotted against their respective performance index. The contour version of the plot is shown in figure 7.24.

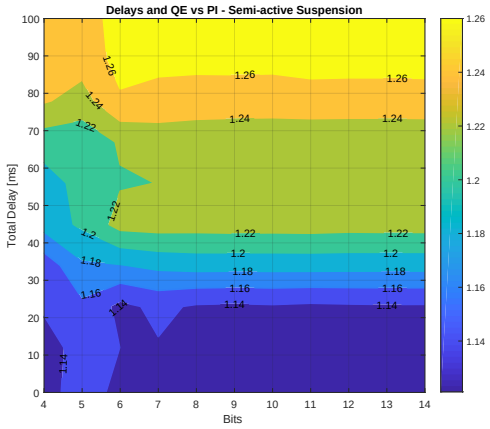

Figure 7.27: Effect of synchronization of total delay and number of bits against performance index for both semi-active by sweeping the delays

Inference: For semi-active suspension, there is a performance difference in the system up to a bit size of 6 and is found to be sensitive in the mid delay value around 30 to 80 ms. The sensitivity of signal error is lowest around the lower delay region. It is also found that there is no improvement in the performance of the system beyond the bit size 6. Finally, from this figure, it can also be clearly noted that the delays have a higher influence on the performance than the signal errors.

7.3 Controller

In this thesis work, two different controllers were evaluated to compensate for the delays in the system. First, a smith predictor is implemented for the semi-active and active suspension system. The reason of choice for this controller is its simplicity, and also it is modular, i.e it works together with the semi-active controller rather than a complete replacement of the controller. Finally, an LQG controller was implemented for the active suspension system as well. The results for these controllers are as shown.

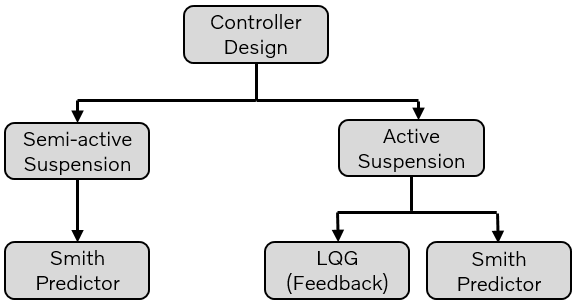

Figure 7.28: Structure of controller

7.3.1 Smith predictor - Semi-active suspension

The fundamental theory behind Smith predictor is given in chapter 2. Here, the results from the final simulation run in IPG carmaker for semi-active suspension with smith predictor are shown and discussed in detail.

7.3.2 Time domain

The results from the simulation are first compared in the time domain. The Smith predictor is simulated in the positive-negative ramp test run at constant velocity with three different test case: Skyhook without any delay or compensation in the system, Skyhook with 100 ms delay and compensation in the system and finally a smith predictor with 100 ms delay. All three comfort metrics: Roll, Pitch and Heave velocity with respect to time are plotted as shown,

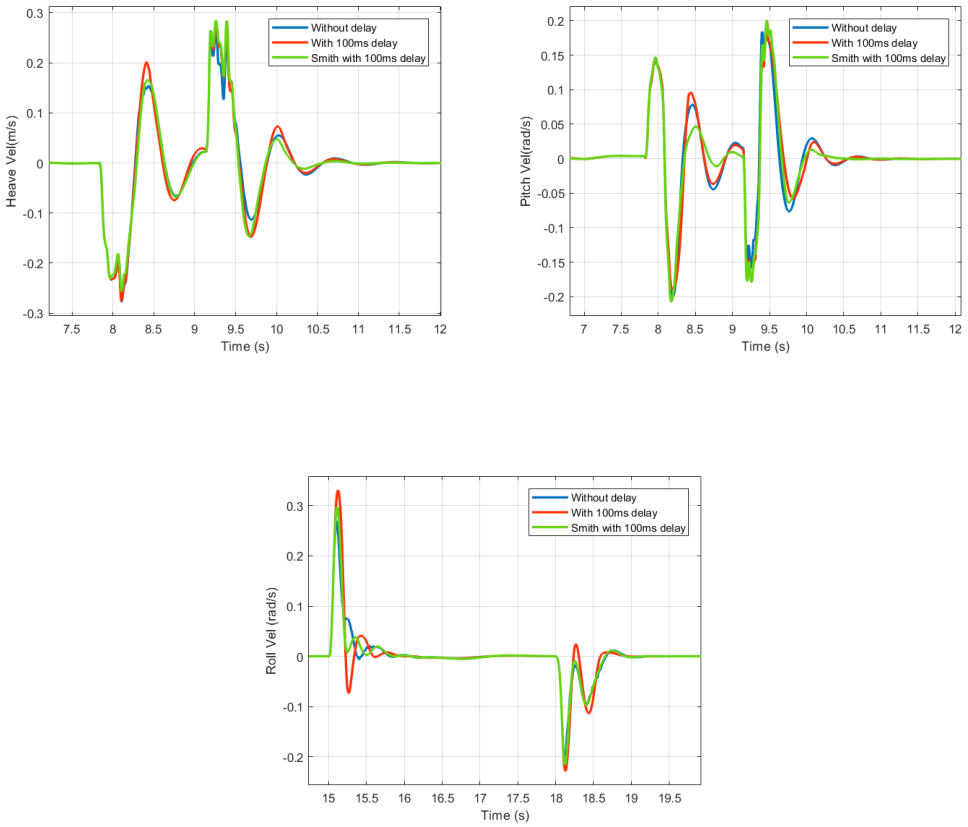

Figure 7.29: Time domain

Inference: As can be seen from the figure 7.29, the smith predictor tracks the system without delay with minor error only in the case of heave motion. The difference in error is high for both pitch and roll motion case. These difference could be due to the limitation on the complexity of the mathematical model within the skyhook.

7.3.3 Frequency domain

Next, the results of the controller with smith predictor's performance were plotted in the frequency domain by taking the transfer function from the road displacement to heave acceleration to analyse the heave performance and they are plotted on the left side in figure 7.30. The transfer function from steer to roll angle, to analyse the roll motion performance is plotted on the right side on the figure. Here the smith predictor was evaluated from 0 to 100 ms with four different samples. The final results are as shown,

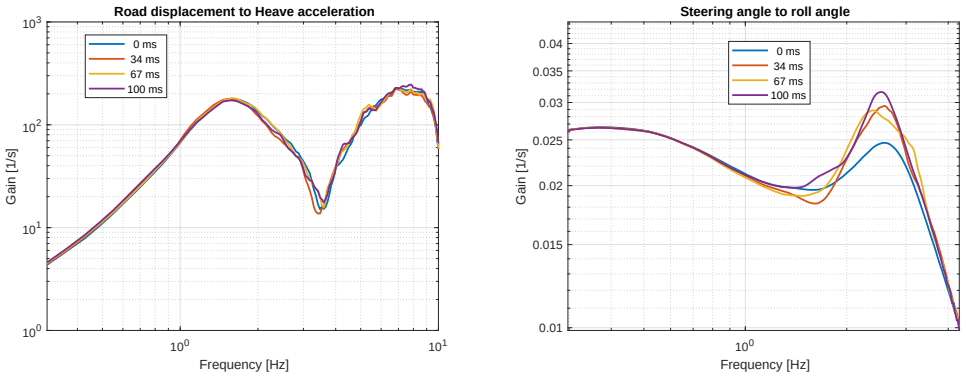

Figure 7.30: Frequency domain

Inference: The figure on the left, it can be noted that when the delays added into the system, the smith predictor compensates the delays with minor performance difference at certain frequency compared to a typical semi-active suspension without any compensation in figure 7.13. The transfer function of steer to roll angle is plotted on the right side. Here, the performance of the smith predictor is not as good as the Heave performance. It seems to find difficulty in tracking the performance with no delay but the performance difference between different delay values is reduced to a great extent in comparison to the semi-active suspension with only skyhook controller in figure 7.18.

7.3.4 RMS bar chart

Here the semi-active suspension with the smith predictor was evaluated with the stochastic road with index C test case. From this analysis, the RMS of the heave acceleration along with the performance difference is evaluated. Here the vehicle was simulated from 0 to 200 ms with 20 different samples. The final results are as shown,

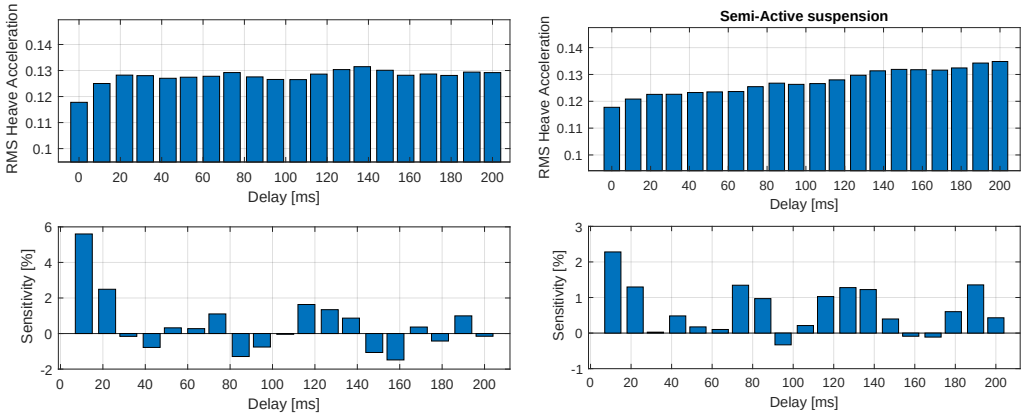

Figure 7.31: RMS bar chart

Inference: In 7.31, the figure on the left is the final result with the smith predictor and the one on the right is the result from the semi-active suspension with the skyhook controller which is plotted again for comparison. From the two figures, it can be noted that smith predictor gives better performance in comparison to the semi-active suspension with skyhook controller alone.

7.3.5 Smith Predictor - Active suspension

7.3.6 Time domain

The results from the simulation are first compared in the time domain. The Smith predictor is simulated in the positive-negative ramp test run at constant velocity with three different test case: Smith predictor without any delay or compensation in the system, Smith predictor with 40 ms delay and/or compensation in the system and finally a LQR with 40 ms delay. All three comfort metrics: Roll, Pitch and Heave velocity with respect to time are plotted as shown,

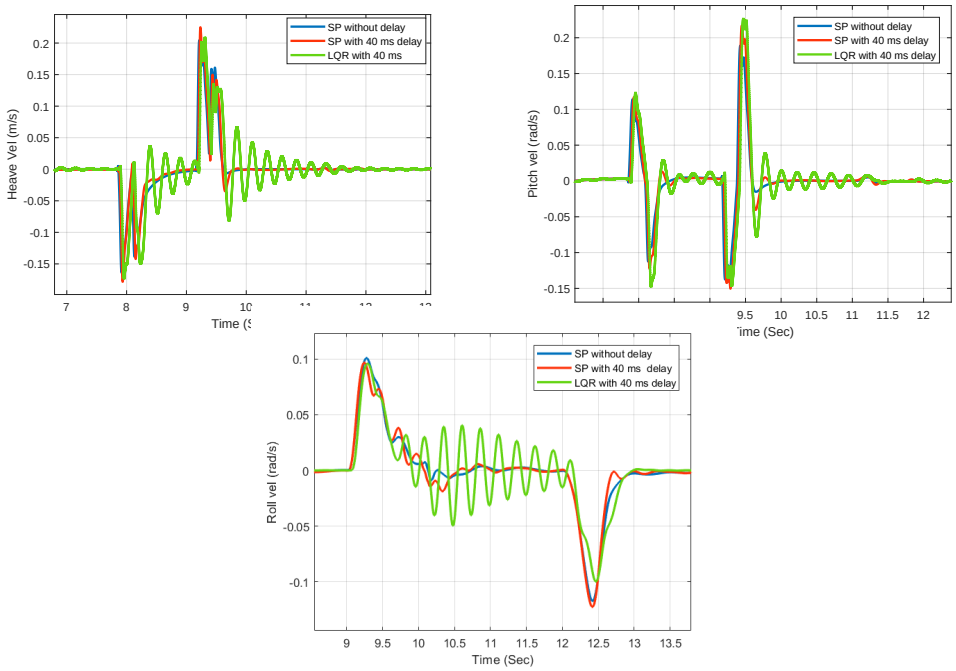

Figure 7.32: Time domain

Inference: As can be seen from the figure 7.32, the smith predictor tracks the system without delay with minor error in all the three test cases as heave, roll and pitch motion. Finally, the result of the LQR controller with 40 ms is also plotted to show that performance of the smith predictor is better than that of the LQR with delay.

7.3.6.1 Frequency domain

Next, the results of the controller with smith predictor performance were plotted in the frequency domain by taking the transfer function from the road to heave

acceleration to analyse the heave performance, and steer to roll angle to analyse the roll motion performance. Here the smith predictor was evaluated from 0 to 50 ms with three different samples. The final results are as shown,

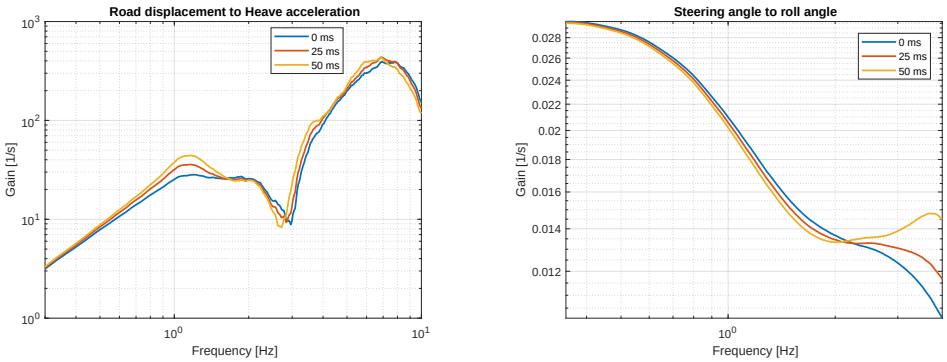

Figure 7.33: Frequency domain

Inference: The figure on the left is the transfer function plot of the road displacement to heave acceleration. it can be noted that when adding a delays into the system, the changes in the system is quite small and robust compared to a typical active suspension without any compensation, especially in primary ride. But still, there is a heavy performance degradation in the secondary ride is similar to the system with no delay. On the other hand, the transfer function of steer to roll angle is plotted on the right plot. Here, it can be noted that the smith predictor is quite better performance compared to the system with no delay.

7.3.6.2 RMS bar chart

Here the active suspension with the smith predictor was evaluated with the stochastic road with index C test case. From this analysis, the RMS of the heave acceleration along with the performance difference is evaluated. Here the vehicle was simulated from 0 to 120 ms with 17 different samples. The final results are as shown,

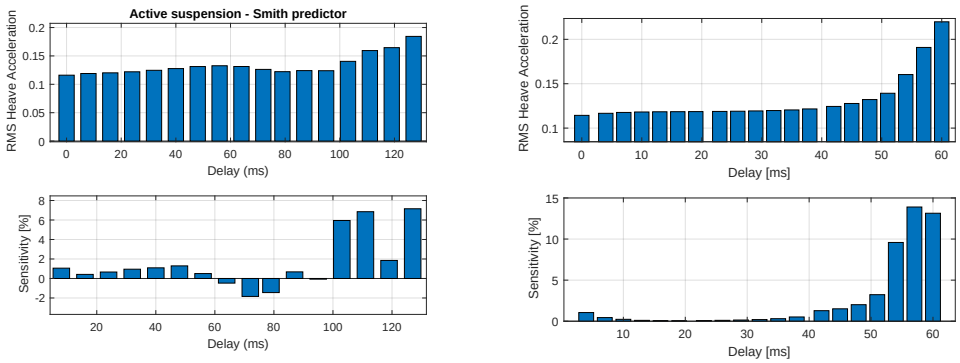

Figure 7.34: RMS bar chart

Inference: In 7.34, the figure on the left is the final result with the smith predictor and the one on the right is the result from the active suspension with the LQR controller which is plotted again for comparison. From the two figures, it can be noted that smith predictor is very much stable till 100 ms and gives better performance in comparison to the active suspension with LQR controller alone.

7.3.7 LQG - Active suspension

The fundamental theory behind LQG controller is given in chapter 2. Here, the results from the final simulation run in IPG carmaker are shown and discussed in detail.

7.3.7.1 Time domain

Here, the results from the simulation are compared in the time domain. This is to show the effectiveness of the controller. The controller is simulated in the positive-negative ramp test run at constant velocity with three different test case: LQG without any delay or compensation in the system, LQG with 60 ms delay and compensation in the system and finally an LQR with 40 ms delay. All three comfort metrics: Roll, Pitch and Heave velocity are plotted as shown,

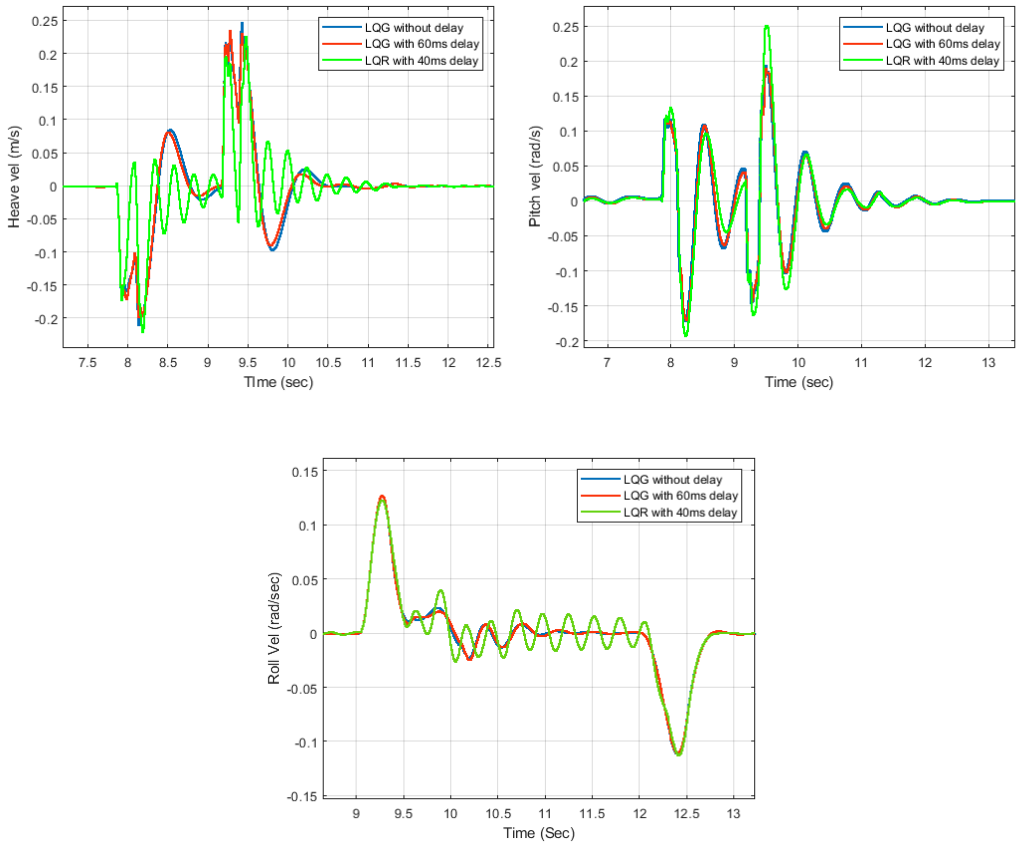

Figure 7.35: Time domain

Inference: As can be seen from the figure 7.35, the delay compensated LQG tracks the system without delays with minor error in all three heave, pitch and roll motion. Finally, the result of the LQR controller with 40 ms is also plotted to show that performance of the LQG is better than that of the LQR with delay.

7.3.7.2 Frequency domain

Next, the results of the controller performance were plotted in the frequency domain by taking the transfer function from the road to heave acceleration to analyse the heave performance, and steer to roll angle to analyse the roll motion performance. Here the delay compensated LQG was evaluated from 0 to 100 ms with four samples. The final results are as shown,

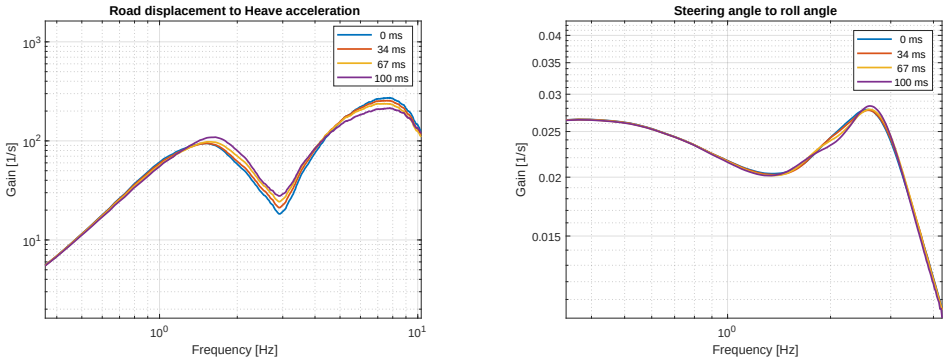

Figure 7.36: Frequency domain

Inference: The figure on the left is the transfer function plot of the road displacement to heave acceleration. it can be noted that when adding the delays into the system, the changes in the system is quite small and robust compared to a typical active suspension without any compensation. But still, there is slight performance degradation in the primary ride and slightly better performance in the secondary ride in comparison to the system with no delay. On the other hand, the transfer function of steer to roll angle is plotted on the right plot. Here, it can be noted that the LQG is quite robust without any major performance degradation in the system.

7.3.7.3 RMS bar chart

Here the active suspension with the delay compensated LQG was evaluated with the stochastic road with index C test case. From this analysis, the RMS of the heave acceleration along with the performance difference is evaluated. Here the vehicle was simulated from 0 to 200 ms with 20 different samples. The final results are as shown,

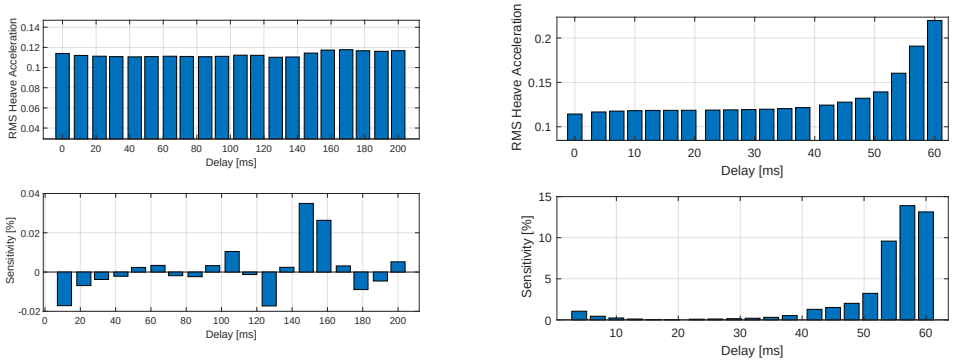

Figure 7.37: RMS bar chart

Inference: In figure 7.37, the one on the left is the final result with the delay compensated LQG controller and the one on the right is the result from the active suspension with the LQR controller. From the two figures, it can be noted that the LQG with compensation is very robust to delay with the change in performance less than 0.04%.

8

Discussion and Conclusion

In this chapter, the main conclusions are drawn from the thesis work and are described along with future scope and improvements. First, some of the key learning outcomes and findings are recalled again and are discussed in terms of modelling, performance analysis and controller. Then some important concepts and methods that were evaluated in this thesis project that is valuable and can be considered for future work are discussed. Then some of the methods and analysis of the project that can be neglected for future works are discussed as well. Furthermore, the main research question and deliverables are then recalled and discussed in detail. And finally, the future works are discussed as well.

8.1 Learning outcomes:

These are some of the main learning's from the project.

- **Delay modelling:** Delays are a function of many different external factors. They are quite stochastic and random like noise and errors. So it is not possible to model them from first principles but can be modelled using mathematical and probabilistic tools.
- **Performance analysis:** Analysis of the semi-active suspension system is not as straight forward as the active suspension system as the semi-active suspension is not capable of adding energy to the system. Nevertheless, the delay in the sensor signals results in a loss of optimality and the performance of the system. What makes the analysis difficult is that because delays tend to improve the performance at a certain frequency region. This was noticed both in [26] and from the experimental results. But in overall, the performance decrease as was shown in this thesis work.
- **Controller:** Two ways to prevent performance degradation with loss of optimality. But first, the fundamental goal of the problem is described.

  The figure 8.1 below represents the timing of the control signal at different nodes for the reduced model shown in figure 6.3

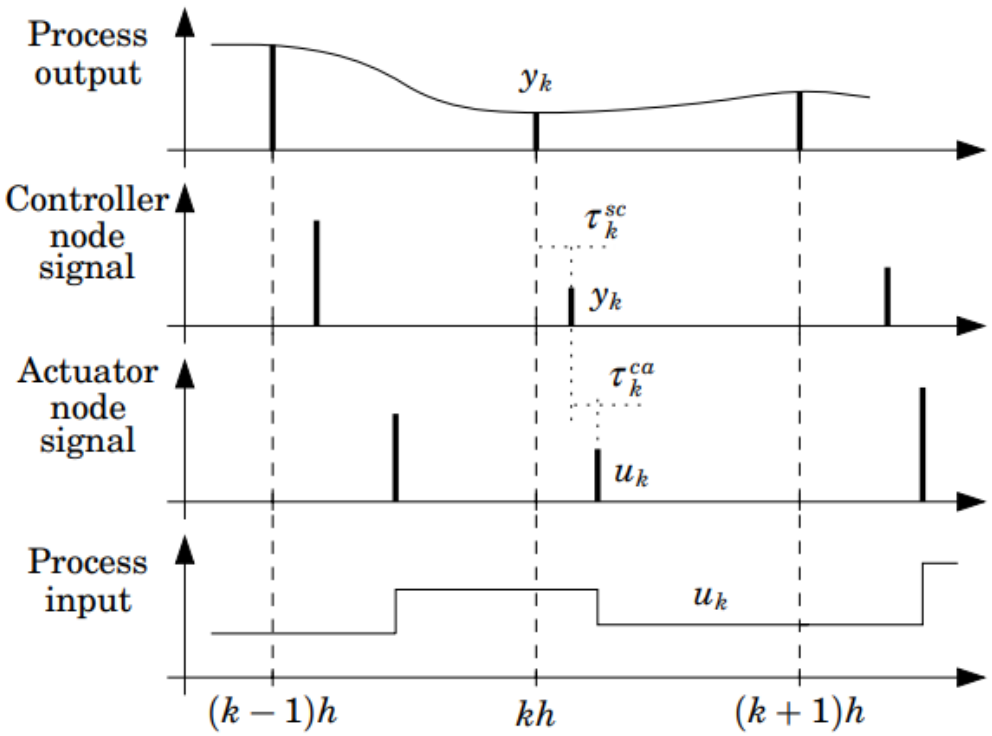

Figure 8.1: Delay timing [14]

As can be seen from the figure 8.1 there are two delays τ_{sc} and τ_{ca}, at the controller and the actuator node. The fundamental core objective is to have the information signals (Solid black lines) exactly inline with a dashed line. Two different methods that could achieve this are by either making improvements from the hardware side by using fast sensors, processor etc or it can be achieved from software side by predicting the signal, which was the focus of study in this thesis work. Now this requirement of prediction rules out the traditional feedback controllers and move towards other filter estimation or compensation techniques.

The requirement of an prediction technique is an accurate model of the vehicle and delay. If the delay model is more accurate, the control signal (Black solid line) would be as close to the optimal (dashed line). Having an accurate vehicle model influences the height (Magnitude) of the line.From the thesis work, it was found that having an accurate delay model is more important than the vehicle model.

8.2 What worked:

Several concepts and analysis were carried out in this thesis work. Some of the most important and valuable analysis that were quite useful are discussed again:

- In the case of the performance analysis, the ride diagram seemed to show a good level of a performance difference in comparison to other metrics. Apart from that, RMS and difference in percentage seemed to be a good measure as well as it gives a numerical value in the performance difference.

- The constant delay and quantization model were quite useful for the fundamental analysis. They were quite simple and easy to implement and were sufficient enough to answer most of the important questions that were addressed in this thesis work.

- In the case of the controller, LQG was quite good in terms of robustness, but its performance in comparison to the LQR is not optimal. But it should be noted that the tuning approach in LQR is quite different from the manual tuning in the LQG. So there is a possibility to further improve the system performance by tuning with different methods. Smith predictor worked well as well, but performance in comparison to the base skyhook controller without any delay is slightly poor.

8.3 What didn't work:

In this section, some parts of the thesis work that are more likely of less value and can be neglected for future works are discussed:

- In the case of the delay model, both delay model based on Gaussian distribution and Markov chain were implemented. The performance difference between these models in comparison with constant delay is not much. Nevertheless, this type of delay models would be useful as the layers of assumptions are removed, and the need for accuracy gets more important. It should also be noted that these models are only as good as their model parameters, which are usually extracted from the experimental data.

- In the case of performance analysis and metrics, the weighted RMS, response ratio and performance based on cost function didn't seem to give much information for analysing comfort in the presence of delays and can be neglected for future works. Other metrics like histogram, covariance and statistical data are not quite intuitive, but it might be worth implementing to see some interesting trends for detailed analysis.

- Some of the controllers that are studied in the thesis work are LMI based control, neuro-fuzzy smith predictor, smith predictor [27] and Modified smith predictor [27]. Out of these, the LMI was quite difficult to implement and was pure analytical, which would have made it not suitable for non-linear systems. Hence it was neglected. The performance of the neuro-fuzzy smith predictor was quite good, but it required a complete change of the controller, and it comprises of many rules, thus increases the complexity. Since in the case of semi-active suspension, the target was to improve the current skyhook con-

troller, a compensator like a smith predictor is more suitable as it worked on top of the existing controller. Also, two different configurations of the smith predictor were tried in addition to the standard configuration based on [27]. But due to time constraint and complexity, it was also neglected.

These are some concepts that are evaluated using a quarter car to keep the analysis simple. The choice of whether to further implement this in the car-maker boiled down to simplicity and usefulness. Finally, the LQG with delay compensation and smith predictor is chosen.

8.4 Discussion:

- *How the signal delays affect the active and semi-active suspension in terms of comfort, and in which test cases these performance degradation becomes prominent?*

  Delays, in general, tend to increase the amplitude level on all three degrees of freedom motion: heave, pitch and roll, when they are excited. In case of semi-active suspension, as we add delays, the amplitude tends to increase in most cases in the simulation. From the objective results, it was noticed that delays tend to increase the pitch amplitude more in comparison to that of the heave amplitude. From the subjective test, the test driver commented that there is not much variations in amplitude but felt that the response of the vehicle to be very weird and different.Similarly, in the case of active suspension, as the delays were added, the amplitude increase with oscillatory behaviour. In some cases, if the delays are too high, it could result in system instability.

  For the test case, refer to 7.3.

- *Which sensor has the most impact on the performance of the system when considering the signal delay and how much delays can be tolerated?*

  In this thesis work, the sensors that are within the scope of the study are level and accelerometer sensor. For both active and semi-active suspension, the accelerometer sensor delays showed to be the most sensitive compared to the level sensor delay. But the experimental results contradict this inference by indicating that the level sensor to the most sensitive to performance degradation.

  As for maximum tolerability, for the active suspension, it's quite straight forward as it has stability margin beyond which the system gets unstable and from simulation, the value was found to be 60 ms delay on both level and accelerometer sensor. But in the case of semi-active, a delay value of 40 ms on the level and 160ms on accelerometer sensor delay was chosen to be tolerable. At this particular delay value, the performance of the skyhook was found to be very similar to the passive suspension.

- *What are the effects of unsynchronized signal delay on the performance of the active and semi-active suspension.*

  From both the simulation and experimental data, it was found that having a synchronized signal can significantly help in improving the performance of the system than having signals that are not synchronized. For example, 50ms delay on both level and accelerometer is better, almost twice, in terms of performance than having 50ms only on the level sensor.

- *How much accuracy of resolution of the signal delay do we need before the performance degradation becomes prominent.*

  From figure 7.27, it was found that the ADC should have at least 6-7 bit quantization levels before the performance of the system drops for both level and accelerometer sensor.

- *Which modelling technique is most suitable for modelling the time-varying signal delays.*

  Three different delay models were implemented, and the differentiation between these models in simulation is quite less for the semi-active system. This in addition to the lack of experimental data with the same simulated controller and vehicle model made it quite difficult to conclude.

- *To what extend will the simulation environment be able to capture the expected vehicle performance in the presence of signal delay?*

  The results from the simulation environment seem to contradict some results from the experimental data. One of the contradiction is that the effect of signal delays for the semi-active system is more prominent and exhibits a significant difference in the experimental data than in the simulation environment. Another contradiction is that the level sensor delay is more sensitivity to performance degradation than the accelerometer sensor delay in the experiment, whereas the opposite is true in the simulation environment.

8.5 Future works:

- It would be interesting to branch out the problem from analysing the system with delay in two locations (i.e in between sensor and controller) to multiple locations and evaluate their behaviour.

- It would be interesting to measure the delay in the current system. This would help to accurately model the mathematical delay models. This might not be super useful in analysing the system performance but would be valuable when

designing the controller.

- One experiment that would be interesting is to test the current suspension system with inexpensive sensors and then try to compensate the delay from the SW side, and evaluate its performance with the current sensor and controllers. There will be some performance loss but it would be interesting to see by how much.

- The analysis was carried off for only one particular vehicle model. It would be interesting to carry out the study for a different vehicle and damper models.

- To study two parameters, sweep seems to be sufficient. But to study a large set of parameters and how they influence each other, some tools from data science and visualization would be very useful, and it is worth exploring that field for performance studies. For example, the Pearson correlation coefficient can show how different parameters affect the final performance of the system in the magnitude of -1 to 1.

Bibliography

[1] Happee, R. and Dhaens, M.(2020):How do you prevent motion sickness in autonomous cars, Monroe Intelligent Suspension on collaboration with TU Delft. may 2020. [Video source].

[2] Aly, A. and Salem, F.A. (2013): Vehicle Suspension System Control: A Review, International Journal of Control, Automation and Systems, vol. 2, no.2, July, pp. 46-54.

[3] Christopher,B. and David, J.(1991): Notes on Control with Delay, The University of Rochester, Computer Science Department, August, pp. 7-9.

[4] Fridman E.(2014): Introduction to Time-Delay Systems. [electronic resource]: Analysis and Control [Internet]. 1st ed. 2014. Springer International Publishing; [cited 2020 Apr 13]. (Systems Control: Foundations Applications).

[5] Savaresi.S, Poussot-Vassal.C, Spelta.C, Sename.Ö, Dugard.L,(2010). Semi-Active Suspension Control Design for Vehicles. Butterworth-Heinemann.

[6] Postlethwaite and Ian.(1996): Multivariable Feedback Control: Analysis and Design, JohnWiley Sons, Inc. , , ISBN: 0471943304.

[7] Kulscar B.(2017) Class Lecture, Topic: Linear Control System Design. SSY285, Department of Electrical Engineering, Chalmers University of Technology, Gothenburg,.

[8] Segers.J (2008). Analysis Techniques for Race car Data Acquisition, Second Edition. SAE International

[9] Jazar, R.N.(2017): Vehicle Dynamics: Theory and Application, Springer International Publishing, 2017,ISBN: 9783319534411.

[10] IPG Carmaker reference manual Version 7.0.2.

[11] Fredrik Skoglund,(2020): Strategies for Road Profile in Adaptive Suspension Control, Department of Electrical Engineering, Vehicle Systems, Linköping university.

[12] Elham Goudarzi,(2019): Improving ride comfort using control system design for Active Damper, Department of Mechanics and Maritime sciences, Chalmers university of technology.

[13] Kjellberg, F. and Sundell, S.(2018): Real- time non-linear model predictive control for semi-active suspension with road preview, Department of Electrical Engineering, Chalmers university of technology.

[14] Nilsson, J. (1998). Real-Time Control Systems with Delays. Department of Automatic Control, Lund Institute of Technology (LTH).

[15] Zadeb L A.(1952): Operational analysis of variable delay system" Proc. IRE, vol. 40,May 1952, pp. 564 - 568

[16] S. G. Margolis and J. O'DonneU,(1952): J. Rigorous treatments of variable time delays, May 1952 pp. 564-568.
[17] Seddon, P. and Johnson,R.A.(1963): The simulation of variable delay, IEEE Trm. IEEE Tram. Electron. Cornput.. vol. EC-12. June 1963 pp. 307-309, .
[18] Johnson.R. A.(1972): Functional equations approximations, and dynamic response of Compur. (Short Notes), vol. C-17, pp. 89-94, Jan. 1968. systems with variable time delay," IEEE Tram. Auioma . Conlr. vech. Notes and Corresp.). vol. AC-17, June 1972 pp. 398-401, .
[19] Strandemar, K.(2005): On objective measures for ride comfort evaluation Department of Signals, sensors and systems, (Doctoral dissertation, KTH).
[20] Singh A.k(2018): Quantization process and Quantization noise. [Online](Video source), Available from:https://www.youtube.com/watch?v=ez7NnC6Mu2M
[21] Sarangapani.J, Xu.H (2015). Optimal Networked Control Systems with MATLAB. CRC Press
[22] Wang, Fei-Yue, Liu, Derong,(2006). Networked Control Systems. Springer-Verlag, London,2008.
[23] Jalilian.F (2014): Investigation of Power Harvesting Potential from Vehicle Suspension Systems. MSc Thesis. Department of Electrical and Computer Engineering,University of Victoria.
[24] J. D. Ivan Cvok (2019). Comparative performance analysis of active and semi-active suspensions with road preview control. IAVSD (2019).
[25] Strandemar.K (2005). On Objective Measures for Ride Comfort Evaluation. PhD Thesis. Department of signal, sensors and systems, Royal Institute of technology (KTH), Stockholm, Sweden, 2005
[26] Eslaminasab.N, Golnaraghim.M.F (2007): The Effect of Time Delay of the Semi-Active Dampers on the Performance of On-Off Control Schemes, ASME 2007 International Mechanical Engineering Congress and Exposition, Vol. 9, 2007.
[27] Tamas, G., Molnar, A., Hajdu, D and Insperger, T.(2018): The Smith predictor, the modified Smith predictor and the finite spectrum assignment: a comparative study, s, Department of Applied Mechanics,Budapest University of Technology and Economics.
[28] Mirkin.L, J.Palmor Z, Control Issues in Systems with Loop Delays, Faculty of Mechanical Engineering, Technion—IIT, Haifa 32000, Israel

A

Active suspension

A.1 Effect of signal delays

A.1.1 Sinus steering

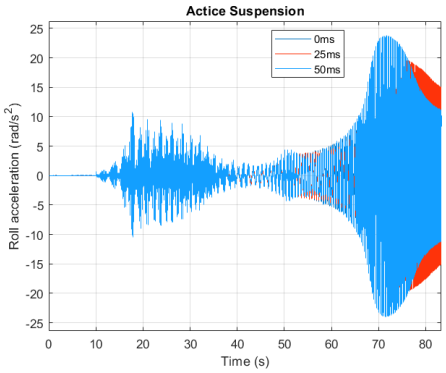

Figure A.1: Time domain plot for different delay

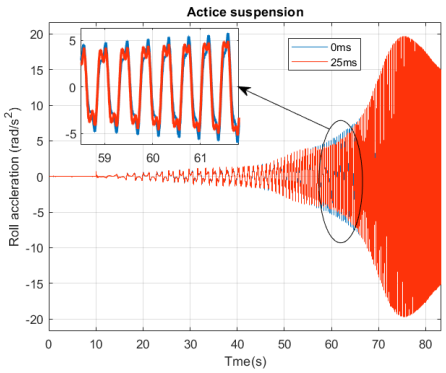

Figure A.2: Region where delays increase the performance in active suspension

A.2 Effect of synchronization

A.2.1 Stochastic road index-c

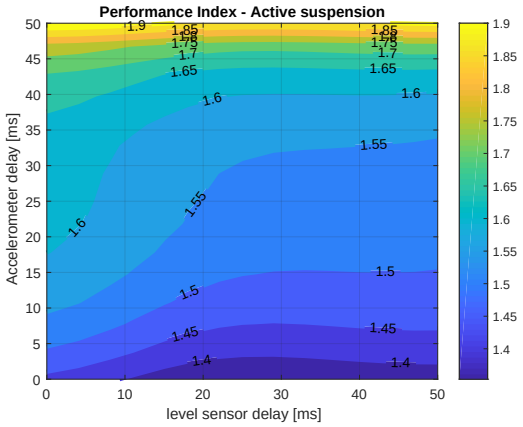

Figure A.3: Effect of synchronization of Accelerometer and level sensor delay against performance index for active suspension by sweeping the delays

A.2.2 Transfer function plot

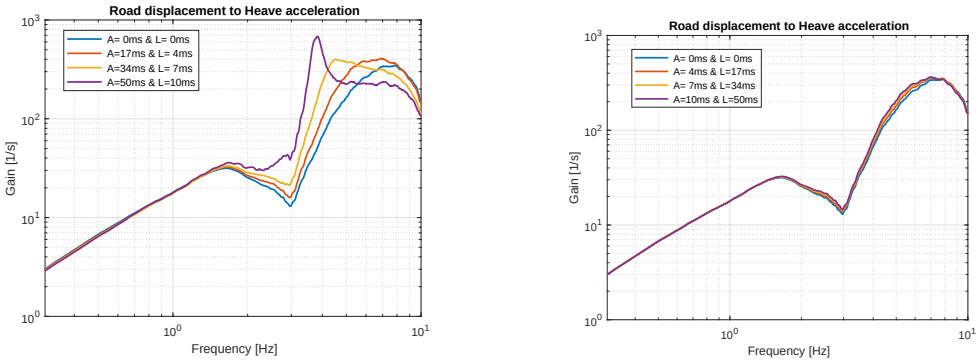

Figure A.4: Transfer function plot of unsynchronized delays for Active suspension

A.3 Effect of signal error

A.3.1 Quantization and delay sweeps

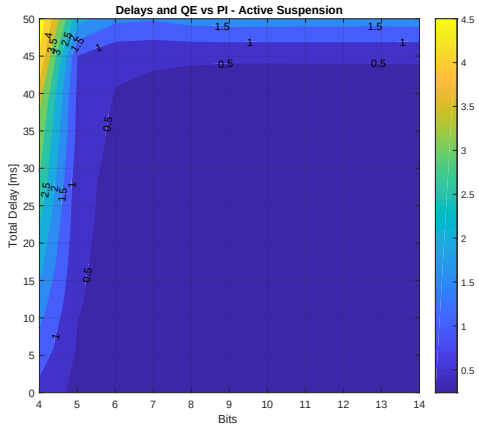

Figure A.5: Effect of synchronization of total delay and number of bits against performance index for active suspension by sweeping the delays